October 2019

Self-Exfoliating and Reactive Polymer (SERP) as A Protection Against Chemical Warfare Agents (CWAs)

SOEUN KIM

SELF-EXFOLIATING AND REACTIVE POLYMER (SERP) AS A PROTECTION AGAINST CHEMICAL WARFARE AGENTS (CWAs)

A Dissertation Presented

By

SOEUN KIM

Submitted to the Graduate School of the

University of Massachusetts Amherst in partial fulfillment

of the requirements for the degree of

DOCTOR OF PHILOSOPHY

September 2019

Department of Polymer Science and Engineering

SELF-EXFOLIATING AND REACTIVE POLYMER (SERP) AS A PROTECTION AGAINST CHEMICAL WARFARE AGENTS (CWAs)

A Dissertation presented

By

SOEUN KIM

Approved as to style and content by:

_____

Kenneth R. Carter, Chair

_____

Ryan C. Hayward, Member

_____

Dhandapani Venkataraman, Member

_____

E. Bryan Coughlin, Department Head

Department of Polymer Science and Engineering

ACKNOWLEDGMENTS

I would like to acknowledge all those who have supported me during my graduate study and who have contributed to this thesis. First, I would especially like to thank my dissertation advisor, Professor Kenneth R. Carter for his guidance and support during my graduate study. He gave me many chances to attend conferences and collaborate with others from different research affiliations. He spent so much times doing corrections on my academic writing since my project has many quarterly and annual reports. He is always supportive and open to group members when we need his help. Also, I would like to thank for waiting for me when I had been in hospital for so long. Without his support and patience, I would not have achieved my Ph.D.

I would also like to acknowledge my committee members, Professor Ryan Hayward and Professor Dhandapani Venkataraman for your invaluable time, great insights, and challenging questions. You are both experts in the area of my research, and meeting with you is always inspiring.

I would like to thank the past Carter group members. I would thank Dr. Jacob John, Dr. Andrew Davis, and Dr. Yinyong Li, Mikhail Kuchuk, Dr. Jaewon Choi, Dr. Jared Harris, Dr. Charlotte Mallet, Dr. Sachin Bhaladhare, Dr. Kara Martin, Dr. Yiliang Zhou, Laura Parker, Trouble Mandeson, Anise Grant and Lauren Grondin for their help. I would also like to acknowledge the current members of Carter group, Allen Chang, Hanna Yu and Jerred Wassgren. I would like to thank my friends Hyeyoung Kim, Jooyoung Chang, Dukman Yu, Gajin Jeong, Minjeong Lee, Byoung-jin Jeon, Paul Kim,

Feyza Dundar, Irene Howell, Shruti Rattan, Aditi Naik, Laura Lanier, Gayathri Niveditha, Xiyu Hu, Tetsu Ouchi, from PSE and Miwha han, Soon-mi Kim, Maritza Casa from Amherst for having a such a good friendship. I will never forget them and would like to continue this relationship even after leaving PSE.

I would like to acknowledge collaborators Tianxi Yang (Professor Lile He group, Department of Food Science), Gibson P.W. and Chris Doona (Natick Army Research Center), Dr. Francesco Fornasiero (Lawrence Livermore National Laboratory), Prof. Jerry Shan (Rutgers University) and Prof. Timothy M. Swager (MIT)

My grateful acknowledgments go to the Polymer Science and Engineering faculty and staff. I would specially thank Lisa Groth for her help in dealing with tons of documents and keeping track of my milestones.

I would like to thank to my previous advisor Kwang-un Jeong (Prof. Chonbuk National University, Department of Polymer Nano Science & Technology) who encouraged me to study in United States and has given much advices since I joined his group in 2009 until today.

I would like to acknowledge the financial support of the Chemical and Biological Technologies Department of the Defense Threat Reduction Agency (DTRA-CB) via grant BA12PHM123 in the “Dynamic Multifunctional Materials for a Second Skin D[MS]2” program.

Finally, I want to acknowledge beloved, parents, sister (so-young), and brother (il-do) for their unconditional support. They trust any choice I make and encourage me to pursue my dream.

ABSTRACT

SELF-EXFOLIATING AND REACTIVE POLYMER (SERP) AS A

PROTECTION AGAINST CHEMICAL WARFARE AGENTS (CWAs)

SEPTEMBER 2019

SOEUN KIM, B.S., CHONBUK NATIONAL UNIVERSITY

M.S., CHOUNBUK NATIONAL UNIVERSITY

M.S., UNIVERSITY OF MASSACHUSETTS AMHERST

PH.D., UNIVERSITY OF MASSACHUSETTS AMHERST

Directed by: Professor Kenneth R. Carter

According to the US army report, there are still significant numbers of stockpiles of chemical warfare agents (CWAs) produced during the Second World War. CWAs production and stockpiling were officially outlawed by the Chemical Weapons Convention of 1993. Nevertheless, some fanatics around the world use CWA as a weapon of mass destruction, such as the Sarin gas attack in Syria in 2013. Since the discovery that toxic pentavalent organophosphorus (OP) compounds has facilitated the development of CWAs as well as insecticides, research on developing protective materials against those toxins have become a priority. Simply, those poisonous molecules are referred to as a “nerve agent” because it prevents nervous system from transferring messages by forming a covalent bond with nerve enzyme, referred to as acetylcholinesterase. As a result of this chemical interference, organs are tightly constricted and muscles cannot relax displying noticeable physical symptoms:

contraction of the pupils, excessive mucus, tears and sweat, nausea, vomiting, chest tightness, loss of bowel control like urinating and defecating, and eventually coma or death. Remarkably, even trivial amount of toxins (LD_{50}: ~10 μg/kg) is enough to cause those severe results. Those OP-based compounds can be facilely hydrolyzed by strong base, such as sodium hydroxide and converted to non-toxic compounds. However, this chemical reaction is highly vigorous, generating excess heat. Therefore, it is important to develop a mild catalyst, which can be employed in fabrics or mask for protective garment applications. This can be achieved by selecting organo-based, nucleophiles such as amines, or pyridine-aldoxime. With these organo-based nucleophilic materials, it may be possible to fabricate personal protective equipment to prepare for sudden CWA attacks.

The ultimate goal of this project is the fabrication of a protective polymer which can be easily coated on fabric, essentially creating a “second skin”. Protection can be achieved by blocking permeation of toxins through layer and simultaneously detoxifying molecules through chemical modification Furthermore, we challenge ourselves to regenerate fresh reactive layers by physically destructing contaminated area, referred to as a self-exfoliation. Chapter 1 briefly describes the concept of self-exfoliating and reactive polymer (SERP) layer as a protection against CWAs and how to experimentally accomplish and evaluate. Chapter 2 introduces a stimuli-responsive, self-exfoliating polymer with promising acid-sensitive, acetal/ketal-based crosslinkers that exhibit self-exfoliation at room temperature. Synthesis of acid-sensitive crosslinker and their acid-hydrolysis kinetics were studied. Chapter 3 focuses on developing a

nucleophilic polymer as a CWA reactant to decontaminate organophosphate-based nerve agents. Chapter 4 evaluates a reactive polymer layer by investigating moisture-vapor transmission rate (MVTR), permeation of nerve agents through polymer films by using Surface-Enhanced Raman Spectroscopy (SERS). Chapter 5 describes conclusions and future work.

TABLE OF CONTENTS

ACKNOWLEDGMENTS iv

ABSTRACT vi

LIST OF FIGURES xi

CHAPTER

1.SELF-EXFOLIATING AND REACTIVE POLYMER (SERP) AS A PROTECTION AGAINST CHEMICAL WARFARE AGENTS (CWAs) 1

2.ACID-STIMULI RESPONSIVE POLYMER FOR SELF-EXFOLIATION 5

2.1 Introduction: Acid-sensitive Polymers and Hydrolysis Kinetic Study 5

2.2 Project Goal 8

2.3 Experimental 9

2.3.1 Methacrylate-functionalized Acetal/Ketal-based Crosslinker 9

2.3.2 Hydrolysis Kinetic Study by ^{1}H NMR: Water-soluble Crosslinker 16

2.3.3 Hydrolysis Kinetic Study by UV-Vis Spectroscopy 17

2.3.4 Hydrolysis Kinetic Study by GC-MS: Insoluble Crosslinked film 18

2.4 Results and Discussion 20

2.4.1 Acid-sensitive crosslinkers 20

2.4.2 Kinetics of hydrolysis of CL3 by ^{1}H NMR 22

2.4.3 Degradation study of CL4m and CL4p by UV-Vis spectroscopy 24

2.4.4 GC-MS degradation study of network films crosslinked by acetals 28

2.5 Conclusion 36

3.REACTIVE POLYMERS WITH NUCLEOPHILIES FOR NEUTRALIZING ORGANOPHOSPHATE-BASED NERVE AGETNS 38

3.1 Introduction 38

3.2 Project Goal 40

3.3 Preliminary Approaches 41

3.3.1 Bulk Hydrogel Films Crosslinked by Acid-sensitive Crosslinkers Containing Quaternary Ammonium Halides (Cl or F) as a Nucleophile 41
3.3.1.1. Preparation of QAC or QAF-based catalyst containing films 41
3.3.1.2. ^{31}P MAS NMR study 42
3.3.1.3. Preliminary Results 43
3.3.1.4. Summary 45
3.3.2 Nucleophilic Polymers Functionalized from Acid-degradable NPs 47
3.4 Experimental: Photo-cross linkable and Nucleophilic Linear Polymer 57
3.5 Results and Discussion 63
3.6 Conclusion 74
4.EVALUATION: MOISTURE VAPOR TRANSMISSION RATE (MVTR), CWA PERMEATION STUDY AND SELF-EXFOLIATION STUDY 76
4.1 Introduction 76
4.2 Project Goal 78
4.3 Experimental, and Results and Discussion 78
4.3.1 Moisture Vapor Transmission Rate (MVTR) 78
4.3.2 Permeation test using Franz Cell and GC-MS 79
4.3.3 CWA Permeation By Surface-enhanced Raman Spectroscopy (SERS) 81
4.4 Conclusion 83
5.CONCLUSION 85
6.FUTURE WORK 87
REFERENCES 88

LIST OF FIGURES

Figure **Page**

1.1. Current military garment for protecting against chemical warfare agent threat (http://www.militarysystems-tech.com/).....2

1.2. Schematic illustration of Self-Exfoliation and Reactive Polymer (SERP) as a protection against CWAs (above) and its multi-responsive mechanism (below).....3

1.3 Chemical structures of nerve agents and nerve agent simulants.....4

2.1 Synthetic scheme: divinyl-functionalized acetal/ketal-based crosslinkers[20].....9

2.2 ^{1}H NMR of CL2.....11

2.3 ^{1}H NMR of CL3 as prepared (a mixture of desired crosslinker CL3 and unreacted PEG-MA with 1 to 3.38 molar ratio).....12

2.4 ^{1}H NMR of CL4m.....13

2.5 ^{13}C NMR of CL4m.....14

2.6. ^{1}H NMR of CL4p.....14

2.7. ^{13}C NMR of CL4p.....15

2.8 ^{1}H NMR of V-CL4m.....16

2.9 (a) Hydrolysis of CL4m-based networks and (b) schematic representation of network degradation experiment for the GC-MS study[20].....18

2.10. GC-MS from mixture of mMBA and hexadecane (internal standard) in hexane (a) and calibration curve (b): To construct calibration curve, each solution contains different concentration of mMBA with same concentration of internal standard (hexadecane). From the GC-MS, calibration curve can be

built from response ratio between two molecules vs amount ratio from concentration ratio[20].....20

2.11 Acid catalyzed degradation of CL3: (a) ^{1}H NMR spectra before and after degradation, and (b) the corresponding hydrolysis kinetics at pH 4 and 5 versus time[20].....23

2.12 UV-Vis spectrum: Generation of mMBA during hydrolysis of CL4m (a) pH 1; (b) pH 2; (c) pH 3; (d) pH 4.....26

2.13 UV-Vis spectrum: Generation of mMBA during hydrolysis of CL4p (a) pH 1; (b) pH 2; (c) pH 3; (d) pH 4.....26

2.14 Acid catalyzed degradation of (a) CL4m and (b) CL4p at pH1, 2, 3 and 4.....27

2.15 GC-MS of degradation of HEMA crosslinked films (3.2 mol% of CL4m): (a) pH 1; (b) pH 2; (c) pH 3; (d) combined results after 144 hr. Scanning time means retention time. 29

2.16 (a) Plot of $\ln([M]_t/[M]_0)$ in different buffer solutions versus incubation time and (b) plot of the half-life of crosslinkers (CL4m) in the network as a function of pH 31

2.17 (a) Plot of $\ln([M]_t/[M]_0)$ for networks with different crosslinker concentration versus incubation time and (b) plot of the half-life of crosslinkers (CL4m) in the network as a function of crosslinker concentration. 32

2.18 Acid degradation study of hydrophobic crosslinked MMA films by CL4m at different pHs 33

2.19 Thiol-ene networks: (a) hydrolysis of thiol-ene based networks, (b) plot of $\ln([M]_t/[M]_0)$ in different buffer solutions versus incubation time and (c) plot of the half-life of crosslinkers in the network as a function of pH.....34

3.1 Chemical structure of monomers and CWA catalysts.....41

3.2 Disposable insert kit (left) and 0.4 cm ZrO2 rotor.....43

3.3 ^{31}P MAS NMR spectra showing DFP and hydrolyzed product DIIP, and their structures.....43

3.4 DFP neutralization kinetic plots and % DFP remaining vs time for SE003, SE006 and SE007 44

3.5 Schematic illustration of self-exfoliating and reactive polymer (SERP) as a bulk film and its key results (a) and DFP neutralization kinetic plot..... 46

3.6 Methacrylate-functionalized ATRP initiator: MABr..... 48

3.7 ^{1}H NMR of MABr 48

3.8 PS-co-DVD/MABr core-shell nanoparticles: PSBr..... 49

3.9 SEM Image of PSBr NPs..... 50

3.10 Synthesis of vinyl-functionalized nucleophilic monomers..... 50

3.11 ^{1}H NMR of HisMA 51

3.12 ^{1}H NMR of MIA 52

3.13 ^{1}H NMR of MIAD..... 53

3.14 ^{1}H NMR of SIA 54

3.15 ^{1}H NMR of SIAD..... 54

3.16 ^{1}H NMR of SPP 55

3.17 Synthesis scheme: nucleophilic polymer functionalized NPs by performing ATRP reaction..... 56

3.18 Kinetic plot of DFP neutralization catalyzed by 23 mM AMBD buffer, 4-pyridine aldoxime (PAM) with D_2O and PAM with 23 mM AMPD buffer (left) and half-life of DFP at each condition (right)..... 57

3.19 ^{1}H NMR of VBBP 59

3.20 ^{1}H NMR: p(NIP-VBBP-VBCl)..... 60

3.21 ^{1}H NMR: p(NIP-VBBP-VBI) 61

3.22 ^{1}H NMR: p(NIP-VBBP-VBIPAM) 62

3.23 Schematic illustration: preparation of a breathable thin film combining terpolymer, crosslinker and PEI 62

3.24 DFP neutralization study by the reactive film: experimental set up and ^{31}P NMR spectrum after 30 min exposure to DFP 63

3.25 Synthetic pathways used to make the PAM-containing terpolymer. The iodization of the benzyl group was found to be necessary to allow reaction of PAM while at the same time avoiding hydrolysis of NIP to AAc in resulting PAM-functionalized terpolymer. 64

3.26 ^{1}H NMR: effect of room temperature on hydrolysis of NIP and PAM functionalization to vinylbenzyl chloride 65

3.27 Determination of reaction order 66

3.28 ^{1}H NMR: mixture of PAM-functionalized 4-vinylbenzyl iodide and PAM 67

3.29 Reaction mechanism and rate constants defined for the hydrolysis of DFP catalyzed by PAM (left), equations for defining half-life for DFP hydrolysis from pseudo-first order kinetic (right)[23] 67

3.30 Schematic illustration: neutralization of DFP catalyzed by nucleophiles and ^{31}P NMR spectra. 68

3.31 Kinetic plots of DFP neutralization catalyzed by terpolymer with 49 mol% of VBClPAM (a) and terpolymer with 22 mol% of VBClPAM in different solvent mediums 69

3.32 DFP neutralization kinetic plots for comparing polymer solution concentration using same polymer (a) and mol% of VBClPAM in terpolymer using two different polymer (b) in two different 2-amino-2-methyl-1,3-propanediol (AMPD)-based buffer solution (5 mM and 23 mM) in D_2O 70

3.33 DFP neutralization kinetic: catalyzed by p(NIP-VBBP-VBIPAM) with assistance ot PEI (left) and 23 mM AMPD (right) 71

3.34 Water-soluble poly(NIP-co-VBIPAM) with different compositions (O means water-soluble, Δ means poorly water-soluble) 72

3.35 DFP neutralization kinetic study: effect of polymer (p(NIP-co-VBIPAM) with 90:10) concentration and buffer solutions 72

3.36 DFP neutralization kinetic study: effect of polymer with different compositions and buffer solutions.....73

4.1 Permeation cell: F739 (a) and Franz cell (www.permeagear.com) 77

4.2 Dynamic Moisture Permeation Cell (DMPC), image provided from Natick 78

4.3 Surface and cross-section image of breathable thin film on ePTFE and MVTR values. 79

4.4 Calibration curve for GC-MS measurement of permeated DCP 81

4.5 Schematic illustration of Surface-enhanced Raman Spectroscopy; target CWA simulant (paraoxon) 81

4.6 Visually shown depth-mapping of SERS exhibiting CWA permeation through crosslinked terpolymer 83

CHAPTER 1
SELF-EXFOLIATING AND REACTIVE POLYMER (SERP) AS A PROTECTION AGAINST CHEMICAL WARFARE AGENTS (CWAs)

Up-to-date chemical protection garments can reduce the risk of chemical exposure by using smaller pore size than toxins in fabric structures, where toxins cannot penetrate through the barrier materials or are based on heavyweight full-barrier protection or permeable adsorptive protective over-garments that cannot meet the critical demand of simultaneous high comfort and protection, and provide a passive rather than active/dynamic response to the environmental threat. However, toxins can eventually permeate through the barrier materials via absorption, diffusion, or desorption at the molecular level, rendering them to single or limited-use protective clothing.[1] To overcome this limitation, and enhance the comfort and protection of warfighters in the battlefield and during operations in diverse climates, new technologies and material assemblies are required for the fabrication of advanced multifunctional garments that allow high water vapor transport rates (MVTR) while blocking toxic chemicals and bio-threats. There is a continuing need for technological advancements to ameliorate the dangers presented by weaponized biological and chemical agents and their use by either identified forces or terrorist organizations. The nature and severity of these threats is well-known and is an active area of research with the majority of work being in the area of threat detection rather than threat reduction. 3

We are developing new approaches for in-the-field protection from organophosphate-based nerve chemical warfare agents (CWAs), exploring the use of reactive nucleophilic compounds embedded in a thin protective layer. Upon CWA

challenge, the latter actively reacts with the toxin, neutralizes the threat and then self-exfoliates, removing the compromised layer and exposing fresh protective under-layers. This process mimics the function of natural living skin where blistering and peeling occurs when overcome by dangerous external factors. The artificial exfoliation requires specially designed stimuli responsive materials. The stimuli in this case are the highly acidic byproducts formed during the neutralization of highly nucleophilic CWAs. We are developing layers that when exposed to CWAs, first neutralize the threat as it diffuses into the layer and concurrently the acidic byproducts of the neutralization initiate reactions that destabilize the contaminated regions of the matrix leading to exfoliation of the compromised areas and re-exposing fresh uncontaminated protective layers.

Figure 1.1. Current military garment for protecting against chemical warfare agent threat (http://www.militarysystems-tech.com/)

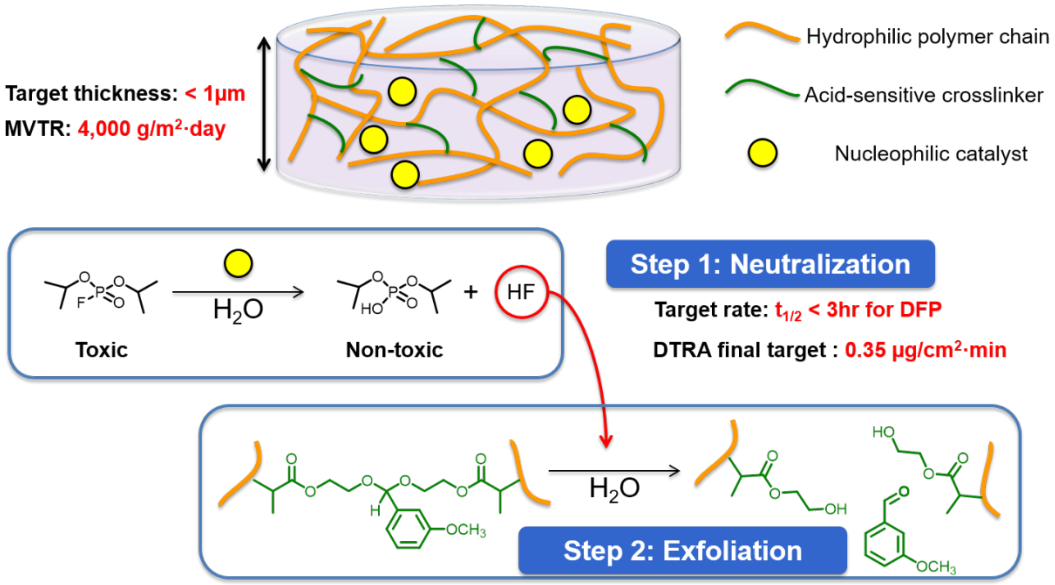

Figure 1.2. Schematic illustration of Self-Exfoliation and Reactive Polymer (SERP) as a protection against CWAs (above) and its multi-responsive mechanism (below)

Self-exfoliating and reactive polymer (SERP) as a protection against CWAs is composed of nucleophilic reactants or catalyst for decontaminating organophosphate-based nerve agents (**Figure 1.2)**, and acid-sensitive crosslinkers to induce self-exfoliation by using a transition from insoluble network to soluble linear polymer. Here, we are specifically targeting organophosphate-based nerve agents which can be simply hydrolyzed to non-toxic OP compounds by nucleophiles. This reaction also produces an acidic byproduct such as HF or HCl. This harmful acid can trigger hydrolysis reaction on the acid-sensitive crosslink junction. From this hydrolysis reaction of crosslinker, we can reveal self-exfoliate of contaminated area while also consuming the harmful acid.

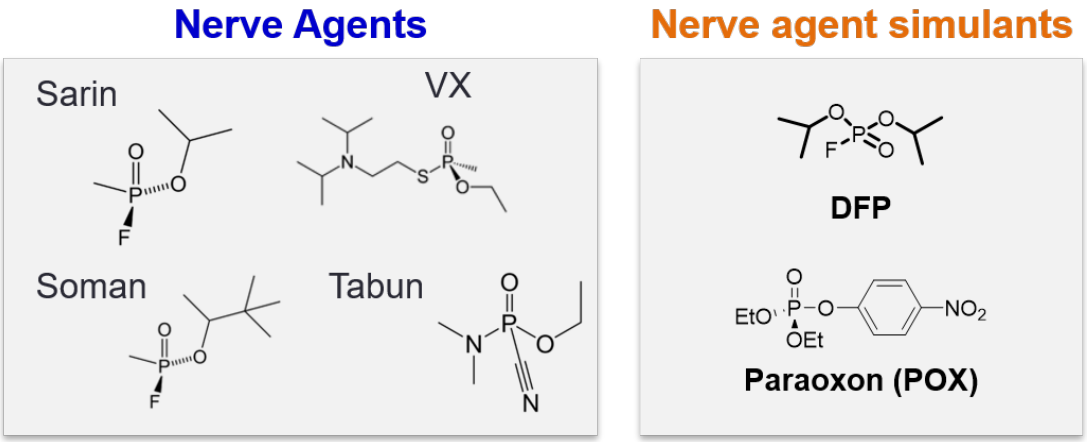

Figure 1.3 Chemical structures of nerve agents and nerve agent simulants

CHAPTER 2

ACID-STIMULI RESPONSIVE POLYMER FOR SELF-EXFOLIATION

2.1 Introduction: Acid-sensitive Polymers and Hydrolysis Kinetic Study

pH-sensitive polymers and gels have been intensively studied among the stimuli-responsive systems that can show spontaneous physical or chemical changes in response to external stimuli such as temperature, mechanical stress, and ionic strength. These pH-sensitive polymer systems can be used in bio-related areas such as in drug-delivery systems (DDS), as well as diagnostic and sensing applications because of the various pH ranges found in human organs and pH differences between normal tissue and tumor tissue.[4-8] For example, using changes in pH as the external stimuli can drive reversible changes in volume by tuning the ionization states of polyelectrolytes or even irreversibly change solubility via cleavage of acid-degradable crosslinked positions in the crosslinked or linear polymer.[9] Polymers containing acid-degradable linkages have also been exploited in lithographic patterning where high temperature or strong acids are often required to strip resist after patterning.[10-12] The use of these acid-sensitive materials not only provide protection of the silicon substrates from undesired damage but also leads to milder condition for post-process substrate cleaning, thus lowering production costs.

There are a variety of acid-degradable systems based on chemistries including tertiary esters, orthoesters, acetal/ketals, imines, hydrazones, and cis-aconityls – many

of these are also frequently used as protective groups in organic synthesis.[9] For example, polystyrene based nanogels crosslinked by tertiary ester dimethacrylates have been reported and their degradation was demonstrated by treating the samples at 90 ºC for 24 hr leading to their conversion from spherical gel particles to soluble linear polymers.[13] Acid-sensitive brush polymers were grown from silicon substrates utilizing a tertiary ester-based tethering group. Layers with different brush thickness were demonstrated and these brushes could be easily removed by treatment with aqueous media.[14] Among the many acid-sensitive functional groups, acetal based crosslinkers have various advantages including ease of synthesis, easy hydrolysis at room temperature that occurs within reasonable time at various acidic pH ranges, stability at neutral or mildly alkaline conditions, and versatile tuning of degradation rate by changing the substituent group at the acetal position.

The degradation rates of hydrogels or polymers which are covalently bonded with acid-degradable monomers have been studied using a variety of methods. Hydrophilic water-soluble materials can be easily characterized in water-based pH buffer solutions without any complications due to diffusion. These measurements can be made using ^{1}H NMR by observing the disappearance of proton signal corresponding to acid-sensitive functional groups,[15] or by tracking molecular weight changes using gel permeation chromatography (GPC).[16] Acid-degradable linear polymers have been synthesized via step-polymerization involving the Michael addition reaction with acetal containing monomers, direct acetal forming polymerization using diols with divinyl ether[17], or acyclic diene metathesis (ADMAT) from divinyl monomers with Grubbs' catalyst.[5] All

these procedures require long reaction times, high monomer purity, and precise control of stoichiometry for high molecular weight. Most linear step-growth polymers will not retain their shape after degradation because the resulting products consist of smaller molecules which can be easily washed away after hydrolysis. In the case of materials crosslinked by simple radical polymerization, the monomers themselves can be selected from those having more than one polymerizable group. After hydrolysis, only the crosslinker units will be severed while the linear portion of the polymer remains mainly intact. This can lead to partial shape retention and lends utility of these types of materials to be used in molding operations where the networks can be formed by thermal or UV-initiated polymerization. For these reasons and others, acid-degradable crosslinked films are ideal candidates for the development of self-exfoliating garments, which can facilitate the selective removal of contaminated areas by acidic stimuli but maintain its overall original integrity. The pH range which triggers this degradation could be specifically varied depending on external stimuli.

While networks that controllably degrade in the presence of external stimuli have many potential applications, there has been little activity in studying the acid-catalyzed hydrolysis kinetics of ketal and acetal functional groups present in network films. It is challenging to quantitatively measure how quickly acid-sensitive groups can be hydrolyzed in crosslinked systems, mainly due to the slow diffusion of aqueous buffer solutions and the relatively small mass loss during the decomposition of the crosslinker units. In the case of acid-sensitive nano- or micro-gel particles, the degradation rate can be indirectly examined by observing particle size changes, for example by using

dynamic light scattering (DLS) while taking into account any swelling effect.[18] The hydrolysis of acid-degradable crosslinked polymer films can be discontinuously measured by monitoring fractional mass loss by repeatedly incubating gels in buffer solution and drying.[19] However, if the mass loss during hydrolysis is too small, it can be very difficult to measure the mass change after each degradation cycle.

2.2 Project Goal

In this project, various acid sensitive dimethacrylate-functionalized acetal/ketal-based crosslinker monomers were synthesized. Acetal and ketal were chosen due to their acid sensitivity at ambient temperature at which self-exfoliation under CWA attack happens. ^{1}H NMR and UV-Vis spectroscopy were employed for hydrolysis kinetic study under different acidic environments. Acid-degradable network films simply composed of hydrophilic or hydrophobic commercially available monomers with the synthesized crosslinkers will be prepared and their degradation kinetics will be investigated by using Gas Chromatography-Mass Spectroscopy (GC-MS). Overall, hydrolysis rate of crosslinked system will be controlled with hydrophilicity of comonomers and crosslinking density (mol % of crosslinkers). Eventually, we can understand how fast acid-sensitive groups can be hydrolyzed at certain conditions and this information will be employed in combination with reactive polymers for decontaminating OP compounds.

2.3 Experimental

2.3.1 Methacrylate-functionalized Acetal/Ketal-based Crosslinker

Vinyl-terminated acetal/ketal-based, acid-sensitive crosslinkers can be prepared by reaction of alcohol with acetone or aldehyde in acatalytic amount of acid. By tuning substituent group and hydrophilicity, hydrolysis rate is expected to be controlled.

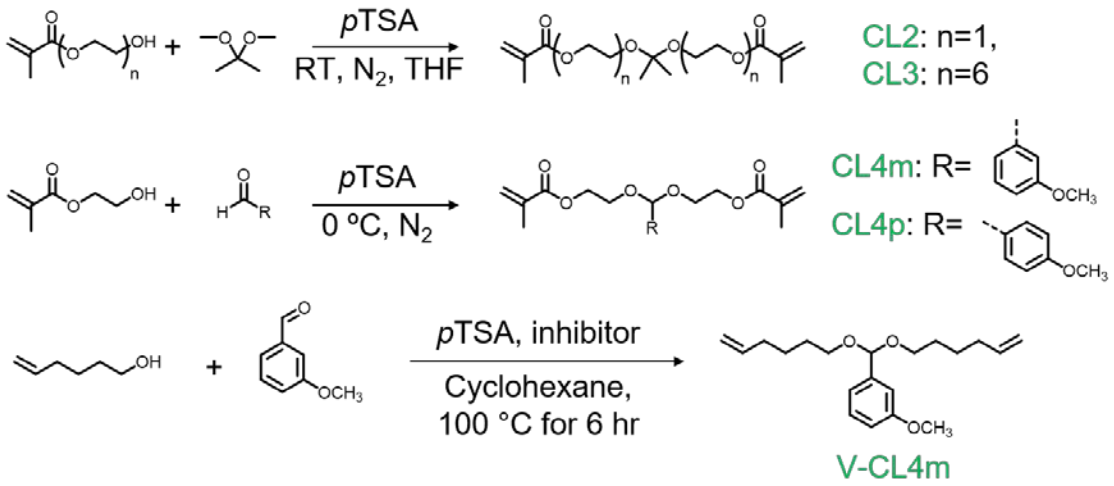

Figure 2.1 Synthetic scheme: divinyl-functionalized acetal/ketal-based crosslinkers[20]

Materials used for synthesis are Hydroxyethylmethacrylate (HEMA, Acros Organics, 97%), methyl methacrylate (MMA, Acros Organics, 99%), poly(ethylene glycol) methacrylate (PEG-MA, average M_n: 360 g/mol, Aldrich), 2,2-dimethoxypropane (DMP, Acros Organics, 98%), *p*-toluenesulfonic acid monohydrate (*p*TSA, Aldrich, 98.5%), molecular sieves (4Å) (Alfa Aesar), *p*-methoxybenzaldehyde (*p*MBA, Alfa Aesar, 98%), *m*-methoxybenzaldehyde (*m*MBA, Alfa Aesar, 98%), 5-hexen-1-ol (TCI, 95%), triethylamine (TEA, Acros Organics, 99%), anhydrous tetrahydrofuran (THF) (EMD chemicals, 99.9%), cyclohexane (Fisher Scientific, 99%), pentaerythritol

tetrakis(3-mercaptopropionate) (PTMPA, Aldrich, 95%), pH buffer solution (pH1~5, Fluka) were used without further purification. Azobisisobutyrontitrile (AIBN, Aldrich, 98%) was recrystallized before use.

Instruments used for characterizing are ^{1}H and ^{13}C NMR spectra were recorded on a Bruker Avance 400 (400 MHz) spectrometer. Chemical shifts were referenced relative to residual solvent peaks in deuterated solvents, chloroform ($CDCl_3$) and deuterium oxide (D_2O). UV-Vis spectroscopy was performed on a Cary 50 UV-Vis absorption spectrometer with 1 cm path length quartz cuvettes at room temperature. GC-MS was performed using a HP 5890 GC-MS (Agilent DB-5ms column consisting of a fused silica capillary, 30 m length, 0.2 mm inner diameter and 0.325 μm film thickness) injecting 2 μL of dilute solution and ramping from room temperature to 350 °C.

Synthesis of crosslinkers are described as follow. CL2: Synthesis based on a literature procedure was followed and optimized.[7] In a 250 mL round bottom flask, 0.55 g of *p*TSA (2.91 mmol, 0.07 equiv.) were dissolved in THF and molecular sieves were then added to the solution. After 15 min, 13.53 g HEMA (104 mmol, 2.5 equiv.) and 4.3 g 2,2-DMP (41.6 mmol, 1 equiv.) were added and the mixture was stirred for 6 hours at room temperature. The reaction was quenched by adding ~3 mL TEA (pH > 7), the molecular sieves were removed by filtration and solvent was evaporated in vacuum. After removing solvent, the transparent liquid residue was purified by column chromatography with silica gel (ethyl acetate:hexane:TEA=10:90:1, v/v). The resulting product was obtained as a slightly yellow viscous oil (40% yield). ^{1}H NMR of CL2 (400 MHz, $CDCl_3$, TMS standard, r.t.): δ=6.10 (m; 2H), 5.55 (m; 2H), 4.26 (t; 4H), 3.69

(t; 4H), 1.93 (s; 6H), 1.37 (s; 6H).

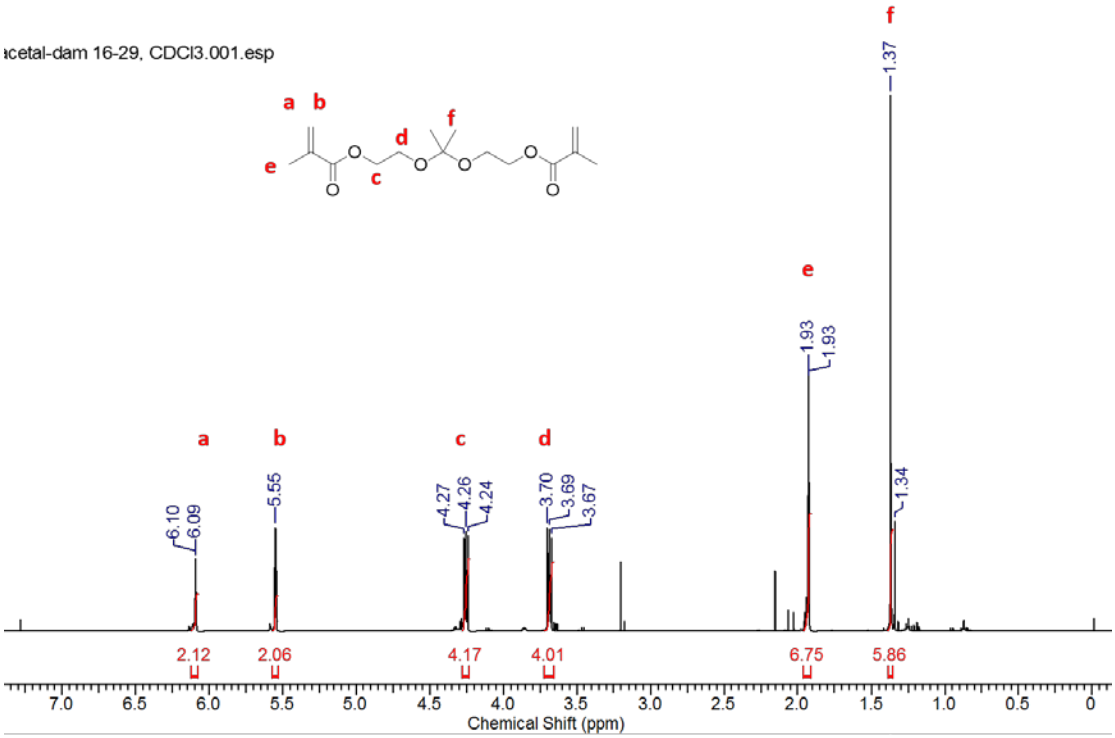

Figure 2.2 ^{1}H NMR of CL2

We utilized a similar procedure to synthesize CL3 as described above for CL2 except substituting 5 g PEG-MA (13.89 mmol, 2.3 equiv.) in place of HEMA. The reaction was quenched by adding with ~0.5 mL TEA (pH > 7) and the molecular sieves were removed by filtration and solvent was evaporated in vacuum. Product was obtained as a viscous yellow liquid. By comparing the integration ratio in ^{1}H NMR ($CDCl_3$) spectra it was confirmed that it is mixture of unreacted PEG-MA and CL3 (3.38:1). CL3, with the un-functionalized PEG-MA impurity was used without further purification

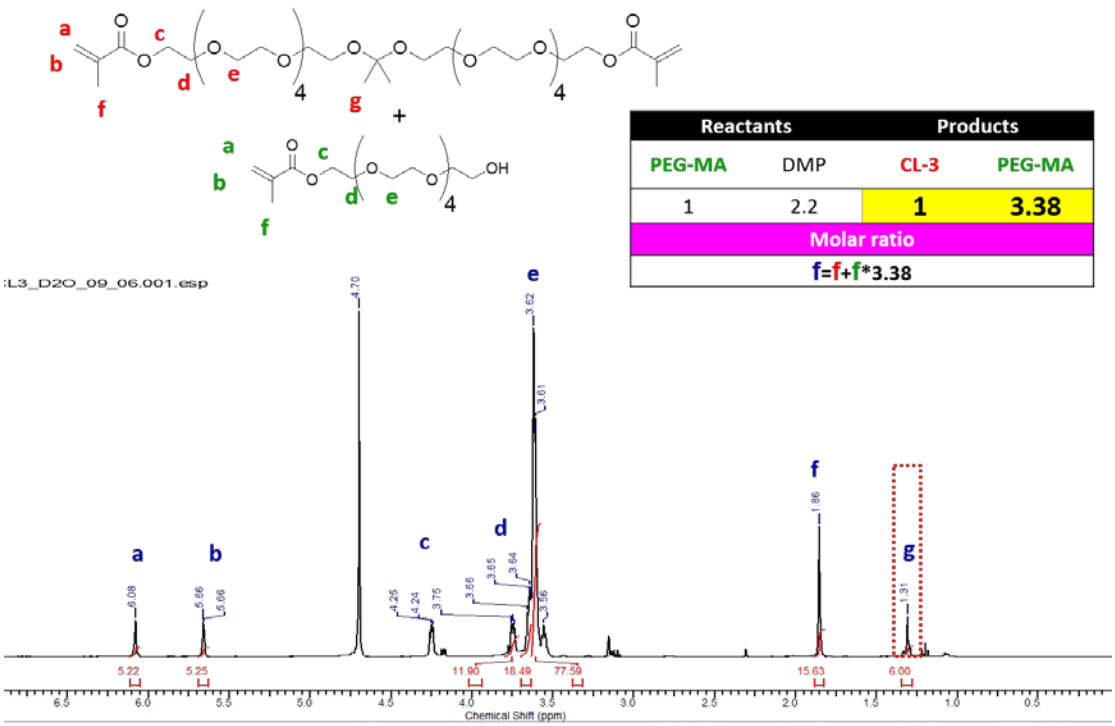

Figure 2.3 ^{1}H NMR of CL3 as prepared (a mixture of desired crosslinker CL3 and unreacted PEG-MA with 1 to 3.38 molar ratio)

*p*MBA or *m*MBA 5 g (36.7 mmol, 1 equiv.) and 19.1 g HEMA (146.8 mmol, 4 equiv.) were charged in a 100 mL round bottom flask and placed in an ice-bath in the presence of 0.49 g *p*TSA (2.57 mmol, 0.07 equiv.) and stirred over 4 Å molecular sieves for 6 hours. The reaction was quenched by adding ~1 mL TEA and the solution was diluted with tetrahydrofuran (THF) and molecular sieves were filtered. The crude product was purified by column chromatography with silica gel using a solvent mixture (hexane: dichloromethane: TEA = 85:5:10, v/v) as the eluent. The compounds CL4p and CL4m were both obtained as colorless transparent viscous liquid in approximately 35 % yield. ^{1}H NMR of CL4p (400 MHz, $CDCl_3$, TMS standard, r.t.): δ=7.4 (d; 2H), 6.9 (d; 2H), 6.12 (m; 2H), 5.65 (s; 1H), 5.57 (m; 2H), 4.33 (t; 4H), 3.81 (s; 3H), 3.75 (t; 4H), 1.95 (s; 6H), ^{13}C NMR of CL4p (100 MHz, $CDCl_3$): δ=167.25, 159.77, 136.15, 129.87, 127.94, 125.71, 113.58, 100.97, 63.70, 62.68, 55.24, 18.30, ^{1}H NMR of CL4m

($CDCl_3$): δ=7.29 (d; 1H), 7.04 (t; 2H), 6.87 (d; 1H), 6.12 (m; 2H), 5.65(s; 1H), 5.57 (m; 2H), 4.35 (t; 4H), 3.80 (s; 3H), 3.75 (t; 4H), 1.95 (s; 6H), ^{13}C NMR of CL4m (100 MHz, $CDCl_3$): δ=167.20, 159.67, 139.23, 136.14, 129.31, 125.69, 118.98, 114.18, 112.14, 100.89, 63.64, 62.85, 55.17, 18.27.

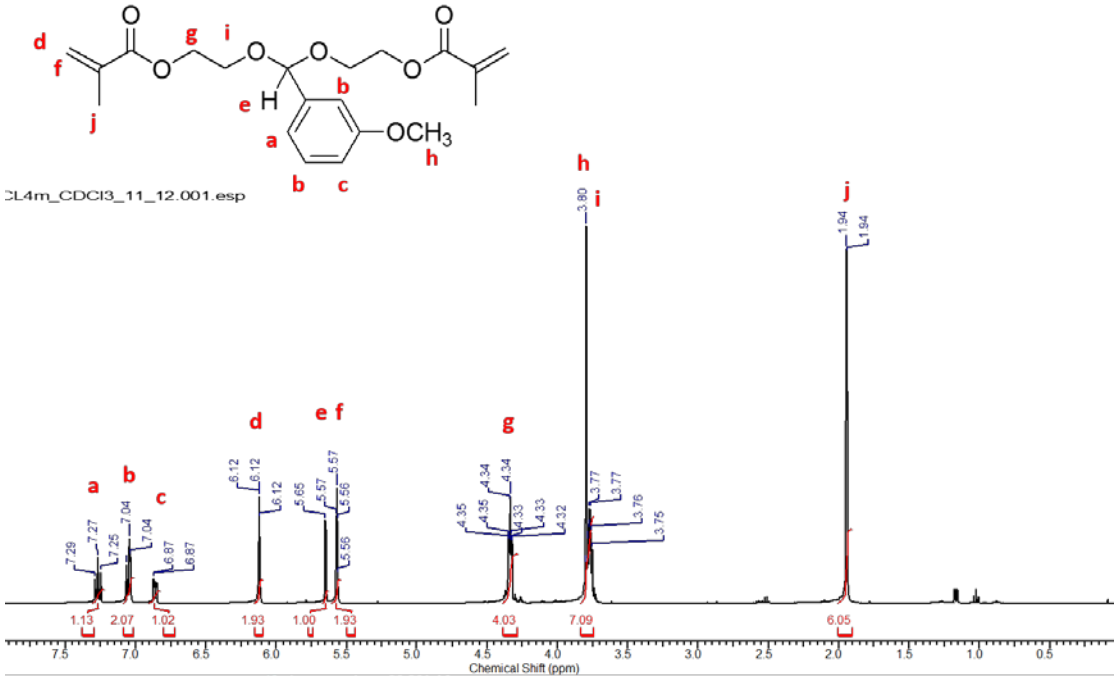

Figure 2.4 ^{1}H NMR of CL4m

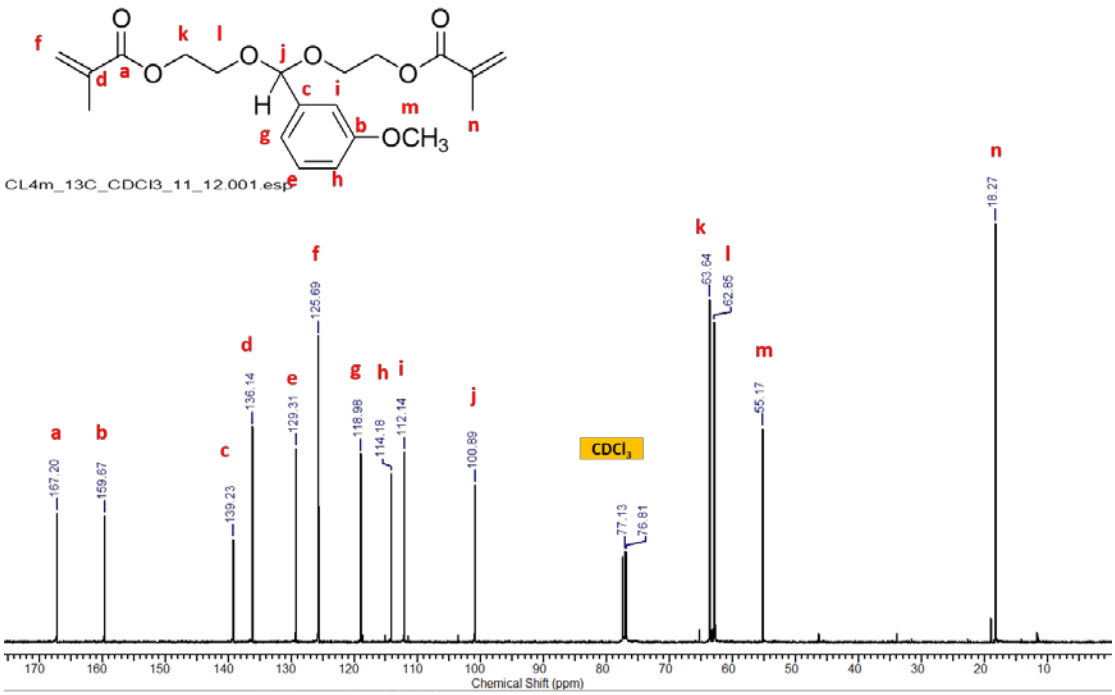

Figure 2.5 ^{13}C NMR of CL4m

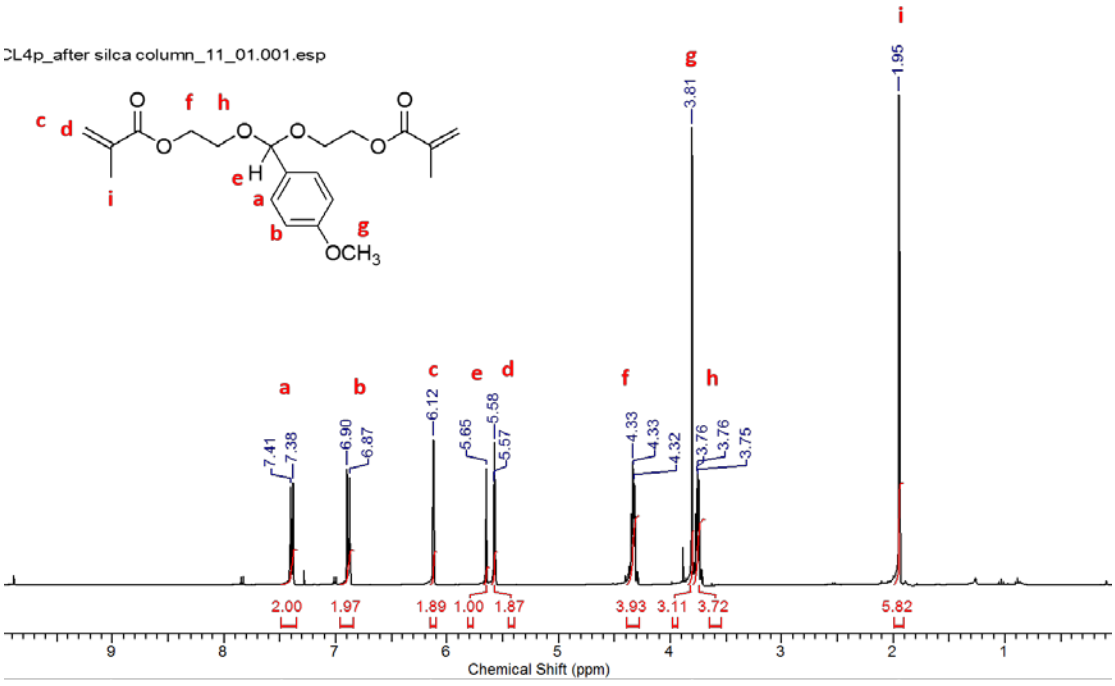

Figure 2.6. ^{1}H NMR of CL4p

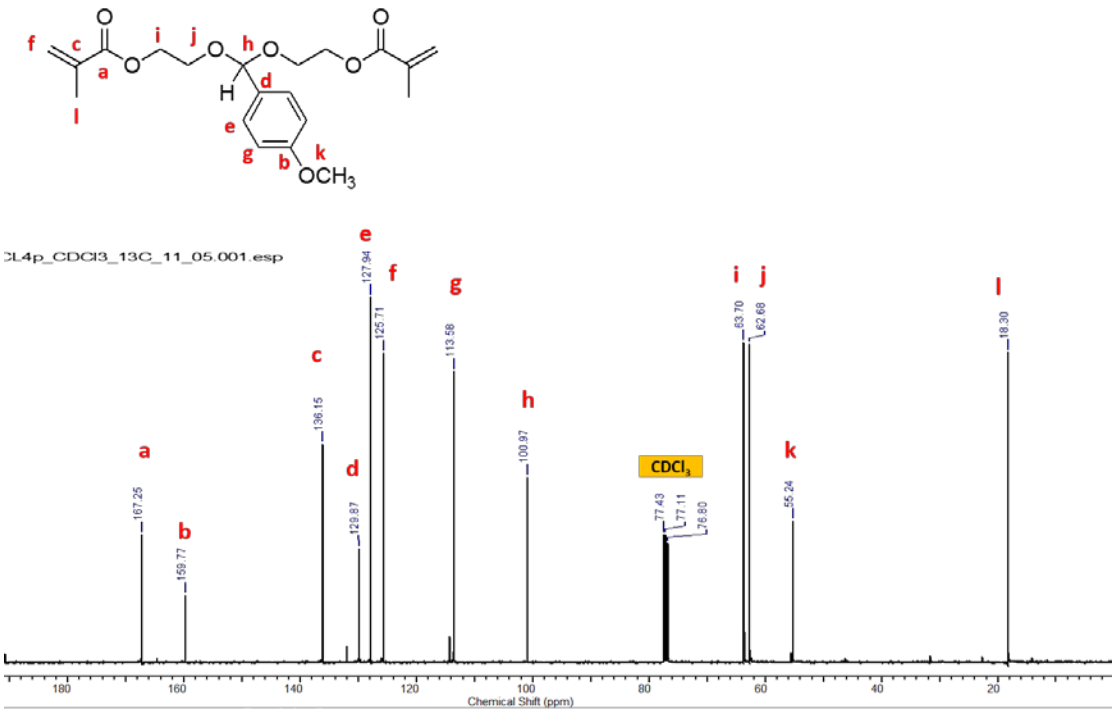

Figure 2.7. ^{13}C NMR of CL4p

A 40 mL round bottom flask fitted with a Dean-Stark trap filled with 25 mL of cyclohexane was charged with 3 g 5-hexen-1-ol (0.03 mol, 3 equiv.), 1.36 g *m*MBA (0.01 mol, 1 equiv.) and 0.02g *p*TSA (0.1 mmol, 0.01 equiv.), and 40 mL cyclohexane. The solution was refluxed at 100 °C for 18 hr and distilled water was periodically removed from the trap. After cooling to room temperature, the reaction was quenched by adding ~ 1mL TEA. The crude product was purified by column chromatography with silica gel using mixture of hexane: dichloromethane: TEA (85:5:10, v/v). as the eluent. V-CL4 was obtained as colorless transparent liquid (Yield: 80 %). ^{1}H NMR of V-CL4m (400 MHz, $CDCl_3$, TMS standard, r.t.): δ=7.3 (t; 1H), 7.07 (d; 2H), 6.89 (d; 1H), 5.84 (m; 2H), 5.50 (s; 1H), 5.0 (m; 2H), 3.84 (s; 3H), 3.58 (t; 4H), 2.09 (m; 4H), 1.64 (m; 4H), 1.51 (m; 4H)

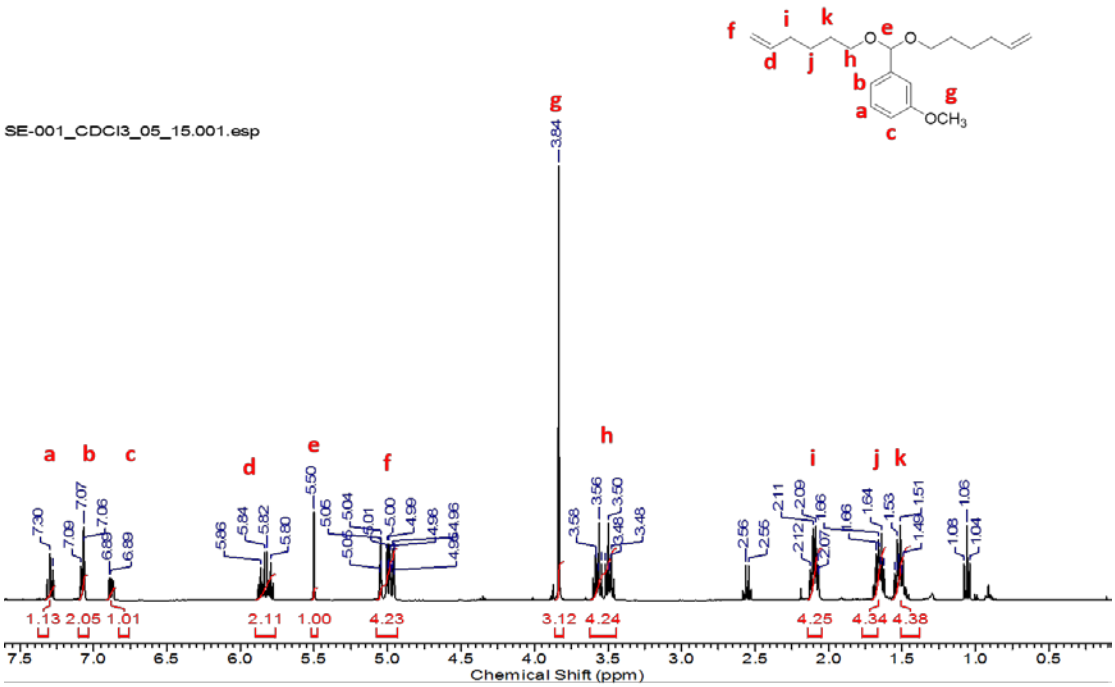

Figure 2.8 ^{1}H NMR of V-CL4m

2.3.2 Hydrolysis Kinetic Study by ^{1}H NMR: Water-soluble Crosslinker

If the molecule is water-soluble, hydrolysis kinetics will be straightforwardly achieved by observing ^{1}H NMR spectra with different time intervals. The phosphate buffer solution with specific pH in deuterium oxide (D_2O) can be prepared by mixing with a known volume of the primary salt solution and diluted with D_2O. Samples will be kept at room temperature in between measurements. The ratio of hydrolyzed molecule and intact molecule at time *t* will be determined by comparing the disappearance of the protons on acetal/ketal group, or appearance of protons of acetone or aldehyde from ^{1}H NMR spectra. The half-life of hydrolysis can be determined as $(ln2)/k_d$, where k_d is a negative value of the slope obtained by plotting $ln([M]_t/[M]_0)$ vs incubation time *t* where $[M]_t$ and $[M]_0$ are the relative peak integrations at time *t* and

initial time.

A stock solution of deuterium phosphate buffer solutions was prepared by mixing adjusters (see Table below) with a known volume of the primary salt solution and diluted to a total volume of 2 mL with D_2O. (KCl: potassium chloride, KHP: potassium hydrogen phthalate, DCl: deuterium chloride, NaOH: sodium chloride)

Table 1. Preparation of D_2O buffer solutions[20]

pH1	2.5 ml of 0.2 M KCl + 6.7 ml of 0.2 M DCl
pH2	2.5 ml of 0.2 M KCl + 0.65 ml of 0.2 M DCl
pH3	5 ml of 0.1 M KHP + 2.23 ml of 0.1 M DCl
pH4	5 ml of 0.1 M KHP + 0.01 ml of 0.1 M DCl
pH5	5 ml of 0.1 M KHP + 2.26 ml of 0.1M NaOH

2.3.3 Hydrolysis Kinetic Study by UV-Vis Spectroscopy

The pH-dependent hydrolysis can be studied by observing the increase of absorbance in the UV-Vis spectra corresponding to the generation and extraction of the aromatic aldehydes, *m*MBA or *p*MBA which are the product of hydrolysis. Absorbance can be measured at different time intervals for each of the pH buffered solutions and used to construct the kinetic plot and calculate the half-life ($t_{1/2}$) of hydrolysis. The kinetic plot was obtained by using following equation, where A_t, A_0, A_∞ are absorbance at time t, initial, and theoretical 100% hydrolysis, respectively.

$$-\ln\left[\frac{[Crosslinker]_t}{[Crosslinker]_0}\right] = = -ln\left[\frac{(A_\infty - A_t)}{(A_\infty - A_0)}\right]$$

2.3.4 Hydrolysis Kinetic Study by GC-MS: Insoluble Crosslinked film

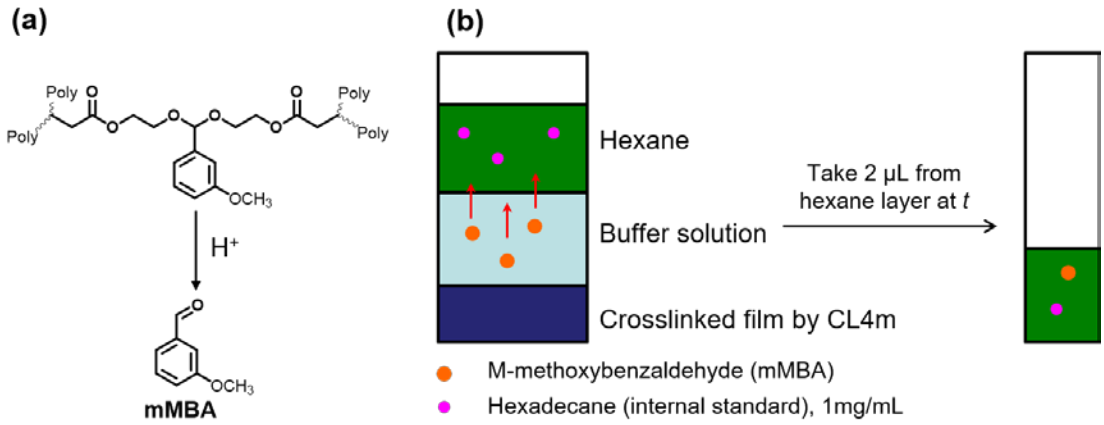

Figure 2.9 (a) Hydrolysis of CL4m-based networks and (b) schematic representation of network degradation experiment for the GC-MS study[20]

Crosslinked films can be prepared in 20 mL scintillation vials by thermally initiated polymerization of monomers and acid sensitive crosslinkers. In a typical polymerization, a vial is loaded with monomer, crosslinker and AIBN as an initiator which can be dissolved in a small amount of organic solvent. Polymerization can be accomplished by heating the vial to 60 ~ 90 °C for 20 min under N_2. After polymerization the crosslinked polymer formed a film in the bottom of the vial. The films are rinsed with hexane several times to extract unreacted monomers and any mMBA that may have formed during the reaction. The films are dried under vacuum at room temperature to remove residual ether. To study network hydrolysis, each vial was filled with pH buffer solution to trigger acidic hydrolysis and hexane to which 1 mg/mL of hexadecane (as an internal standard) will be added. Released mMBA from hydrolysis of network will be only molecule that diffuses into hexane layer. At prescribed times, 2 µL of the hexane phase will be taken by syringe and analyzed by GC-MS. In the case of thiol-ene crosslinked films between V-CL4m and pentaerythritol tetrakis(3-

mercaptopropionate) (2:1 molar ratio), the polymerization was conducted under N_2 using UV irradiation (365 nm) without initiator for 15 min. The exact film compositions are shown in the **Table 2**.

Table 2. Acid-degradable film compositions (molar ratio), hydrolysis solution pH, and $t_{1/2}$ of crosslinker.

Monomer	**Crosslinker**	**pH**	**$t_{1/2}$ (hr)**
HEMA	CL4m		
30	1 (3.2 mol%)	5	Non-measurable
		4	533 hr
		3	160 hr
		2	33 hr
		1	25 hr
10	1 (9 mol%)		125 hr
1	1 (50 mol%)		521 hr
0.5	1 (66 mol%)		713 hr
MMA	CL4m		
30	1 (3.2 mol%)	1 ~5	No degradation observed
4-thiol	V-CL4m		
1	2 (66 mol%)	5	837 hr
		4	460 hr
		3	106 hr
		2	45 hr
		1	25 hr

To study network hydrolysis each vial was filled with pH buffer solution (2 mL) and 2 mL of hexane to which 1 mg/mL of hexadecane (as an internal standard) had been added. At prescribed times 2 μL of the hexane phase were taken by syringe and analyzed by GC-MS. For quantitative study, calibration curve of releasing molecule with internal

standard was constructed.

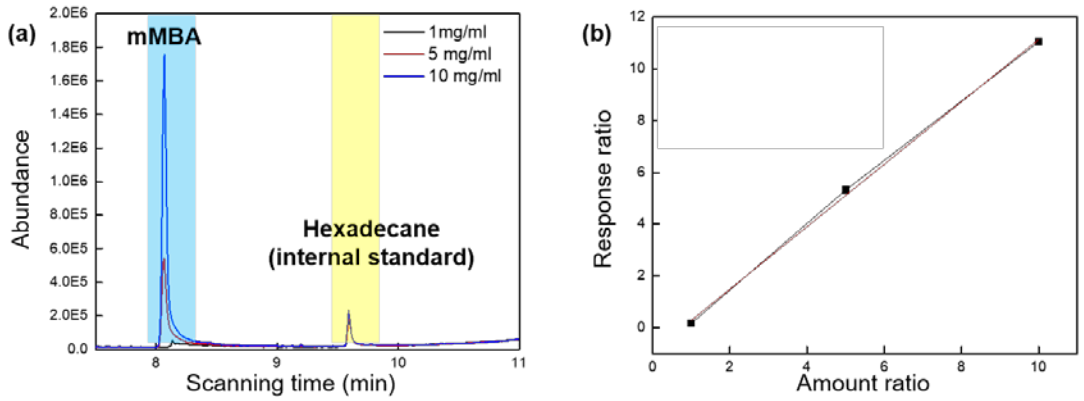

Figure 2.10. GC-MS from mixture of mMBA and hexadecane (internal standard) in hexane (a) and calibration curve (b): To construct calibration curve, each solution contains different concentration of mMBA with same concentration of internal standard (hexadecane). From the GC-MS, calibration curve can be built from response ratio between two molecules vs amount ratio from concentration ratio[20]

2.4 Results and Discussion

2.4.1 Acid-sensitive crosslinkers

The ketal crosslinkers were synthesized by reacting 2,2-dimethoxypropane (DMP) with either HEMA (yielding CL2) or PEG-MA (average M_n: 360 g/mol) (yielding CL3) in the presence of a catalytic amount of *p*TSA with or without solvent. The acetal crosslinkers were made by condensing HEMA with either *p*MBA (yielding CL4p), or *m*MBA (yielding CL4m) with acid catalysis. In the case of V-CL4m, 5-hexen-1-ol was condensed with *m*MBA. In all cases care was taken to remove either the methanol or water formed during the reaction thereby favoring the formation of product and reducing the back reaction. Water removal was accomplished by performing the reaction over dried molecular sieves or through in situ distillation of water or methanol and removal using a Dean-Stark trap to increase yield. In the case of distillation, we

note that raising the reaction temperature to the boiling point of methanol or water sometimes led to an undesirable polymerization of the monomers, especially in the case of the methacrylates, giving a low yield of product. During purification by column chromatography, the slightly acidic silica gel led to undesirable hydrolysis, but this could be avoided by adding small amount of TEA to the eluent. For similar reasons, after column purification, it is very important to avoid evaporating the solvent at high temperature as this also leads to decomposition of the product. The monomers were kept at 0 ºC to prevent degradation or polymerization before use.

CL3 is so sensitive to hydrolysis and hydrophilic due to the PEG content that no purification was attempted after quenching the reaction with TEA and the only post-reaction processes were removal of salts and molecular sieves by filtration. ^{1}H NMR analysis reveals that the ratio of PEG-MA and CL3 was 1: 3.38. This ratio was determined by comparing integration ratio of methacrylate CH_3 (δ=1.9) and acetal CH_3 . The methacrylate-based crosslinkers (CL2, CL4m, CL4p, and CL3) were all isolated in low yields (20 ~ 40 %) which is inevitable due to insufficient removal of water or methanol during the reaction. However, the starting materials are not very expensive. Work continues to find ways of increasing the yields which would be especially useful when using more expensive or less available starting materials. It was also challenging to isolate the acetal products from residual mMBA or pMBA by column chromatography due to the very close R_f values of each material. The exception was V-CL4m which was synthesized in the same manner as the other monomers except we were able to employ a Dean-Stark and run these reactions at a higher temperature to

remove water instead of using molecular sieves. This effective water elimination gives higher yield (80%) compared to low temperature reaction in the presence of molecular sieves. The resistance of 5-hexen-1-ol and V-CL4m to undergo undesired thermal polymerization at elevated temperatures was important. V-CL4m was used for crosslinked films with multi-functional thiol monomers using the thiol-ene reaction and their degradation kinetics were compared to the other methacrylate-based crosslinked films.

2.4.2 Kinetics of hydrolysis of CL3 by ^{1}H NMR

We wish to gain an understanding of the kinetics of acid hydrolysis of the acetal-based crosslinkers in the water-based buffer solutions at certain pH ranges. Our interest stem from reports of the use of similar network materials under physiological conditions, a similar temperature range needed for garment applications. The hydrolysis of the HEMA-based CL2 monomer was difficult to study in aqueous buffer solutions due to its water-insolubility. To improve water solubility of the crosslinker, PEG-MA (360 g/mol) was used to prepare the acetal CL3, using 2,2-DMP instead of HEMA during the condensation. Both CL2 and CL3 share the same acetal linking group structure.

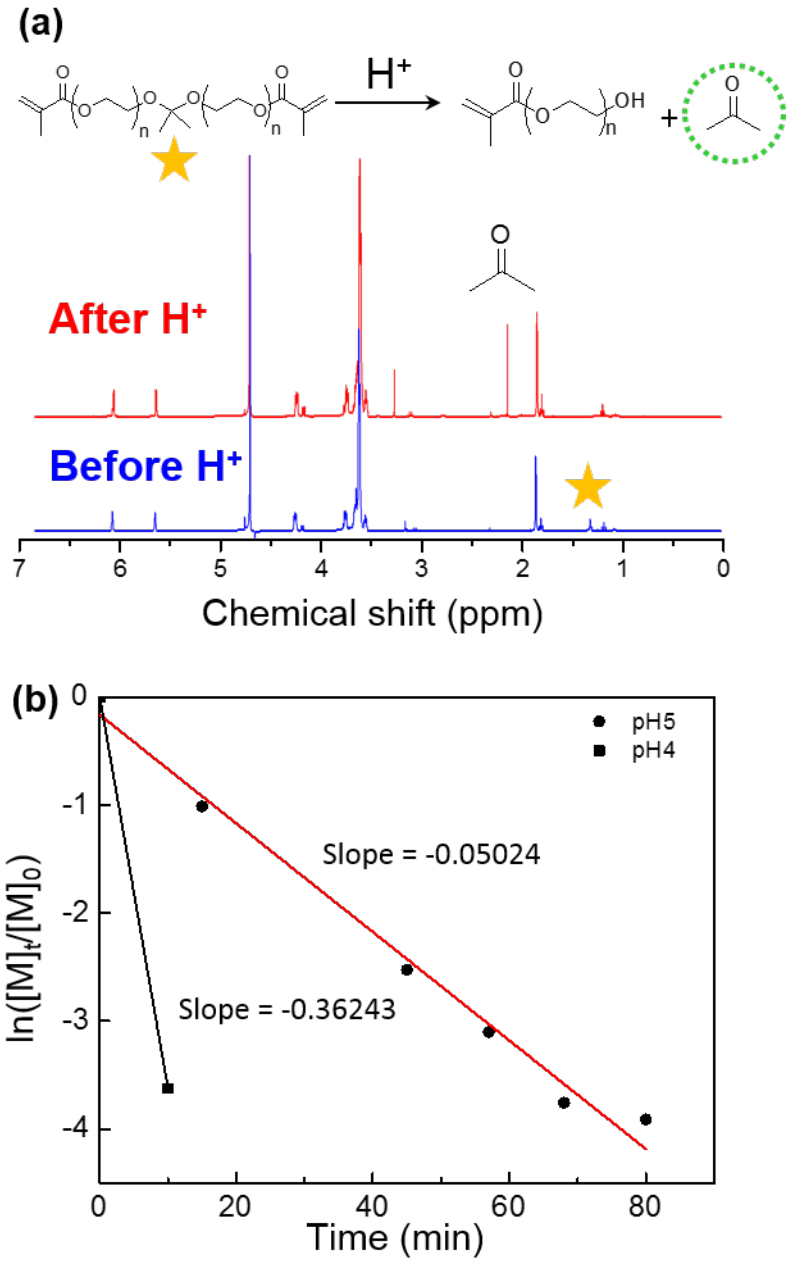

Figure 2.11 Acid catalyzed degradation of CL3: (a) ^{1}H NMR spectra before and after degradation, and (b) the corresponding hydrolysis kinetics at pH 4 and 5 versus time[20]

The ^{1}H NMR degradation study of the water soluble crosslinker CL3 was conducted using a phosphate buffer solution made using deuterium oxide (D_2O) with a range of pH from 1 to 5 and confirmed using a pH meter. Although a ^{1}H NMR kinetic study of CL2 wasn't conducted because of its low solubility, it can be expected that CL2 and CL3 would have different degradation profiles because the polarity of overall structure

will affect the hydrolysis rate, and given that more hydrophilic backbones will have a higher hydrolysis rate compared to a more hydrophobic one due to solvation effects. As an initial state (t=0), ^{1}H NMR was conducted by using pure D_2O at room temperature. $[M]_t$ and $[M]_0$ are the molar concentration of ketal function at time *t* and initial time, respectively, which were obtained using the integration of value of CH_3, δ=1.31 (s; 6H) (***Figure 2.11***). The size of ^{1}H NMR peaks were monitored over time and hydrolysis rates generally increased with decreasing pH. As shown in ***Figure 2.11***b, CL3 completely decomposed in 80 minutes ($t_{1/2}$ < 14 min) at pH 5 and 10 min ($t_{1/2}$ < 2 min) at pH 4. At pH 1~3, the hydrolysis was too rapid to measure by NMR as there were no observable acetal peaks to be found in the spectra. Given the time required to prepare the samples and start the NMR experiment, it is assumed that hydrolysis in these strongly acid solutions takes place in under 1 ~ 2 min. Lowering the pH results in an acceleration of the hydrolysis kinetics as the rate of acetal hydrolysis is proportional to the hydronium ion concentration. For some applications this rate at low pH may be too rapid, therefore, to reduce the hydrolysis rate, acetals based on benzaldehyde, CL4m and CL4p, were synthesized and their degradation kinetics were also investigated.

2.4.3 Degradation study of CL4m and CL4p by UV-Vis spectroscopy

Unlike CL3, the benzaldehyde-based acetals CL4m and CL4p are non-polar and insoluble in the water-based buffer solution, however, both crosslinkers generate *m*- or *p*-methoxybenzaldehyde as a result of acetal hydrolysis, which show strong UV absorbance around 300 nm. Even using a low concentration of crosslinker (0.016 μL/mL), it was possible to detect small amounts of mMBA or pMBA released into

buffer solutions. Samples were prepared in quartz UV cuvettes and studied in real-time by observing changes in absorption between 280 to 320 nm (the maximum peak values varied slightly based on the buffer pH). All the UV-Vis spectra taken are provided in **Figure 2.12**. and **Figure 2.13**. For each experiment absorbance was measured at different time intervals. It was expected that using a substituted aromatic ring with an electron donating methoxy group in the acetal position would reduce the hydrolysis rate compared to CL3. Depending on the methoxy substituent position, *meta* or *para*, hydrolysis rates were also different. The kinetic plots corresponding to CL4m (a) and CL4p (b) are shown in **Figure 2.14** and both show accelerated hydrolysis at lower pH. Using initial slope at each pH, the half-life of hydrolysis for samples was calculated and both CL4 derivatives show a much slower rate of hydrolysis compared to CL3 across all pH ranges. At pH 1, there is no discernable difference measured between CL4m and CL4p (~4 min), while at pH 2~4, CL4m has a slightly longer half-life. This tendency is well matched with the observed trend that acetals (structures based on aldehydes) undergo slower hydrolysis than ketals (based on ketones) due to the absence of the second electron-donating methyl group to stabilize the carbocation intermediate during the hydrolysis.

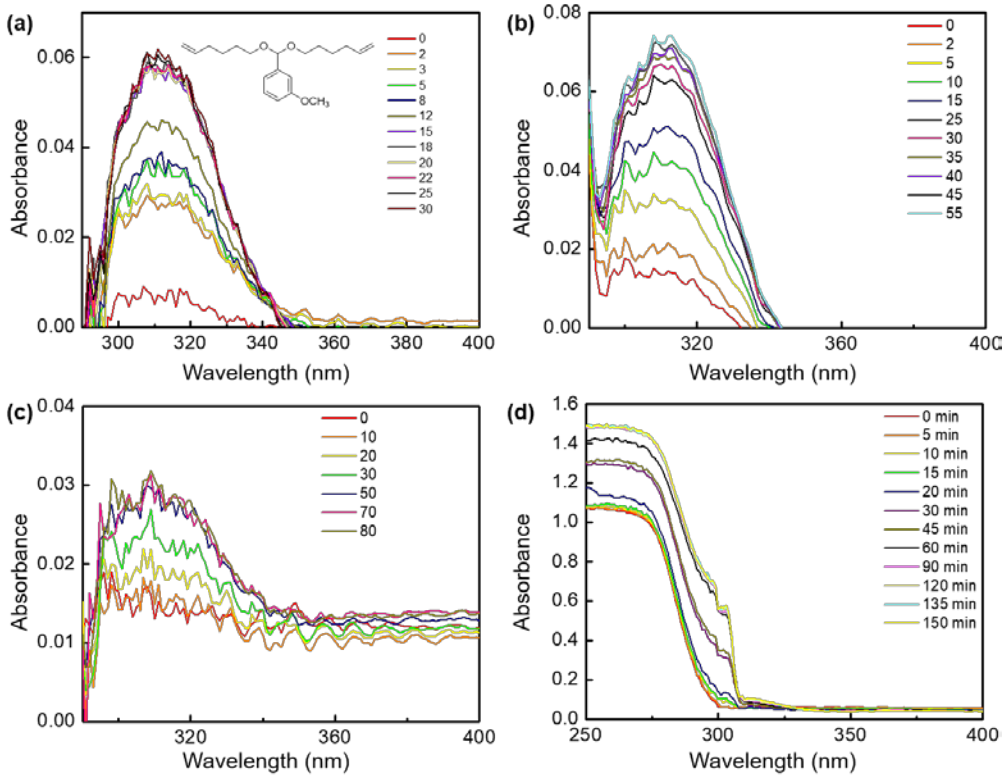

Figure 2.12 UV-Vis spectrum: Generation of mMBA during hydrolysis of CL4m (a) pH 1; (b) pH 2; (c) pH 3; (d) pH 4

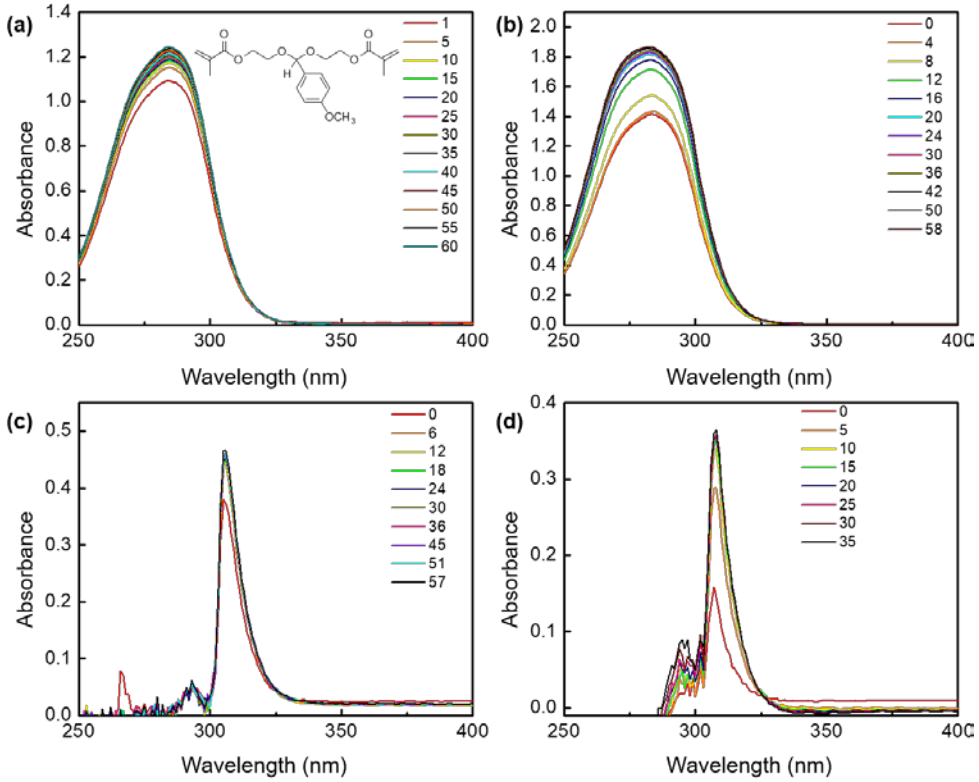

Figure 2.13 UV-Vis spectrum: Generation of mMBA during hydrolysis of CL4p (a) pH 1; (b) pH 2; (c) pH 3; (d) pH 4

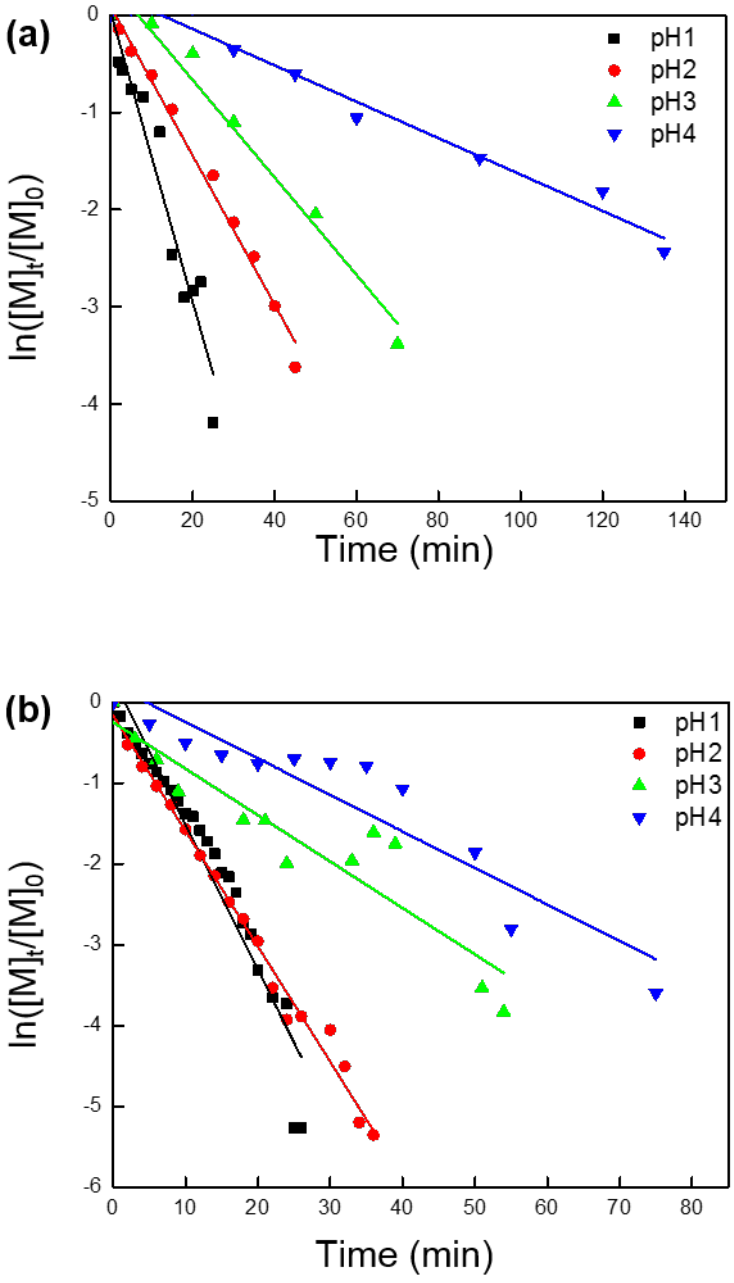

Figure 2.14 Acid catalyzed degradation of (a) CL4m and (b) CL4p at pH1, 2, 3 and 4.

2.4.4 GC-MS degradation study of network films crosslinked by acetals

For the desired application of a reactive, self-exfoliating film, reasonable degradation rates are desired, and it is important to investigate the hydrolysis rate of the network films and solve for variables such as pH, co-monomer compositions, and crosslinking densities. In order to perform continuous measurement of network degradation we chose to look for small molecule fragments released upon hydrolysis of the acetal functionality. Crosslinked films were prepared by thermally initiated radical polymerization of methacrylate-based monomers and crosslinker CL4m. In the case of thiol-ene crosslinked films synthesized by the reaction of V-CL4m and pentaerythritol tetrakis(3-mercaptopropionate), polymerization was conducted under N_2 without initiator under UV irradiation for 15 min. Based on the determined degradation kinetic of the five crosslinkers synthesized, CL4m looked the most promising due to its reasonable hydrolysis rate below pH 4. When using the same crosslinker to make bulk network films, degradation rates were dictated by a combination of pH, hydrophilicity of co-monomers, and the total crosslinking density. Due to the need to detect small amounts of degradation product when monitoring network degradation, we chose GC-MS analysis. To accomplish this, we carried out hydrolysis in aqueous media and extracted the resulting *m*MBA into hexane. A known amount of hexadecane was added to the hexane solution as an internal standard. The overall experiment is outlined in **Figure 2.9**. These experiments make some assumptions that lead to a degree of error in the measurement, such as the assumption that all mMBA generated from the hydrolysis

of the acetal group would be quantitatively extracted into the hexane layer. We also assume that the CL4m monomer was completely incorporated during the network polymerization and is quantitatively present in the crosslinked films. The calculated mass fraction of mMBA is 36 wt% in the CL4m network or 42 wt% in the V-CL4m networks. A calibration curve was made using standard solutions of mMBA by plotting response ratio versus amount ratio (**Figure 2.10**). The response ratio is defined as ratio of area of the mMBA peak and area of the hexadecane (an internal standard) peak. Amount ratio is defined as ratio of amount of mMBA and amount of hexadecane.

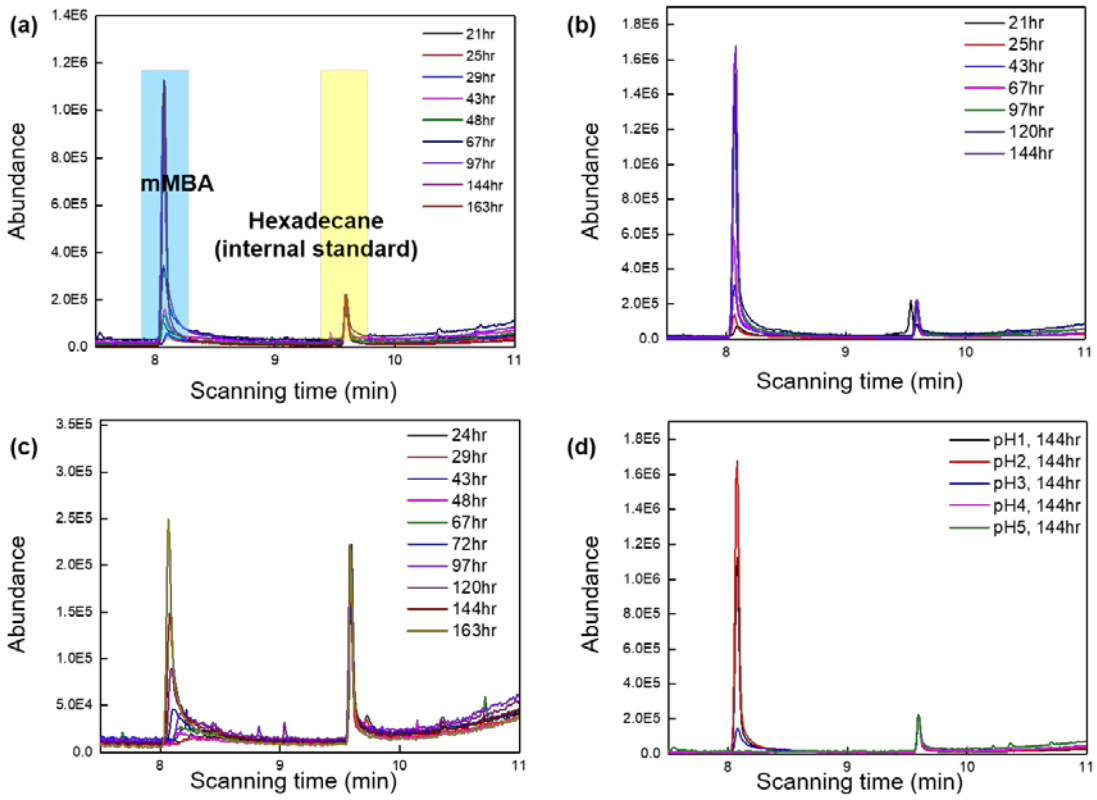

Figure 2.15 GC-MS of degradation of HEMA crosslinked films (3.2 mol% of CL4m): (a) pH 1; (b) pH 2; (c) pH 3; (d) combined results after 144 hr. Scanning time means retention time.

In the case of crosslinked films composed of HEMA and CL4m (30:1 molar ratio - 3.2 mol% of CL4m), $ln([M]_t/[M]_0)$ in different pH buffers was plotted as a function of exposure time and the half-lives were determined (**Figure 2.16**). The rates of hydrolysis were slow, mMBA was not detected for the first 21hr when reacted at pH1 and pH2. A small amount of hydrolysis may have started before this time but detectable amounts of mMBA extracted into hexane were detected by GC-MS only after 21hr. Still, the plots show an increase of mMBA over time. As the acidity of the solutions was reduced, the hydrolysis dropped precipitously and even after 8 days, we were unable to detect any mMBA at pH5. This indicates that these crosslinked films have much slower degradation rate at pH 5 compared to pH 1-4. The first order reaction plots were constructed (**Figure 2.16**) and corresponding half-life time at each pH was obtained using initial slope. The calculated half-lives were 25 hr, 33 hr, 160 hr and 533 hr at pH1, 2, 3 and 4 respectively. These results make it clear that the hydrolysis rates of the acetal groups are much slower after incorporation into networks.

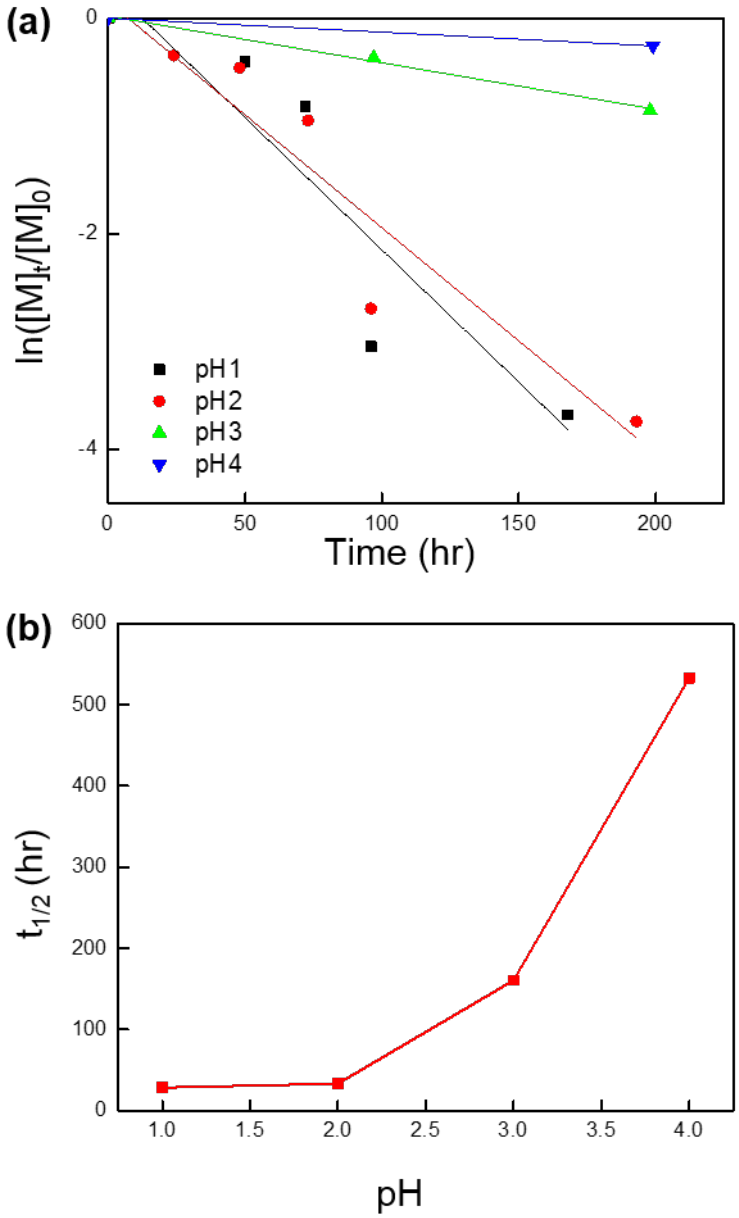

Figure 2.16 (a) Plot of $\ln([M]_t/[M]_0)$ in different buffer solutions versus incubation time and (b) plot of the half-life of crosslinkers (CL4m) in the network as a function of pH

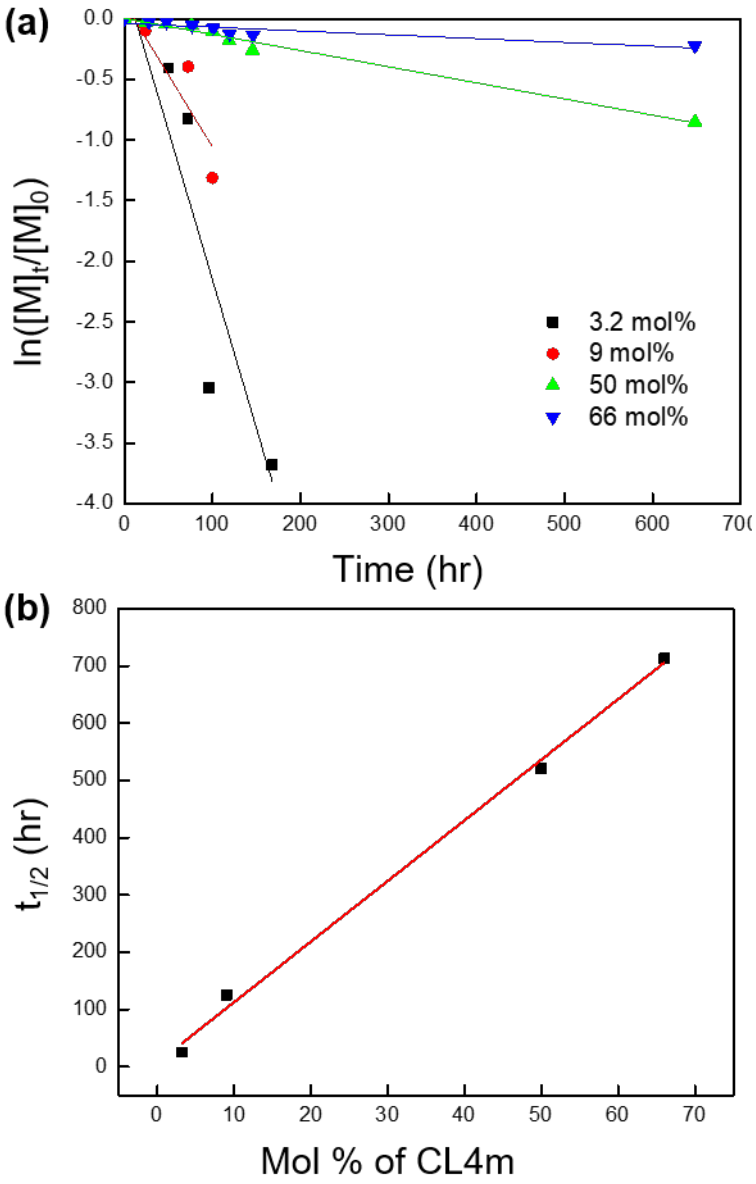

Figure 2.17 (a) Plot of $\ln([M]_t/[M]_0)$ for networks with different crosslinker concentration versus incubation time and (b) plot of the half-life of crosslinkers (CL4m) in the network as a function of crosslinker concentration.

Interestingly, if the same CL4m crosslinker concentration is used, but the commoner is MMA rather than HEMA, the resulting networks fail to show any measurable hydrolysis (**Figure 2.18**). This is because MMA imparts a much more hydrophobic nature to the network slowing diffusion of aqueous buffer and hence lowering the observed rate of hydrolysis. Control of rate of hydrolysis should be selectable by

controlling the relative amounts of hydrophilic or hydrophobic comonomers in the network.

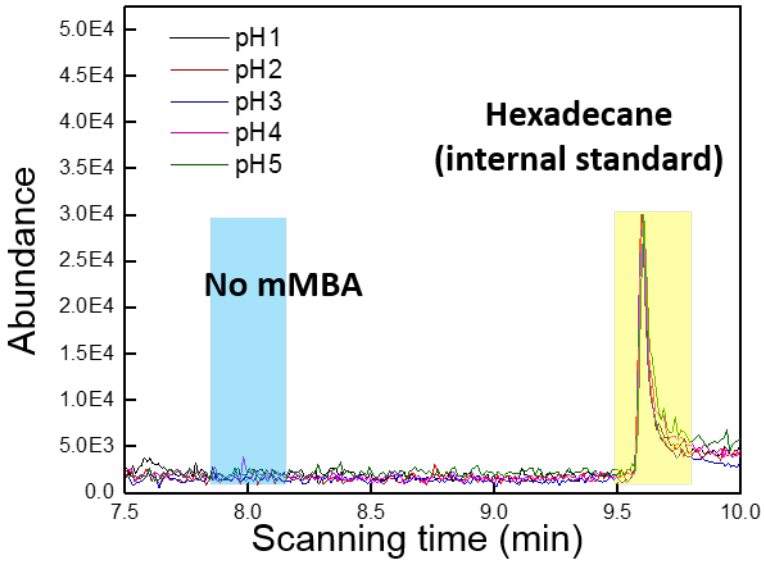

Figure 2.18 Acid degradation study of hydrophobic crosslinked MMA films by CL4m at different pHs

Another variable that can be adjusted to control hydrolysis rate is crosslinking density (**Figure 2.17**). The crosslinking density can be increased or decreased by varying the concentration of CL4m used in the polymerization. The rate of hydrolysis as a function of crosslinking density was examined in pH1 buffer solution. The half-life of hydrolysis for each film was 25 hr, 125 hr, 521 hr and 713 hr at 3.2 mol%, 9 mol%, 50 mol% and 66 mol%, respectively. As expected, the more densely crosslinked films show much slower hydrolysis rate. The buffer solution penetrates, swells, and diffuses much more slowly in the more densely crosslinked films. The half-life of acetal hydrolysis was found to be linearly proportional to the mol% of CL4m in the films.

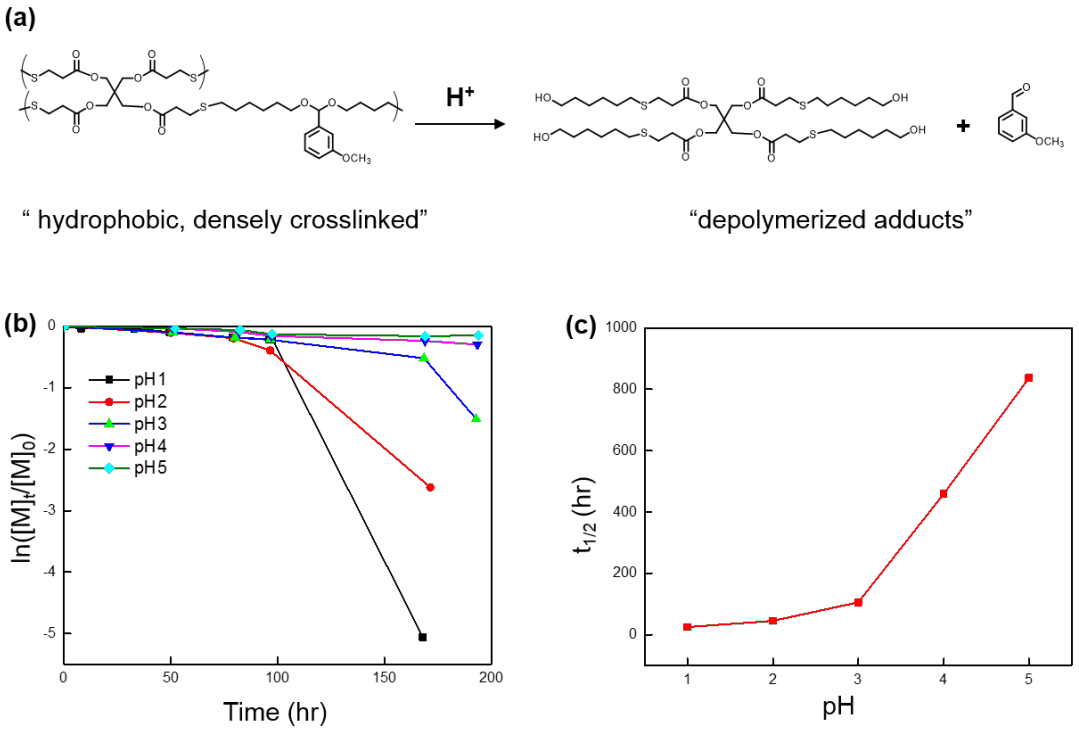

Figure 2.19 Thiol-ene networks: (a) hydrolysis of thiol-ene based networks, (b) plot of $\ln([M]_t/[M]_0)$ in different buffer solutions versus incubation time and (c) plot of the half-life of crosslinkers in the network as a function of pH.

All the networks described to this point were made through free radical chain polymerization processes. We wished to explore step-growth polymerized crosslinked films where the thiol-ene bond formation proceeds via the radical addition reaction between the divinyl monomer (V-CL4m) and a tetra-functional thiol crosslinker (PTMPA). To maximize molecular weight, thiol-ene step-growth polymerization mechanism requires exact stoichiometry between available ene groups and thiol groups. In the case of V-CL2m, 66 mol% is required (33 mol% PTMPA). The crosslinked reaction was facilitated using UV curing (365 nm) without initiator under N_2 at room temperature. After initiation, the reaction proceeds quickly yielding solid, network films. Subsequent acid catalyzed hydrolysis of this resin results in depolymerization and the formation of mMBA (transparent liquid) and a four-armed, star alcohol,

pentaerythritol tetrakis(3-(6-hydroxyhexylthio) propanoate) (888.42 g/mol) (***Figure 2.19***). Unlike methacrylate-based crosslinked films which retain their shapes during the hydrolysis, we could observe a transition to a viscous flowing material during the hydrolysis of the thiol-ene network. The presence of mMBA in the hexane phase was confirmed by GC-MS, which was used to examine hydrolysis kinetics.

The degradation kinetics of the thiol-ene crosslinked films were examined at different pH ranges. Compared to HEMA-based networks, the thiol-ene crosslinked films are more hydrophobic due to absence of free hydroxyl groups, or PEG-like segments in the network and a relatively larger portion of alkyl chains. The thiol-enes are also densely crosslinked, hindering swelling and diffusion of buffer solution. At pH 1 and 2, physical decomposition of the films was visually observed, and parts of the region began to flow after 96 hr in buffer. The half-life at each pH was obtained (***Figure 2.19*** c). The half-life of the acetal group at pH 1, 2, 3, 4 and 5 is 25 hr, 45 hr, 106 hr, 460 hr and 837 hr, respectively. The thiol-ene networks had a much shorter $t_{1/2}$ as compared to the HEMA/CL4m films at pH1 ($t_{1/2}$ = 713 hr) even they have same mol% of crosslinker. Essentially all decomposition during hydrolysis of the thiol-ene polymers converts high molecular weight polymer chains directly to low molecular weight residues, a tetra-functioned molecule and mMBA (**Figure 2.19** a). This results in increased diffusion and permeation of buffer solution, which in turn, continues to increase the rate of depolymerization. Conversely, the HEMA/CL4m films still have partially crosslinked or entangled linear polymer during the hydrolysis because the polymer interconnected structure that was formed via chain-growth polymerization

contains a broad range of number of repeat units between crosslink junctions. We propose that this difference results in the faster hydrolysis observed in the hydrophobic thiol-ene crosslinked films with at the same crosslinker mol%. The vinyl terminated monomer V-CL4m has merits since it can be synthesized in high yield, however, it cannot be utilized in conventional free radical polymerizations due to the low reactivity of the vinyl group. Therefore, its use in network formation is limited to reactions such thiol-ene step polymerization. Hence, selection of appropriate thiol comonomers becomes important and in this study only one was used. This leaves room for improvement in this area and is currently under investigation.

2.5 Conclusion

Through various acid-sensitive acetal and ketal-based groups with different substituents and adjusting the degree of hydrophilicity of the crosslinker unit, we demonstrate chemically tuned molecules that show different room temperature hydrolysis rates at different pH ranges. In the case of 2,2'-DMP-based acetal groups, CL3 revealed the highest acid-sensitivity ($t_{1/2}$ < 14 min at pH 5 and $t_{1/2}$ < 2 min at pH 4). Acetal functional groups based on *meta* or *para* methoxybenzaldehydes (CL4m or CL4p) gave crosslinkers with a reduced hydrolysis. By polymerizing CL4m various comonomers (HEMA or MMA), networks were synthesized, and their hydrolysis rates were measured as a function of pH, network hydrophobicity, and crosslinking density. When the vinyl-terminated crosslinker (V-CL4m) was reacted with a tetrathiol, thiol-ene networks were prepared. This densely crosslinked, hydrophobic polymer exhibited

a much faster hydrolysis rate than HEMA/CL3 based networks with a comparable crosslinking density. These materials are being studied as coatings for protective garments resistant to chemical warfare agents. This basic study of hydrolysis and degradation kinetics of acid-sensitive monomers and networks provides parameters needed to use these materials as stimuli responsive materials. A companion study currently underway in collaboration with the US Army Natick Soldier RD&E Center is examining the kinetics of neutralization of chemical warfare agents within these networks and the moisture vapor transport properties of thin network films. These materials may have additional utility in controlled release applications, advanced patternable resists and several other areas where such control of network stability is desired.

CHAPTER 3

CCREACTIVE POLYMERS WITH NUCLEOPHILIES FOR NEUTRALIZING ORGANOPHOSPHATE-BASED NERVE AGETNS

3.1 Introduction

Since the discovery of severe toxicity in pentavalent organophosphorus (OP) compounds led to development of insecticide as well as weapon of mass destruction (nerve agents), studying the detoxifying of OP-based nerve agents at ambient conditions have been priority.[21,22] Both nerve agents and insecticides act as phosphorylating agents, reacting with the serine moiety of the enzyme, known as acetylcholinesterase.[23] They irreversibly inhibit regulation of the *in vivo* concentration of neurotransmitter acetylcholine resulting in major effects on the nervous system.[24,22] There are various ways to destruct or demilitarize OP-based toxins such as photolysis, oxidation, combustion and microbial degradation.[21-45] The mildest way to detoxify toxic OP-based compounds at ambient condition is nucleophile-assisted hydrolysis reaction which can chemically convert toxins to non-toxic compounds.[24,45] Various nucleophilic functional groups such as oximates, hydroxamates, peroxyanions, and iodosylcarboxylates have been employed to demonstrate their catalytic effect on neutralizing OP-based compounds using real agents or their simulants by incorporating polymers, colloids, micelles or NPs. [21,23,26,27,30–33,35,36] When detoxifying reaction happens in the aqueous medium, the nucleophilic reactivity can be enhanced by forming

a micelle which is capable of increasing the rate of bimolecular reactions by incorporating and concentrating both reactants and solvent in the interfacial region of the colloidal species, which is treated as a reaction region distinct from water, i.e., a pseudo-phase.[40] To produce a protective clothing, we may consider blending nucleophilic-based catalysts with polymer by dispersing them in the polymer coating or forming a covalent bond with polymer. [21,23,26,32,33,35,36,43] There are other nucleophiles (or Lewis acid) such as metal complexes and metallomicelles which is based on transition or lanthanide-metal cations and their complexes.[34,37] Even though their catalytic reactivity is much stronger than organo-based nucleophiles, it is challenging to retain their outstanding reactivity driven from unique surface chemistry and porosity when embedding them in polymer coating.[34,37]

Regarding the choosing of nucleophilic functional groups for protective garment applications, several requirements are necessary. First, nucleophilic catalyst retains strong reactivity to decontaminate OP compounds in several minutes at ambient conditions. Second, the nucleophile should not be corrosive as peroxides, which is capable of damaging organic-based fabrics or human's skin. Also, it should be stable until exposed to targeting toxins. For example, peroxide or alkoxide reveals strong nucleophilic reactivity but are very unstable in atmosphere.[22,38] Given the incorporation of organo-based nucleophilic functional groups within the polymeric system, we may consider some reaction conditions. The nucleophilic hydrolytic reaction needs aqueous medium or humidified state because water eventually triggers neutralization of OP-based compounds. This suggests developing hydrogel type of polymers which can

preserve enough moisture for hydrolytic reaction.[26,36] The moisture can be provided from human's sweat and atmosphere. Since reactive nucleophilic polymers will be coated on or functionalized from fabrics, moisture vapor transmission rate (MVTR) of fabric may decrease resulting from blocking pores in fabric. This problem may be resolved by controlling coating thickness, chemistry (hydrophilicity) and morphology of polymer layers. OP-based nerve agents containing halogens (F or Cl) generate an acid as a byproduct after nucleophilic hydrolysis reaction. This acid can slow down detoxifying reaction by decreasing overall pH since organo-nucleophiles can enhance reactivity through deprotonation in basic buffer solution (pH>8). For protective clothing applications, this acid should be consumed to promote or maintain OP-neutralization reaction rate

3.2 Project Goal

- ✓ Perform neutralization kinetic studies using OP-based nerve agent simulants to determine the most effective organo-based nucleophile.
- ✓ Design a self-exfoliating layer composed of hydrophilic polymers and nucleophilic functional groups and acetal/ketal-based acid-sensitive crosslinkers.
- ✓ Evaluate decontamination of OP-based nerve agents using nucleophilic polymers in nucleophilic and linear form, targeting half-life < 30 min and layer thinkness <10 μm at room temperature, ambient conditions.

3.3 Preliminary Approaches

3.3.1 Bulk Hydrogel Films Crosslinked by Acid-sensitive Crosslinkers Containing Quaternary Ammonium Halides (Cl or F) as a Nucleophile

3.3.1.1. Preparation of QAC or QAF-based catalyst containing films

Protective layer polymer films from CWA are composed of three parts. First, a water like hydrogel assists in hydrolysis reactions. Second, a CWA catalyst acts as an organobase or organonucleophile. Third, acid-degradable crosslinkers which can consume byproducts like HCl or HF from CWA neutralization reaction, physically remove the contaminated part. In order to investigate pure CWA neutralization kinetics, polymer films with different compositions (**Table 3**) were prepared without acid-degradable crosslinkers. Monomer solutions in DMF (~55 wt%) with photoinitiator (0.5 mol%) were spread on 3M duct tape as a substrate and cured under N_2 and UV (365 nm) for 15 min. After cooling, free-standing films were obtained by detaching films from the substrate.

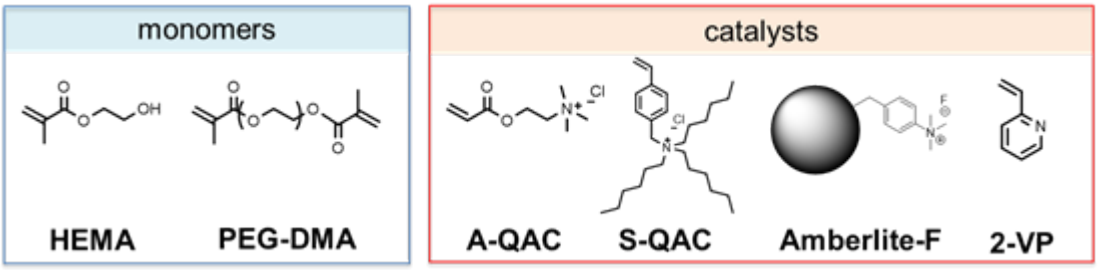

Figure 3.1 Chemical structure of monomers and CWA catalysts

Table 3 Composition of each monomer solution

Sample #	Composition			
	HEMA (equiv.)	PEG-DMA (equiv.)	A-QAC (equiv.)	PI (mol%)
SE003	20	1	5 (23.7 mol%) (19.62 wt%)	0.5
	HEMA (equiv.)	PEG-DMA (equiv.)	S-QAC (equiv.)	PI (mol%)
SE006	20	1	5 (23.7 mol%) (38.7 wt%)	0.5
	HEMA (equiv.)	PEG-DMA (equiv.)	Amberlite-F	PI (mol%)
SE007	20	1	1 wt%	0.5
	A-QAC (equiv.)			PI (mol%)
SE014	1			0.5
	HEMA (equiv.)	PEG-DMA (equiv.)	2-vinyl pyridine (equiv.)	PI (mol%)
SE015	20	1	10 (32.3 mol%)	0.5

3.3.1.2. ^{31}P MAS NMR study

Polymer films (7 ~10 mg) were cut as a small piece and were added to a disposable insert kit. Without capping, the whole thing was placed in the humidity chamber (99% r.h. and 100% r.h.). The mass at each dry and humidified state was recorded to know the exact amount of water absorbed in the polymer film. After 1 day (99 % r.h.) or 3 days (100 % r.h.), insert kit packed with polymer film was taken out and ready for starting measurement. Right before running the NMR, 1 μL of DFP was applied via micro-syringe to the center of the sample. This insert kit was sealed with a cap and then moved to the 0.4 cm ZrO_2 rotor and this rotor was also sealed with a fitted Kel-F cap (Figure 2). ^{31}P MAS NMR spectra were measured periodically to determine remaining starting material and identify degradation products. After finishing measurement, disposable insert kit was taken out and placed in the 1M aqueous NaOH solution to fully neutralize.

^{31}P MAS NMR spectra were obtained at 202.46 MHz (Bruker Avance 500)

spectrometer. The HRMAS spectra were recorded with a 5-mm Brucker 31P gradient probe at 30 °C with the magic-angle spinning rate of 5000 Hz. Between measurement, samples were kept at 30 °C oven.

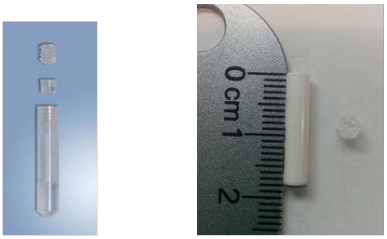

Figure 3.2 Disposable insert kit (left) and 0.4 cm ZrO2 rotor

The chemical shifts corresponding to pure DFP were shown at -7.12 ppm and -13.88 ppm. The hydrolyzed byproduct, DIIP was shown at 0 ppm

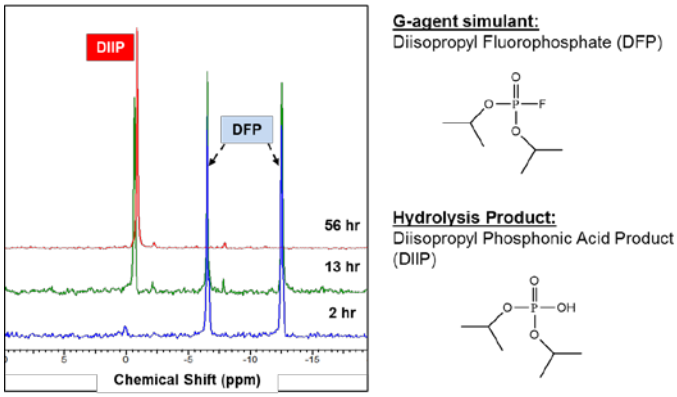

Figure 3.3 ^{31}P MAS NMR spectra showing DFP and hydrolyzed product DIIP, and their structures

3.3.1.3. Preliminary Results

All three samples were placed at 99% r.h. chamber for one day. The exact amount of water is unknown. There was no additional water insertion. As time elapsed, decreasing peaks for DFP and increasing peak for DIIP were observed. By constructing the first-order plot with time, half-life time of DFP was obtained from the slope. Among three samples, SE003 shows the fastest neutralization rate. In the case of SE007, polystyrene-

supporting quaternary ammonium fluoride resin has visible particle size. Depending on the cutting spot of film, the loading amount of catalyst resin can be different. In the case of SE003, DFP remains around 20% after 6 days. SE006 shows 94 % remaining of DFP after 3 days. SE007 shows 48% remaining of DFP after 6 days. The half-life time of DFP is 73 hr, 999 hr and 138 hr for SE003, SE006 and SE007, respectively.

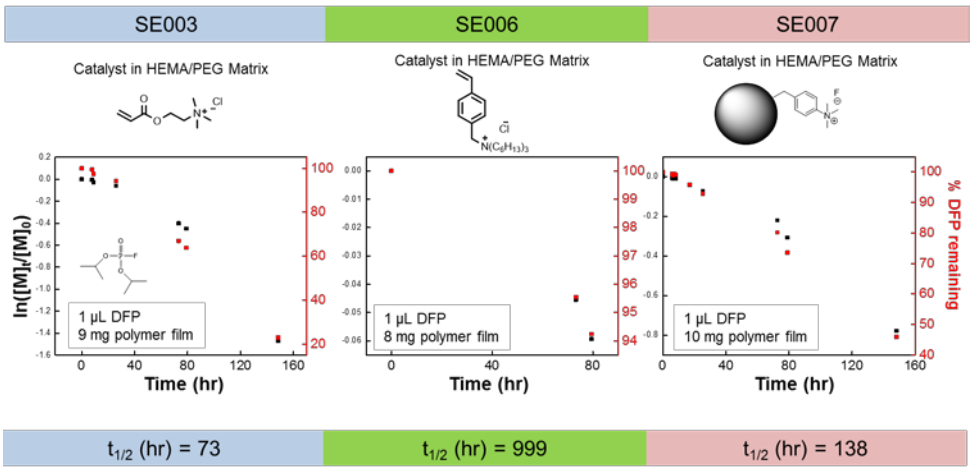

Figure 3.4 DFP neutralization kinetic plots and % DFP remaining vs time for SE003, SE006 and SE007

Acrylate-based QAC containing SE003 film (12 mg) packed in the disposable kit was placed at 100 % r. h. chamber for 3 days. The amount of absorbed water in the film was determined by weighing sample before and after placing in the humidity chamber. Around 8 mg of water was contained by humidity and additional insertion. At higher humidity condition, samples show much faster neutralization. Initial degradation seems to occur slowly, ramping up overtime. This might be due to slow diffusion of DFP into polymer film. It can be both good and bad regarding protection and neutralization, respectively. Much slower neutralization gives us different half-life time depending on observation time. From the results, once DFP starts to be degraded, it seems to accelerate neutralization. Real half-life time from the experiment is between 10 ~ 15 hr

as observed from the graph, which means none of the half-life times from calculation are accurate values. In order to exclude diffusion effects, we might need to perform neutralization study using an A-QAC monomer. The difficulty of doing this experiment is the fact that pure A-QAC monomer is only commercially available and in an aqueous state (80 wt%), which is not applicable for solid-state NMR.

3.3.1.4. Summary

Using ^{31}P MAS NMR, DFP neutralization kinetic study was performed. DFP is one of the G-agent simulants which contain P-F bond. For neutralization, quaternary ammonium chloride or fluoride-based containing films were used as a nucleophile. Depending on humidity, largely different half-life time at the same composition were observed. Acrylate-based QAC containing films showed the fastest neutralization rate (t1/2=22 hr) at 100% r.h. but this is still quite slow. In order to improve neutralization kinetic, first DFP molecule should diffuse quickly into the polymer matrix. Improvements may become by changing monomer compositions, or by using much stronger organic nucleophile.

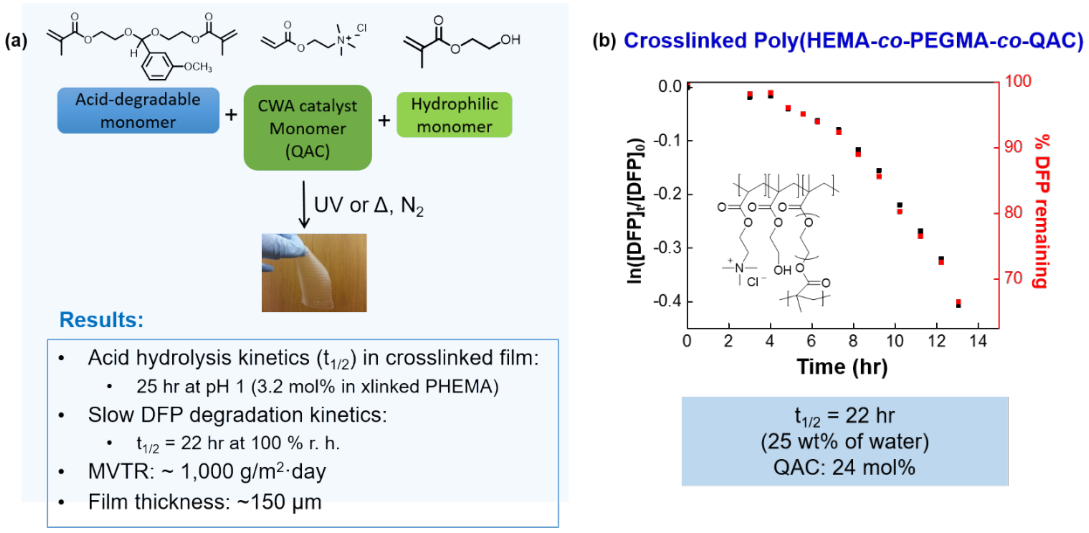

Figure 3.5 Schematic illustration of self-exfoliating and reactive polymer (SERP) as a bulk film and its key results (a) and DFP neutralization kinetic plot

As ***Figure 3.5*****(a)** shows, we initially developed a simple crosslinked self-exfoliating and reactive polymer (SERP) system by mixing dimethacrylate-functionalized acetal-based crosslinker (acid-sensitive), quaternary ammonium chloride (QAC)-based acrylate as a CWA catalyst, hydrophilic monomer (HEMA or PEG-MA), and AIBN (Azobisisobutyronitrile) as an initiator, after which the mixture was cured by using heat or UV irradiation. However, **Figure 3.5(b)** depicts that after the organophosphate-based nerve agent simulant DFP (diisopropylfluorophosphate, LD_{50} Rat: i.p. 1.3 mg/kg) was catalyzed by QAC-containing 100 % humidified hydrogel at room temperature, it was slowly neutralized to non-toxic DIIP (diisopropyl phosphonic acid) ($t_{1/2}$ = 22 hr). This slow hydrolysis rate can be explained by 1) the slow diffusion of DFP into the bulk layer of hydrogel film and 2) the weak catalytic reactivity of QAC. Hydrophilic monomers continued to be dewetted on hydrophobic ePTFE (breathable film) during s spin-coating and doctor-blade coating. Because of dewtting, crosslinked films appeared as a bulk thick hydrogel film with thickness of

150 μm. Also, it was important to explore other organo-based nucleophilic functional groups to enhance neutralization reaction rate. Therefore, we have proposed to make nanoparticle (NP)-type reactive polymer and photo-crosslinkable linear polymer containing stronger nucleophilic functional groups under the expectation that spray-coating of NP solutions and spin-coating of polymer solutions reduce film thickness.

3.3.2 Nucleophilic Polymers Functionalized from Acid-degradable NPs

Nucleophilic nanoparticles are designed to enhance catalytic reactivity due to large surface area and to facilitate making a thin and uniform polymer layer. One of the well-known ways to form a non- dissolvable polymer layer is spray coating of polymer latex. Usually, polymer-based NPs or latex can be easily prepared by conventional emulsion polymerization. As monomers, there will be hydrophilic monomers to attribute hydrogel properties, acetal/ketal-based crosslinkers to reveal acid-sensitivity and a bromoisoburylate-terminated methacrylate monomer as an ATRP (atom-transfer radical polymerization) initiator to polymerize nucleophile-containing monomers.

Methacrylate-functionalized ATRP initiator: MABr was made by follows: 2-hydroxy methacrylate (5 g, 1 equiv.) and triethylamine (8.04 mL, 1.5 equiv.) in THF (70 mL) was placed in a flask under N_2 and cooled to 0 °C. 2-bromoisobutyryl bromide (13.25 g, 1.5 equiv.) was slowly added drop-wise and stirred at room temperature for 6 hr. After reaction, the solvent was removed in vacuum and the crude mixture was extracted with dichloromethane and DI-water several times and dried over $MgSO_4$, filtered, and solvent removed. The product was further purified by column chromatography with

silica gel using eluent (Hex:EA = 6:1, v/v). The monomer was a yellow transparent liquid (yield = 50 %). ^{1}H NMR ($CDCl_3$): δ= 6.12 (m; 1H), 5.58 (m; 1H), 4.37-4.43 (t; 4H), 1.91 (s; 6H).

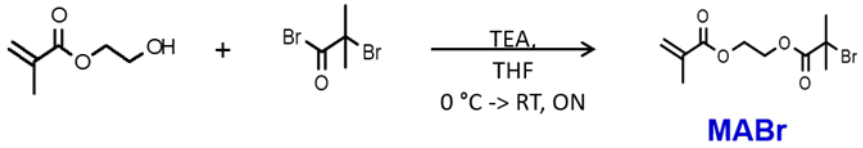

Figure 3.6 Methacrylate-functionalized ATRP initiator: MABr

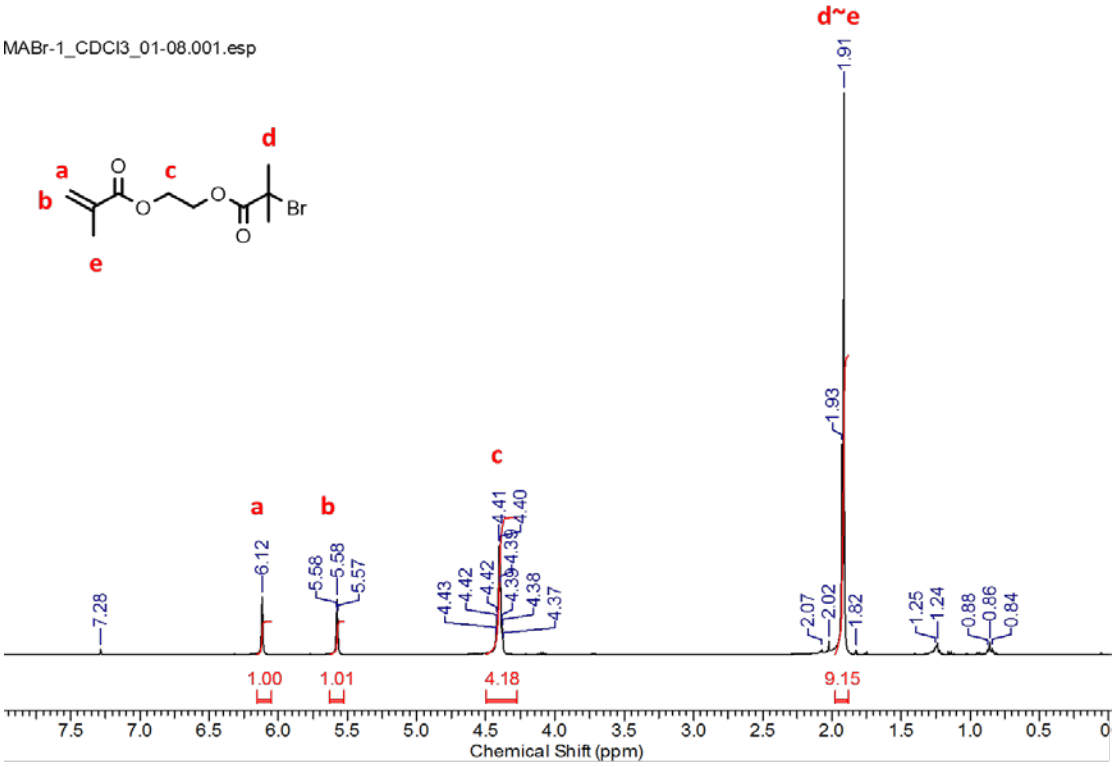

Figure 3.7 ^{1}H NMR of MABr

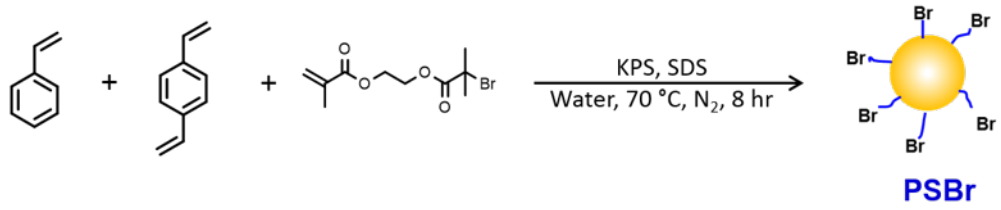

Figure 3.8 PS-co-DVD/MABr core-shell nanoparticles: PSBr

xMABr-Br NPs by emulsion polymerization was performed in the 3 neck-round bottom flasks (25 mL) with a stir bar, divinylbenzene (DVB) (0.05 g, 0.3866 mmol) and potassium persulfate (25 mg, 0.0925 mmol) styrene, sodium dodecyl sulfate (SDS) were dissolved in DI-water (13 mL) and sparged with dry N_2 for 1 hr at room temperature. The initiator solution, potassium persulfate (KPS) in water (3 mL) was also sparged for 10 min and transferred into the flask by syringe. The reaction was refluxed at 70 °C for 1 hr under N_2. At this stage, in which many radicals are very active but most of monomers are consumed, 2-(2-bromo-2-methylpropanoyloxy)ethyl methacrylate (MABr)(1.67 g, 8.74 mmol) in acetone was added. It was refluxed at 90 °C for 45 min or 2 hr under N_2. After reaction, the solution was precipitated in methanol (100 mL). Resulting polymer was obtained as a white powder. The particle size was around 430 ~ 500 nm, observed by scanning electron microscopy (SEM). The overall ratio of [Styrene]:[DVD]:[MABr]:[SDS]:[KPS] = 190:1:9.67:13.9:1.11 or 500:2:20:1:25.

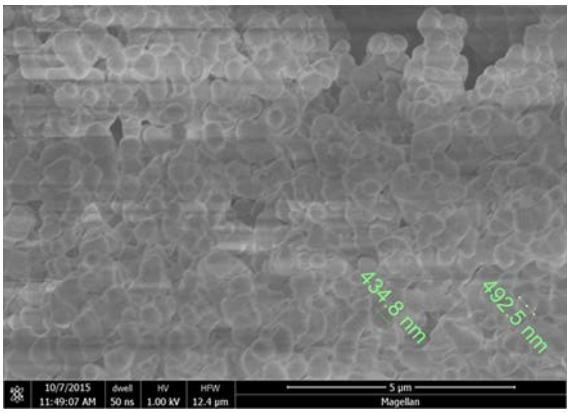

Figure 3.9 SEM Image of PSBr NPs

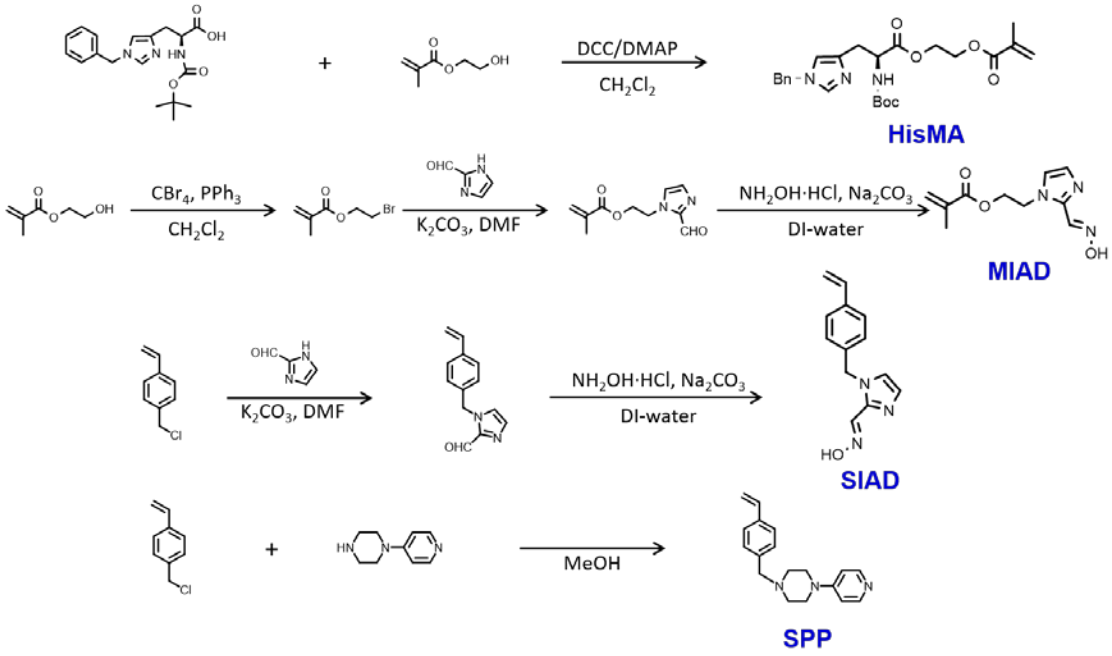

Figure 3.10 Synthesis of vinyl-functionalized nucleophilic monomers

HisMA was synthesized by mixing N-*t*-Boc-Imidazole-benzyl-L-histidine (2 g, 1 equiv.), 2-hydroxyethyl methacrylate (0.904 g, 1.2 equiv.) and *N,N'*-dicyclohexylcarbodiimide (1.192 g, 1 equiv.) in dichloromethane (40 mL) were placed in the flask and cooled to 0 °C. 4-Dimethylaminopyridine (0.066 g, 0.1 equiv.) was added and the reaction was allowed to stir overnight at room temperature. After reaction,

dicylclohexylurea was filtered off and the organic solution was washed with a 1M aqueous HCl solution (200 mL), saturated $NaHCO_3$ solution and brine respectively. The organic layer was dried over $MgSO_4$, filtered and solvent evaporated, and the product was obtained as a transparent viscous yellow liquid.

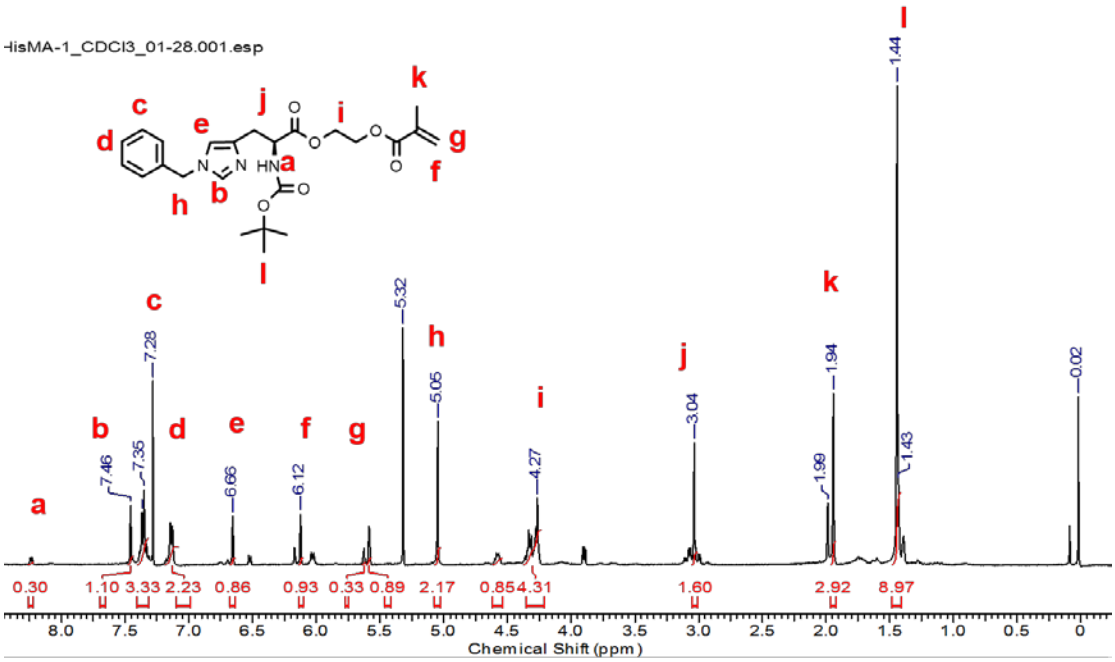

Figure 3.11 ^{1}H NMR of HisMA

MIA was prepared in 100 mL 1-neck round bottom flask, BrMA (2 g, 10.4 mmol, 1 equiv.) and imidazole-2-carboxaldehyde (1 g, 10.4 mmol, 1 equiv.) were dissolved in anhydrous DMF (40 mL) with K2CO3 (1.37 g, 10.4 mmol, 1 equiv.). It was kept stirring at room temperature for 20 hr. During the reaction it was observed that yellow solution turns to brown. After reaction, K2CO3 was filtered and solvent was removed by blowing evaporation. The product was obtained as a sticky brown solid (xx g, xx % yield). 1H NMR of MIA (500 MHz, DMSO, TMS standard, r.t.): δ=9.70 (s; 1H), 7.69 (s; 1H), 7.30 (s; 1H), 5.94 (s; 1H), 5.66 (s; 1H), 4.71 (t; 2H), 4.41 (t; 2H), 1.81 (s; 3H).

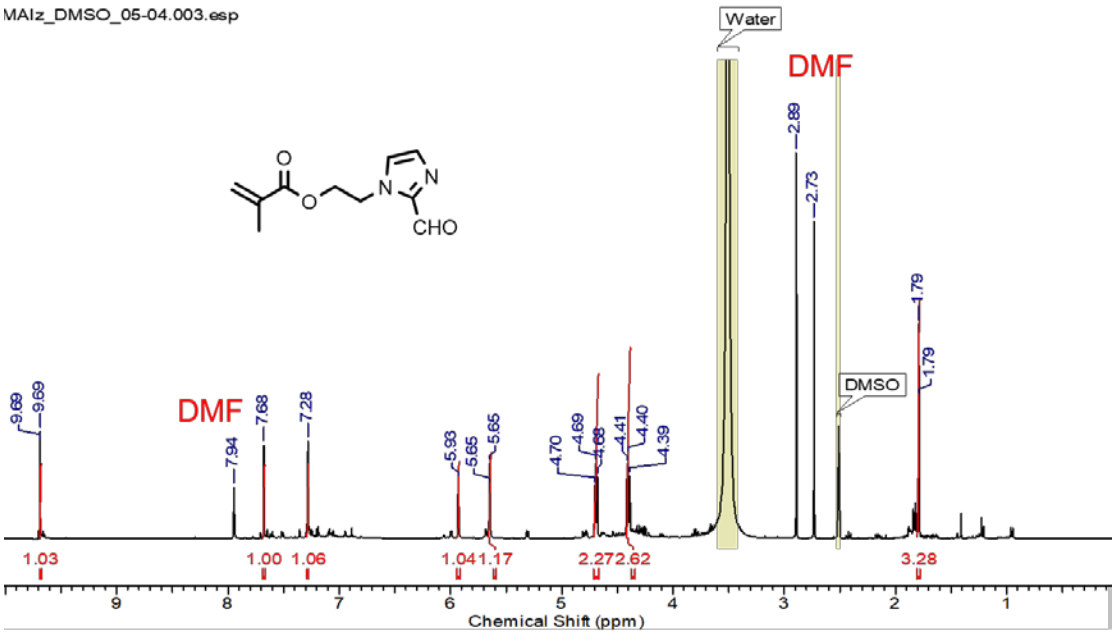

Figure 3.12 ^{1}H NMR of MIA

MIAD was prepared in 100 mL 1 neck round bottom flask, NH2OH·HCl (1.08 g, 15.6 mmol, 1.5 equiv.) was dissolved in 50 mL DI-water and neutralized by adding Na2CO3 (1.65 g, 15.6 mmol, 1.5 equiv.). MAI (2.16 g, 10.4 mmol, 1 equiv.) was dissolved in 10 mL DMF and dropped into aqueous solution. It was kept stirring at room temperature for 5 hr. The brown precipitate was collected by gravity filtration and dried in vacuum oven (xx g, xx % yield). 1H NMR of MIAD (500 MHz, DMSO, TMS standard, r.t.): δ=11.48 (s; 1H), 8.05 (s; 1H), 7.33 (s; 1H), 7.01 (s; 1H), 5.98 (s; 1H), 5.67 (s; 1H), 4.58 (t; 2H), 4.35 (t; 2H), 1.82 (s; 3H).

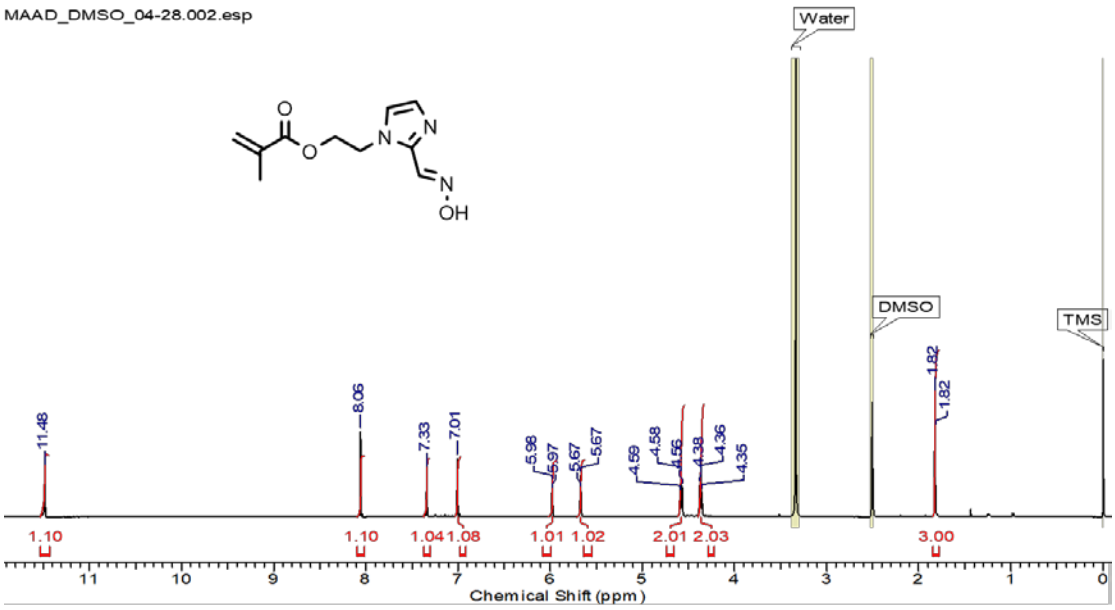

Figure 3.13 ^{1}H NMR of MIAD

1-(4-vinylbenzyl)-1H-imidazole-2-carbaldehyde (SIA) was prepared by making a solution of 4-(chloromethyl)styrene (6.2 mmol), imidazole-2-carboxaldehyde (5.2 mmol) and K_2CO_3 in DMF (20 mL) was stirred overnight at RT under N_2. After this reaction, SIA was obtained as transparent yellow liquid after evaporation of the solvent

1-(4-vinylbenzyl)-1H-imidazole-2-carbaldehyde oxime (SIAD) was prepared by dissolving hydroxyamine hydrochloride (1.5 equiv.) in water and neutralizing with Na_2CO_3 (1.5 equiv.). SIA (1.1 g, 1 equiv.) was added to the solution. The reaction mixture was stirred at room temperature for 1 hr. The oxime product precipitated and was collected by filtration, rinsed with water. It was isolated as a yellow powder

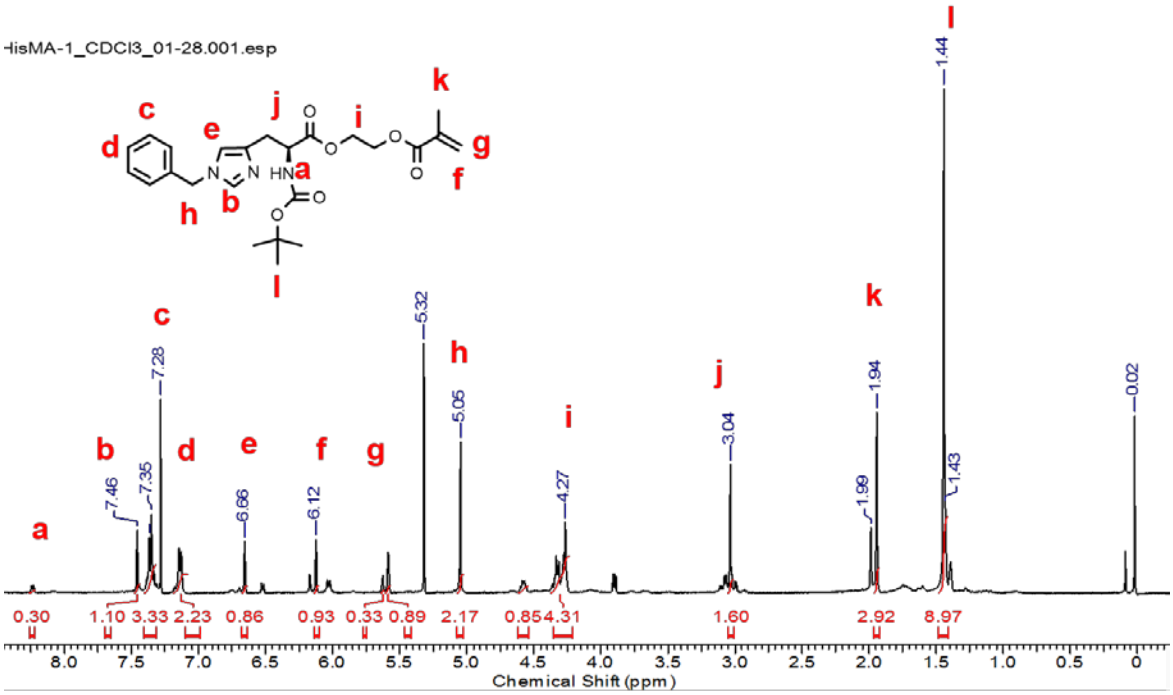

Figure 3.14 ^{1}H NMR of SIA

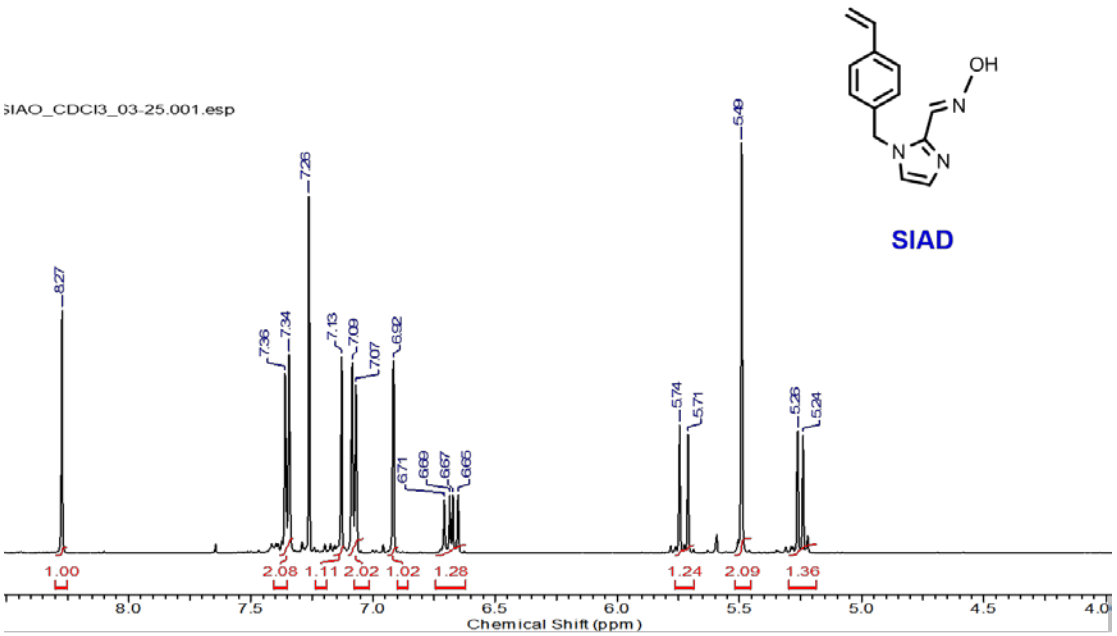

Figure 3.15 ^{1}H NMR of SIAD

Synthesis of SPP was followed via literature (organic letters, 2003, 5, 2445-2447). Briefly, in 100 mL of 1-neck round bottom flask equipped with reflux condenser, N-(4-pyridyl) piperazine (4 g, 24.5 mmol, 2 equiv.) were dissolved in 40 mL methanol and

4-vinylbenzyl chloride (1.87 g, 12.25 mmol, 1 equiv.) was added forming white precipitate. The solution was heated up at 70 °C for 18 hr. After reaction, it was cooled to room temperature. In the solution, 80 mL of aqueous 6N HCl solution was added and washed with ether (80 mL) 3 times. The ether layer was discarded and aqueous 25 M NaOH solution (80 mL) was drop-wised to aqueous layer. Yellow precipitate was collected by vacuum filtration. This solid was dissolved in dichloromethane and purified by column chromatography with silica gel. For packing and adsorption, ~150 mL and ~50 mL of silica gel was used. As an eluent, mixture of ethyl acetate and trimethylamine as 95:5, v/v (Rf~0.3) was used. Resulting product was white powder (2.23 g, 65.3 % yield). 1H NMR of SPP (500 MHz, CDCl3, TMS standard, r.t.): δ=8.25 (d; 2H), 7.37 (d; 2H), 7.31 (d; 2H), 6.72 (m; 1H), 6.63 (d; 2H), 5.73 (d; 2H), 5.25 (d; 2H), 3.54 (s; 2H), 3.32 (t; 4H), 2.56 (t; 4H).

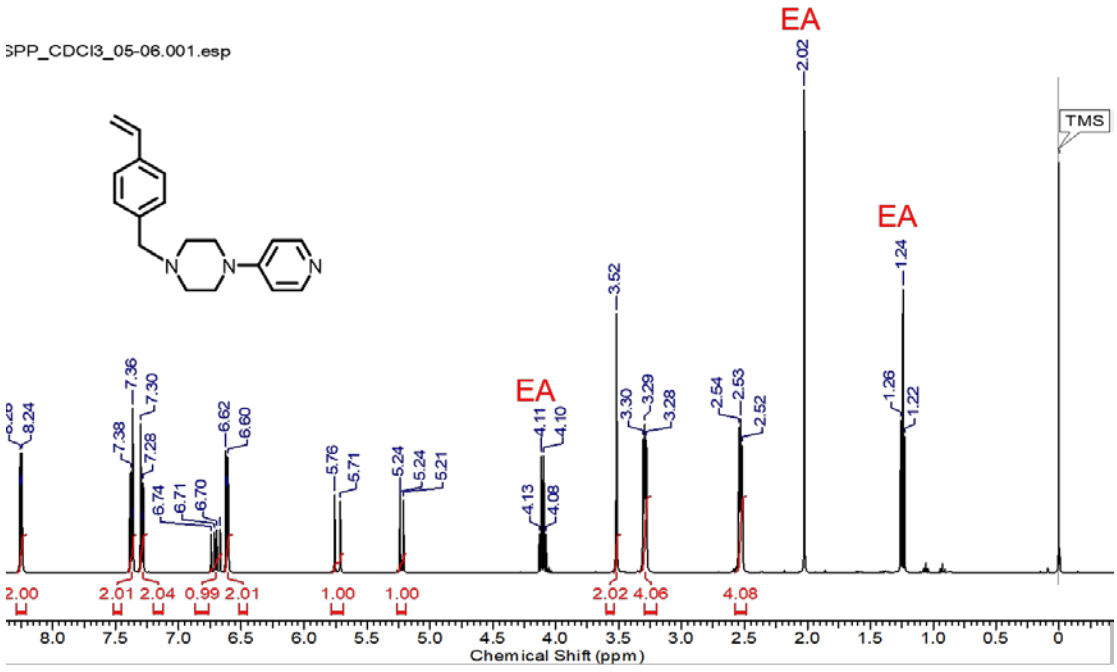

Figure 3.16 ^{1}H NMR of SPP

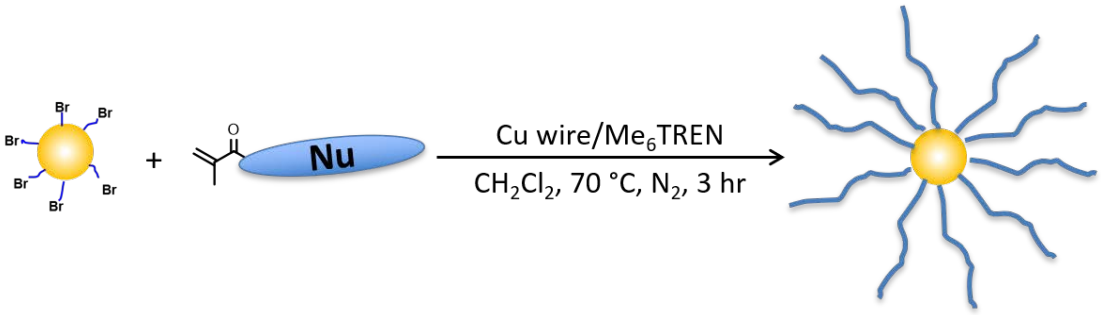

Figure 3.17 Synthesis scheme: nucleophilic polymer functionalized NPs by performing ATRP reaction

HisMA (vinyl-functionalized nucleophilic monomer) in dimethylformamide was sparged with N_2 for 1.5 hr. PSBr particles and Cu wire were charged into a round bottom flask fitted with a stir bar and the flask was flushed with N_2 for 1 hr. The HisMA solution was transferred into the flask by syringe, and the ligand, 0.1 M tris[2-(dimethylamino)ethyl]amine (Me_6TREN) solution in dimethyl sulfoxide (DMSO), was added into the flask. The reaction was heated to 70 °C for 2 hr under N_2. After reaction, solution was poured into methanol and the larger pieces of residual Cu wire were manually removed. The slight green polymer was obtained by filtration.

Polymerization of amine-based vinyl monomers initiated from Br-terminated NPs was not successfully performed which can be confirmed by observing low mass yield (< 3%) showing most monomers were not reacted. There are probable issues which impede reactions such as poor dispersion of NPs macro-initiator during polymerization reaction, amines in monomers binding with copper complex or improper selection of ligand, solvent and copper source. Once NPs synthesized from emulsion polymerization dried out during filtration, they strongly tend to aggregate rendering re-dispersion challenging. Also, purification of NPs after ATRP needs to be scrutinized to

remove impurities such as copper complex, catalyst and unreacted monomers.

3.4 Experimental: Photo-cross linkable and Nucleophilic Linear Polymer

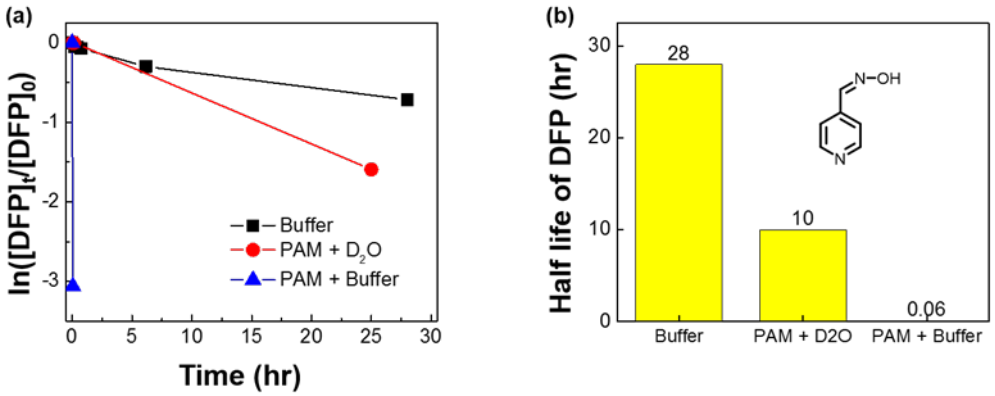

Figure 3.18 Kinetic plot of DFP neutralization catalyzed by 23 mM AMBD buffer, 4-pyridine aldoxime (PAM) with D_2O and PAM with 23 mM AMPD buffer (left) and half-life of DFP at each condition (right)

The PAM is a well-known antidote for immediate injection to combat organophosphate-based nerve agents to reactivate acetocholinesterase. We could see PAM is a promising candidate as a nucleophilic OP-destructive reactant by doing simple experiment and literature search.[26,36] DFP catalyzed by PAM in 23 mM AMPD (2-amino-2-methyl-1,3-propanediol) buffered in D_2O showed even faster decontamination ($t_{1/2}$ of DFP: 0.06 hr) at room temperature. It was investigated by ^{31}P solution NMR.

Materials used for synthesis are 4-hydroxybenzophenone (Alfa Aesar, 98%), 4-vinylbenzyl chloride (Aldrich, 90%), potassium carbonate anhydrous (K_2CO_3, Fishier Scientific), potassium iodide (KI, Fishier Scientific), acetonitrile (anhydrous, Alfa Aesar), pyridine-4-aldoxime (PAM, 98%, Alfa Aesar), diisopropyl fluorophosphate (DFP, Sigma-Aldrich), polyethyleneimine (ca. 30% in Water, TCI) toluene (anhydrous,

VWR), *N*-isopropyl acrylamide (NIP, TCI) was recrystallized in hexane and azobisisobutyrontitrile (AIBN, Aldrich, 98%) was recrystallized in methanol before use.

^{1}H and ^{31}P NMR spectra were investigated by a Bruker DPX 500 spectrometer.

Synthesis of 4-(4-vinylbenzyloxy) benzophenone (VBBP) was performed in a 3-neck round bottom flask (500 mL) with a magnetic stir bar, 4-hydroxy benzophenone (5.95 g, 0.03 mol), K_2CO_3 (8.28 g, 0.06 mol) and KI (6.64 g, 0.04 mol) were dissolved in acetonitrile (150 mL). This solution was refluxed at 50 ºC for 4 hr and solution of 4-vinylbenzyl chloride (VBCl) (6.10 g, 0.04 mol) in acetonitrile (80 mL) was added into the flask. Reaction was stopped by cooling turbid yellow solution to room temperature after heating at 50 ºC for 36 hr. The inorganic salts were filtered out by gravimetric filtration and a yellow chunk was obtained after removing solvent by vacuum rotary evaporation. It was washed with ethyl ether (~100 ml) and filtered out several times. The yellow solid separated from solution was dissolved in acetone (~100 ml) and further purified by column chromatography with silica gel and mixture of acetone and hexane (3:7, v/v) as an eluent. The resulting product was obtained as a slightly yellow powder (5.86 g, yield: 62%). ^{1}H NMR of VBBP (500 MHz, DMSO-d_6, TMS standard, r.t.): δ=7.76 (d; 2H), 7.70-7.64 (3H), 7.57-7.45 (6H), 7.18 (d; 2H), 6.76 (m; 1H), 5.88 (d; 1H), 5.30 (d; 1H), 5.22 (s; 2H).

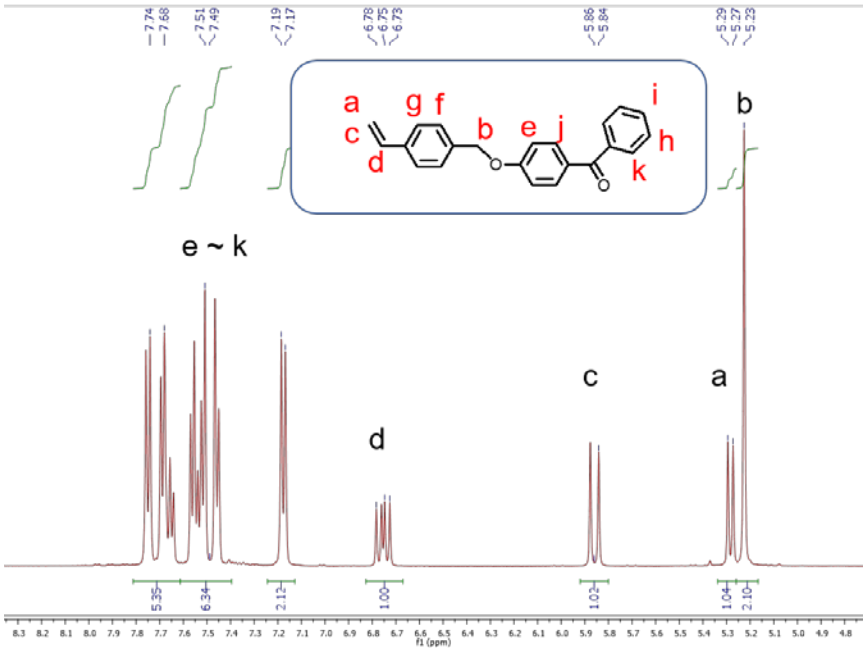

Figure 3.19 ^{1}H NMR of VBBP

Synthesis of photo-crosslinkable terpolymer, p(NIP-VBBP-VBCl) was performed in a 2-neck round bottom flask (50 mL) with a magnetic stir bar, *N*-isopropylacrylamide (NIP) (3.96 g, 0.035 mol, 170 equiv.), VBBP (0.647 g, 2.0588 mmol, 10 equiv.), 4-vinylbenzyl chloride (VBCl) (0.628 g, 4.1147 mmol, 20 equiv.), and AIBN (0.033 g, 0.20588 mmol, 1 equiv.) were dissolved in 25 mL of toluene (20 wt/vol %). This solution was refluxed at 70 ºC for 20 hr under N_2 atmosphere after it was treated with N_2 bubbling for 30 min to remove dissolved oxygen. After cooling to room temperature, this polymer solution was precipitated out in ethyl ether (1L). If polymer solution is too viscous, methanol was slightly added to dilute solution before precipitation. The white product was collected by vacuum filtration with 70% yield (3.7 g). ^{1}H NMR of VBBP (500 MHz, DMSO-d_6, TMS standard, r.t.): δ=7.76 (d; 2H)

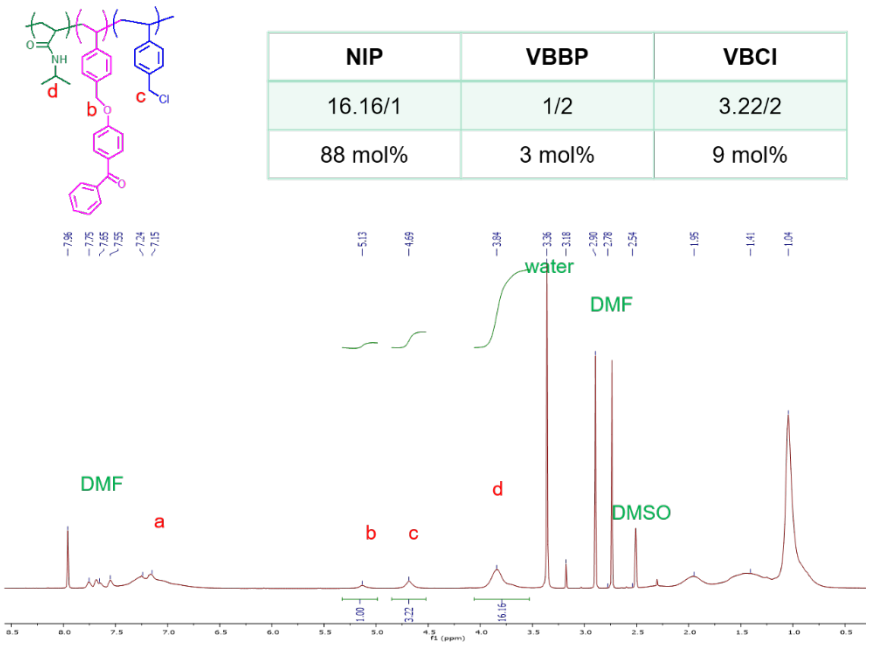

Figure 3.20 ^{1}H NMR: p(NIP-VBBP-VBCl)

Synthesis of p(NIP-VBBP-VBI) was performed in a 1-neck round bottom flask (50 mL) with a magnetic stir bar, p(NIP-VBBP-VBCl) (3.7 g) was dissolved in acetone (40 mL). From ^{1}H NMR spectrum, wt % of VBCl was calculated as 11 wt%. KI (1.33 g, 8 mmol) was added as 3 equiv. of VBCl. This solution was stirred at room temperature for overnight. The polymer solution was diluted with more acetone and inorganic salt was removed by filtration. The solvent of the filtrate was removed by vacuum evaporation. Resulting polymer was obtained as yellow powder.

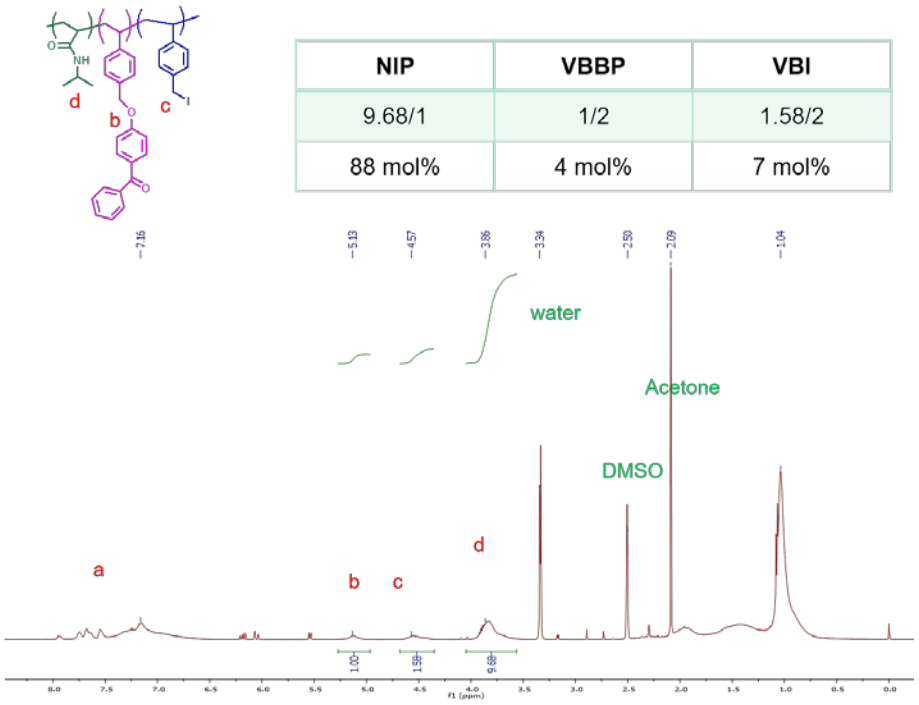

Figure 3.21^{1}H NMR: p(NIP-VBBP-VBI)

Synthesis of p(NIP-VBBP-VBIPAM) was performed by PAM-functionalization reacting p(NIP-VBBP-VBI) (25 g) with PAM (4.88 g, 0.04 mol) in DMF (360 mL) at room temperature for 24 hr. The resulting final polymer was obtained by vacuum filtration after precipitating in diethyl ether. ^{1}H NMR spectrum showed the disappearance of peak at 4.56 ppm and appearance of peak at 5.74 ppm because of PAM-functionalization.

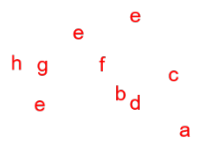

NIP	VBBP	VBIPAM
9.31/1	1/2	1.82/2
87 mol%	5 mol%	8 mol%

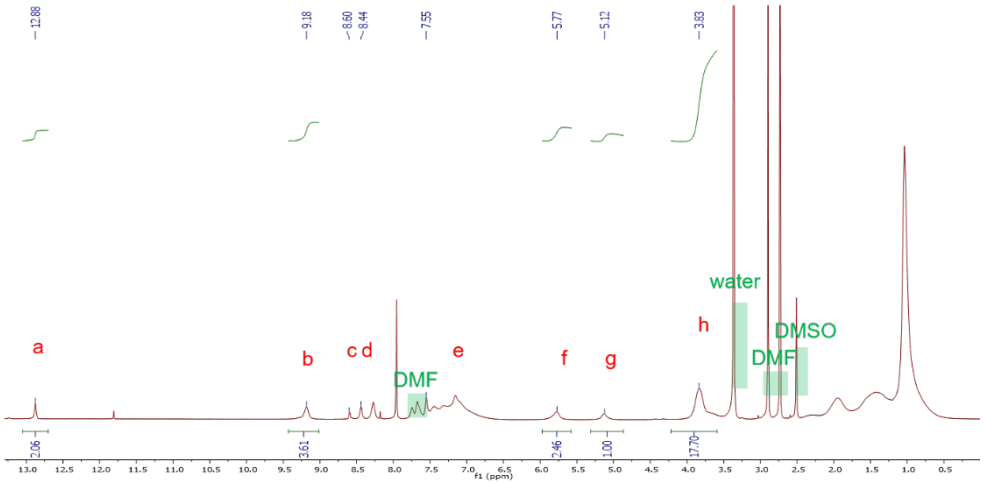

Figure 3.22 ^{1}H NMR: p(NIP-VBBP-VBIPAM)

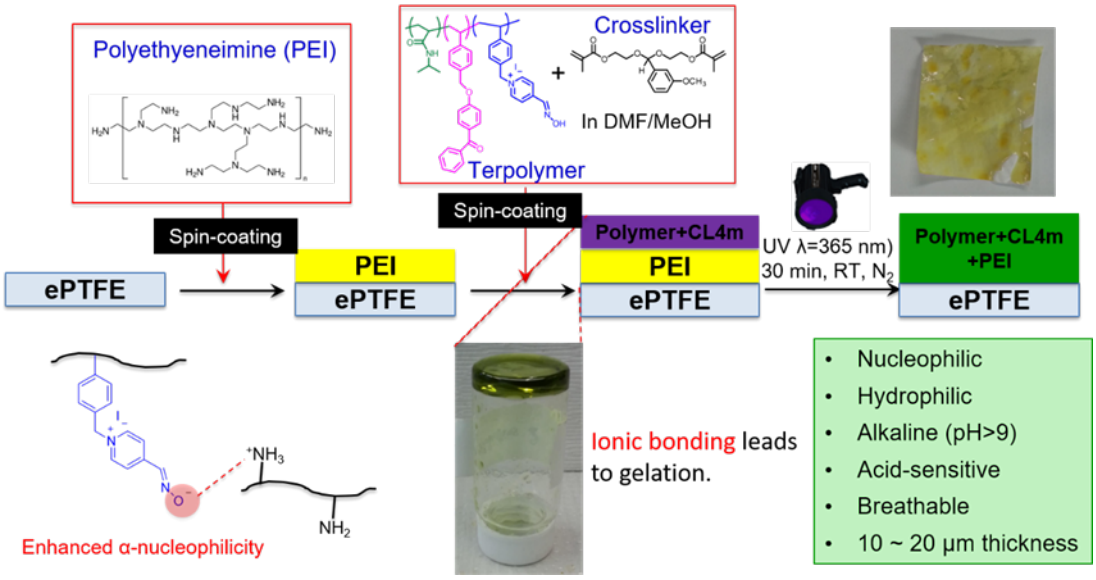

Figure 3.23 Schematic illustration: preparation of a breathable thin film combining terpolymer, crosslinker and PEI

Breathable and protective film was prepared as follow. Polyethyleneimine (PEI) solution (6 wt%) in MeOH was spin-coated on ePTFE. A terpolymer solution with crosslinker in ethanol (terpolymer:crosslinker:ethanol = 0.35 g: 0.007 g: 2.1 g) was then spin-coated on the PEI layer. Subsequently, the sample was UV-cured (365 nm) or allowed to sit for 30 min at room temperature under N_2 purging. The thickness of

polymer (~ 10-20 μm) on the ePTFE was measured via profilometry. Overall, the film is nucleophilic, hydrophilic, alkaline, acid-sensitive and breathable.

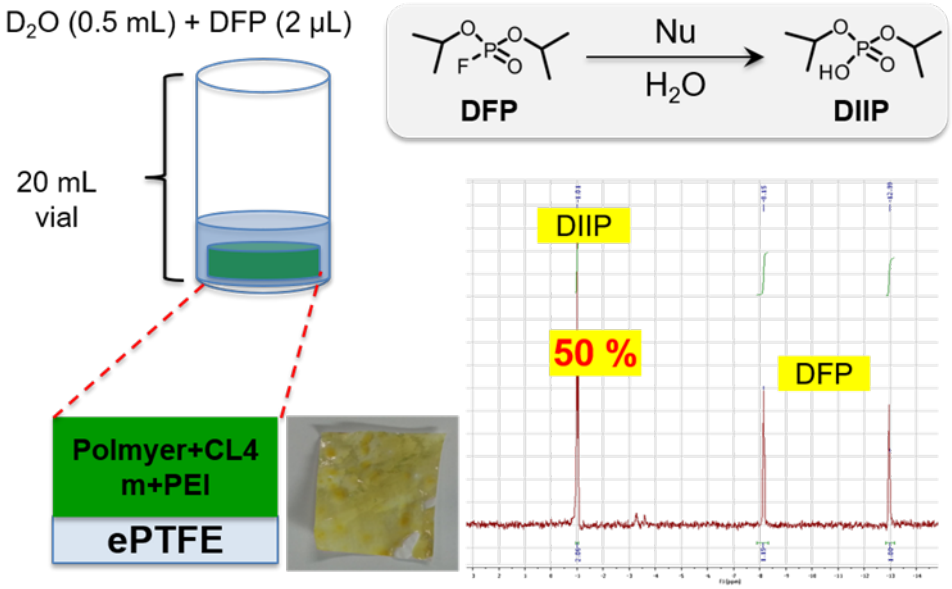

Figure 3.24 DFP neutralization study by the reactive film: experimental set up and ^{31}P NMR spectrum after 30 min exposure to DFP

To test CWA neutralization, a small piece of film was immersed in D_2O (0.9 mL) in a 20mL vial. Two (2) μL of DFP in 0.1 mL of D_2O was introduced into the vial. After 30 min, solution was transferred into a NMR tube for ^{31}P NMR measurement. The spectrum shows that 50 % of DFP was neutralized to DIIP, indicating that half-life of DFP by neutralized solid film is 30 min.

3.5 Results and Discussion

Terpolymer consisting of hydrophilic chains, photo-crosslinkable moiety and nucleophilic CWA catalysts are designed and synthesized. This linear photo-crosslinkable polymer was mixed with previously synthesized acetal-based acid-sensitive crosslinkers in organic solvent. Subsequently, it was spin-coated on substrate and UV-assisted cured resulting in multi-responsiveness including swelling due to

hydrophilic polymer chains, acid-sensitivity from acetal-based crosslinker and OP-compound destructiveness from nucleophilic moiety. Film thickness can be straightforwardly controlled by varying concentration of polymer solution and spin-coating rate.

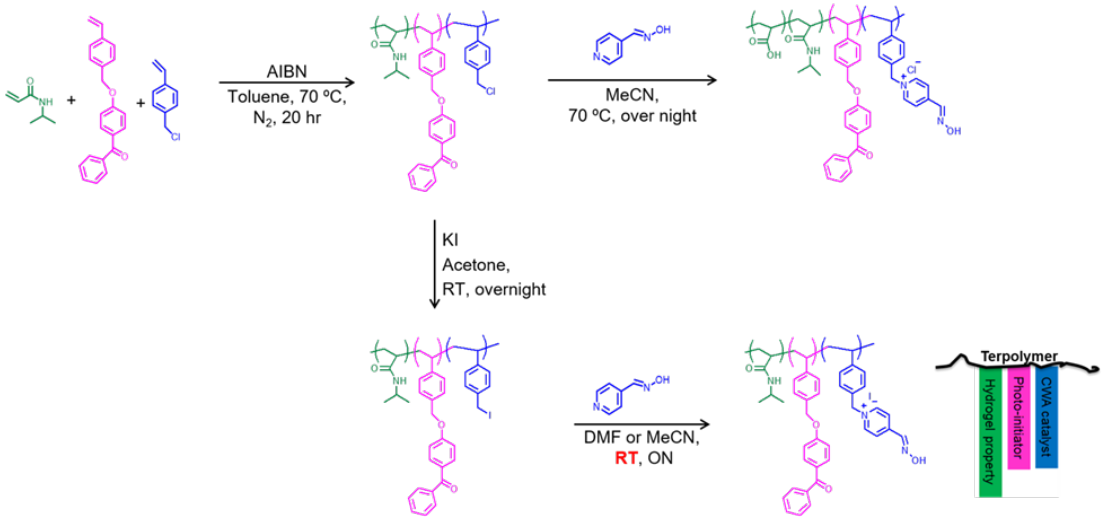

Figure 3.25 Synthetic pathways used to make the PAM-containing terpolymer. The iodization of the benzyl group was found to be necessary to allow reaction of PAM while at the same time avoiding hydrolysis of NIP to AAc in resulting PAM-functionalized terpolymer.

It was necessary to convert chloride group to iodine in order to perform PAM-functionalization reaction at room temperature. We found that there was undesirable hydrolysis of amide group to acetic acid when the reaction was accomplished at high temperature (~70°C) converting alkyl chloride to pyridine-aldoxime chloride.

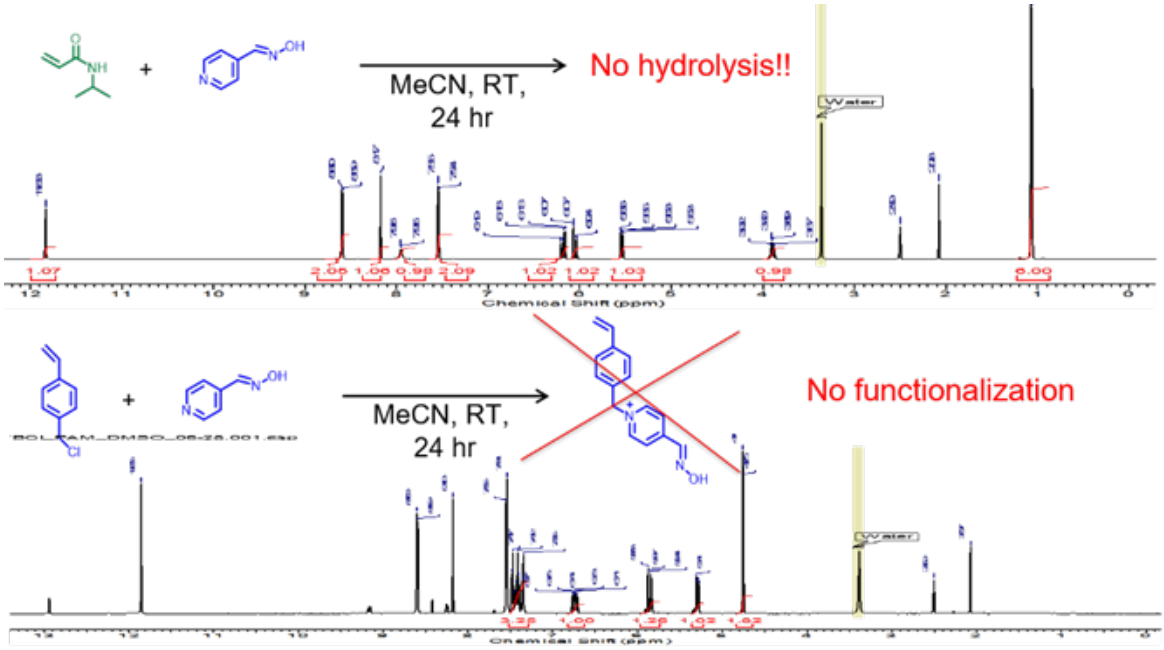

Figure 3.26 ^{1}H NMR: effect of room temperature on hydrolysis of NIP and PAM functionalization to vinylbenzyl chloride

By conducting simple ^{1}H NMR experiments, we could confirm that NIP can be stable in the presence of PAM at room temperature for 24 hrs by observing the peak at 3.83 ppm which corresponds to a proton on isopropyl next to the amine. However, 4-vinylbenzyl chloride monomer could not be functionalized with PAM at room temperature for 24 hrs. Based on this result, we decide to find different conditions to facilitate the functionalization of PAM at room temperature. This was accomplished by incorporating a better leaving group, iodine (I), rather than chloride (Cl).

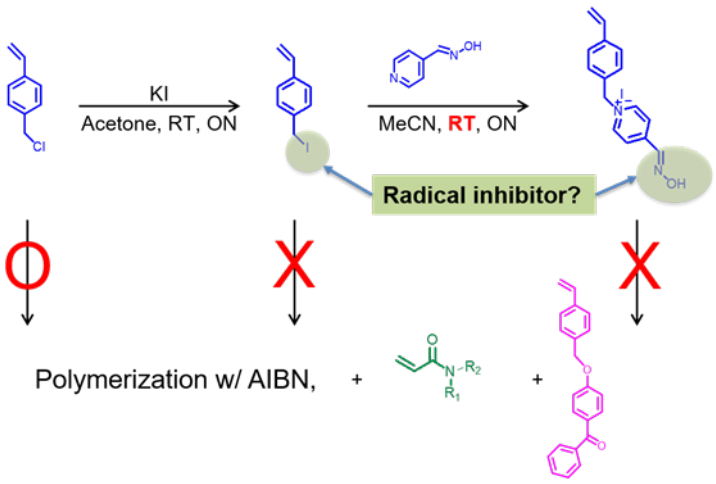

Figure 3.27 Determination of reaction order

At first attempts were made to prepare and polymerize a vinylbenzyl iodide (VBI) monomer or a PAM-functionalized vinylbenzyl iodide (VBIPAM) monomer. Unfortunately, neither approach was successful due to radical inhibitor character of the benzyl iodide or alpha-nucleophile, PAM. Therefore, the post-polymerization functionalization route was used. Also, we confirmed that vinylbenzyl iodide (VBI) can be functionalized with PAM at room temperature for 24 hr by observing the peaks corresponding to oxime (12.90, s) and proton next to quaternary amomum iodine (5.86, s) from ^{1}H NMR shown in **Figure 3.28**.

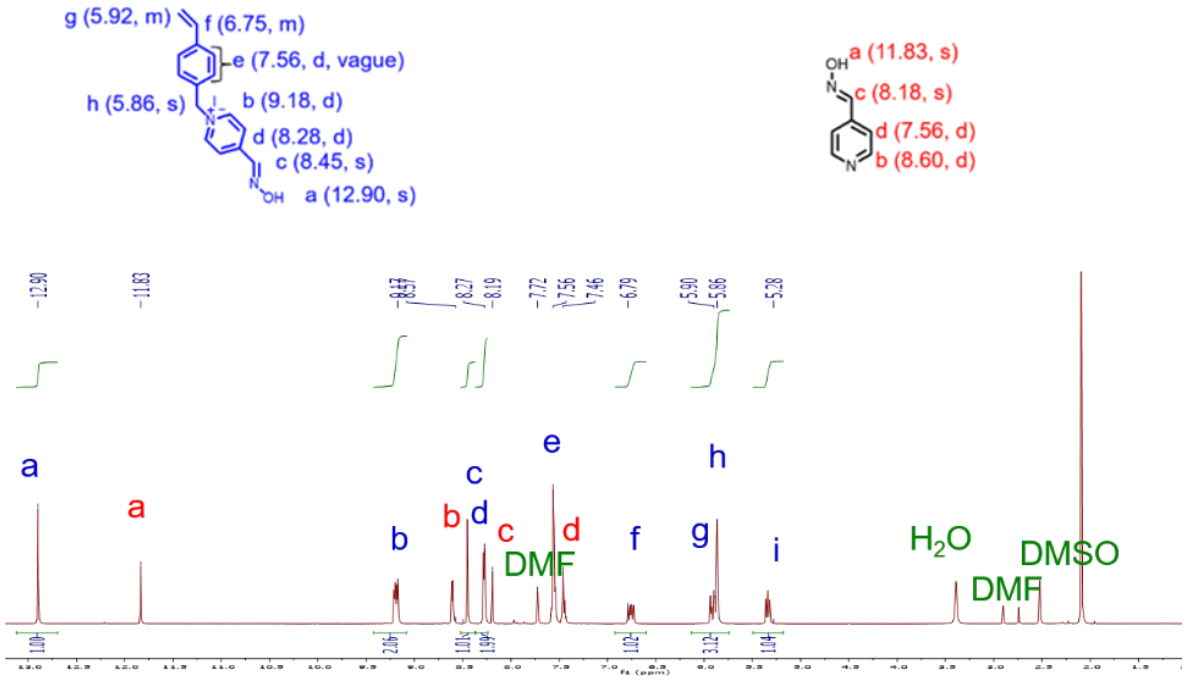

Figure 3.28 ^{1}H NMR: mixture of PAM-functionalized 4-vinylbenzyl iodide and PAM

The main reason why we pay attention to the hydrolysis of amide group to acrylic acid was that the presence of acrylic acid can lower the reaction pH, resulting in a decrease in DFP neutralization rate.

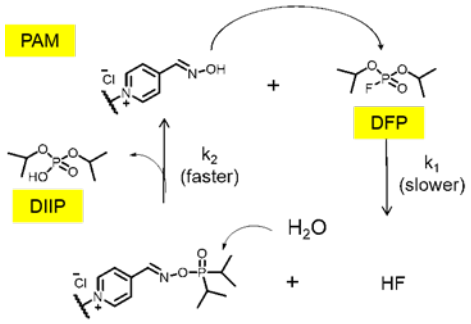

$$\text{Rate} = -d[DFP]/dt \approx k_1[DFP][PAM] \text{ where } k_1 << k_2 \quad (1)$$

$$\text{Rate} \approx k_{obs}[DFP] \text{ where } k_1[DFP] \approx k_{obs} \quad (2)$$

$$\ln[DFP]_t = \ln[DFP]_{t=0} - k_{obs}t \quad (3)$$

$$t_{1/2} = \ln(2)/k_{obs} \quad (4)$$

Figure 3.29 Reaction mechanism and rate constants defined for the hydrolysis of DFP catalyzed by PAM (left), equations for defining half-life for DFP hydrolysis from pseudo-first order kinetic (right)[23]

To demonstrate the catalytic effect of nucleophilic terpolymers, diisopropyl fluorophosphates (DFP) was used as an organophosphorus-based nerve agent simulant and its destruction was observed by tracing ^{31}P NMR spectra. The peaks of pure DFP are shown at -8.2860 ppm and -13.0916 ppm. Integration of those two peaks decreases

and new peak (-0.8207 ppm) corresponding to non-toxic product, diisopropyl phosphoric acid (DIIP) starts to increase as a result of neutralization.

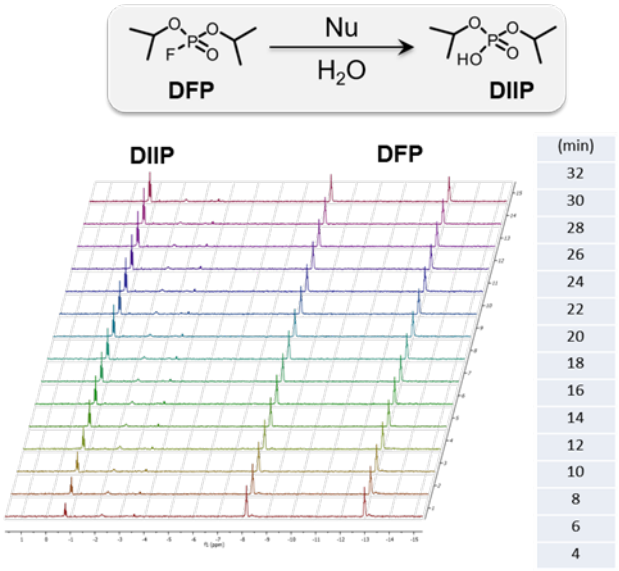

Figure 3.30 Schematic illustration: neutralization of DFP catalyzed by nucleophiles and ^{31}P NMR spectra.

Reaction kinetics of DFP hydrolysis follows a second-order (bimolecular) rate law. To determine the rate constant for DFP hydrolysis, the data will be simply fitted with pseudo-first order kinetics by adjusting the concentration of one of two reactants remains almost constant under the reaction conditions given its much higher concentration ([VBClPAM]>>[DFP]) and considering its catalytic nature. By calculating % DFP remaining from integration of each peak, first-order kinetic plot can be constructed based on following equation: $\ln[[DFP]_t/[DFP]_0] = -K_{obs}t$, where $[DFP]_t/[DFP]_0$ corresponds to % DFP remaining at time t, K_{obs} is the rate constant attained from the slope of plot. Due to experimental limitation, the requirement for pseudo-first order kinetic could not be fully achieved given small molar ratio, [VBClPAM]/[DFP] ≈ 6. This limitation arose because the smallest volume of DFP for clear ^{31}P NMR spectra is 1~2 µL and the highest concentration of polymer solution is

100 mg/mL in 0.5 mL of NMR solvent. To maintain pH higher than 8, 2-amino-2-methyl-1,3-propanediol (AMPD) buffer solution was prepared in D_2O (5 mM or 23 mM).

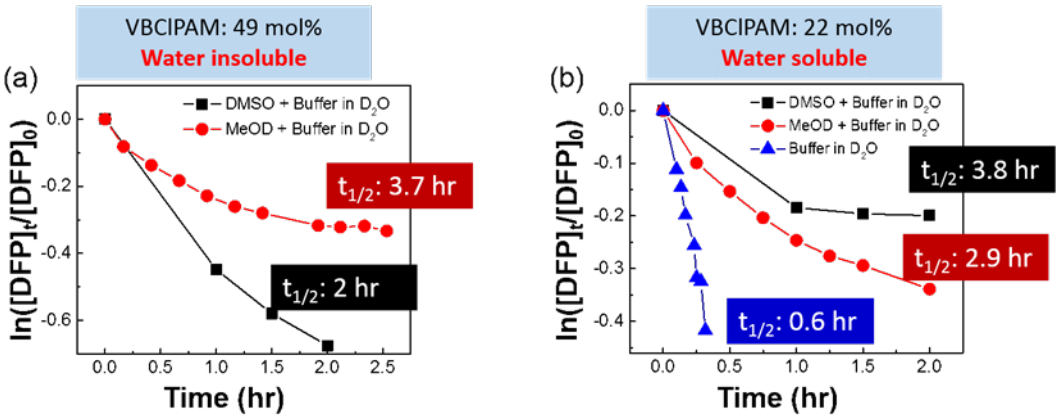

Figure 3.31 Kinetic plots of DFP neutralization catalyzed by terpolymer with 49 mol% of VBClPAM (a) and terpolymer with 22 mol% of VBClPAM in different solvent mediums

DFP neutralization by nucleophilic terpolymer with hydrolyzed acrylic acid was studied. Neutralization of DFP catalyzed by terpolymer with different composition showed distinctive results based on PAM compositions and solvents. Shortly, water-soluble polymer with lower mol% of VBClPAM shows the fastest reaction rate in sole water medium compared to polymer solution with higher mol% of VBClPAM in the mixture of organic solvent such as MeOD or DMSO-d_6. To clarify what reaction conditions (solvent, concentration and pH) can increase the DFP neutralization rate, additional experiments were performed. First, we only focused on water-soluble polymer to exclude solvent effect. Also, molar ratio between DFP and VBClPAM was controlled by adjusting concentration of polymer solution or synthesizing terpolymer with different mol% of each moiety. Furthermore, effects of buffer solution (pH) was also investigated by using 5 mM and 23 mM AMPD buffer solution in D_2O.

Table 4 Summary of DFP neutralization kinetic study: nucleophilic polymer with mol% of each component, molar equivalent of DFP (target): VBClPAM (nucleophilic moiety):AMPD (buffer), concentration of polymer in AMPD-buffered in D_2O

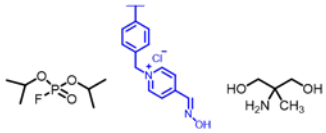

	AAc:NIP:VBBP:VBClPAM	DFP : VBClPAM : AMPD	hr[a]	% DFP[b]	Conc. Of polymer
1	20:49:22:9	1 : 6.03 : 0.26	0.7	58	83 mg/mL
2	19:54:20:7	1 : 2.28 : 1	0.45	0	40 mg/mL
3		1 : 2.28 : 0.22	0.4	80	
4		1 : 5.7 : 1	0.3	20	100 mg/mL
5		1 :5.7 : 0.22	0.3	80	
6	45:0:47:8	1 : 4.37 : 1	0.6	40	40 mg/mL
7		1 : 4.37 : 0.22	0.5	80	

- When[a] DFP destruction rate significantly drops with % DFP[b]
- 1,3,5: 5 mM AMPD, 2,4: 23 mM AMPD

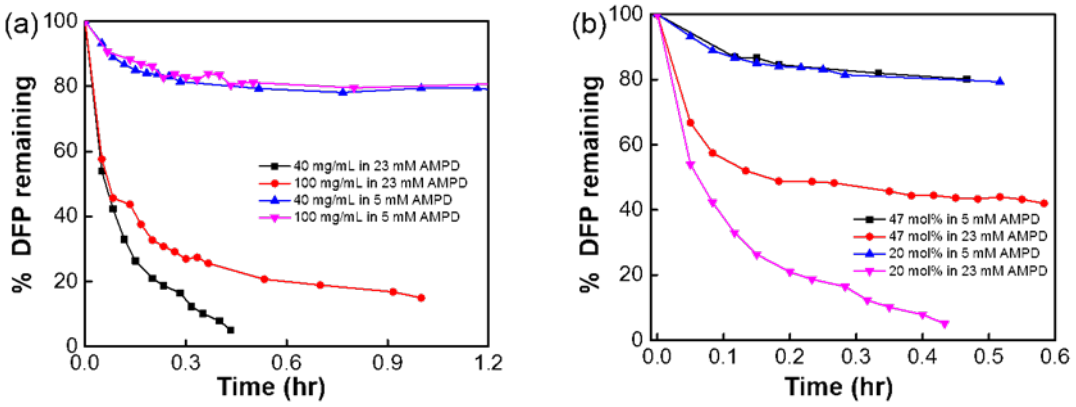

Figure 3.32 DFP neutralization kinetic plots for comparing polymer solution concentration using same polymer (a) and mol% of VBClPAM in terpolymer using two different polymer (b) in two different 2-amino-2-methyl-1,3-propanediol (AMPD)-based buffer solution (5 mM and 23 mM) in D_2O

In the beginning of DFP neutralization (<0.5 hr), concentration of DFP linearly decrease with fast reaction rate (pseudo-first order kinetic). Higher concentration of AMPD buffer solution (23 mM) results in much faster initial neutralization rate than lower concentration of AMPD buffer solution (5 mM) regardless of mol% of VBClPAM or concentration of polymer. Higher concentration of polymer in either 23 mM or 5 mM AMPD buffer solution in D_2O contains larger amount of acrylic acid with

PAM saturates low % DFP destruction. The polymer with higher PAM mol% contains higher acrylic acid mol% at the same time which lowers overall pH of polymer solution. Buffer solution can deprotonate not only pyridine-aldoxime (nucleophile) but also acrylic acid. From this reason, polymer with higher mol% VBClPAM (47 mol%) shows slower initial neutralization and lower % destruction given that only 20% DFP was destructed. It hinders our assumption that polymer with higher PAM mol% will show faster nucleophilic hydrolysis.

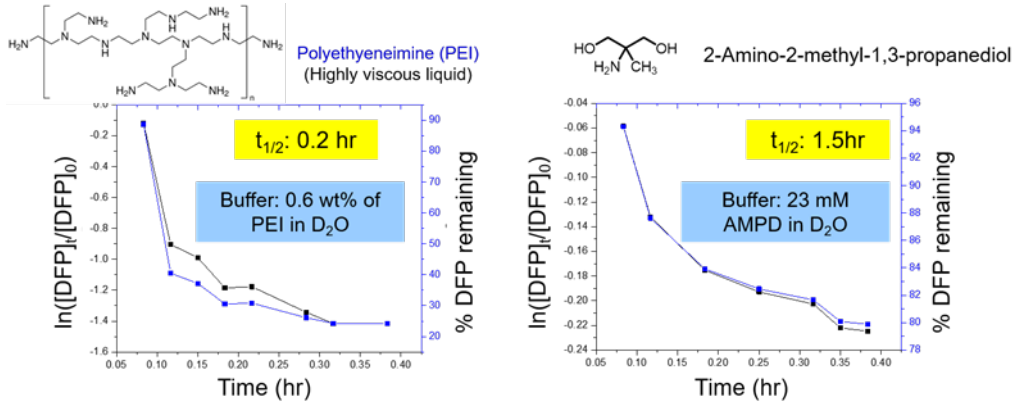

Figure 3.33 DFP neutralization kinetic: catalyzed by p(NIP-VBBP-VBIPAM) with assistance ot PEI (left) and 23 mM AMPD (right)

DFP neutralization by nucleophilic terpolymer without hydrolyzed acrylic acid was studied. To activate the reactivity of PAM, deprotonation of the terminal hydroxyl proton by a base is required. A solution of 2-amino-2-methyl-1,3-propanediol (AMPD - 23 mM) in D_2O ($t_{1/2}$: 1.5 hr) was used as the basic buffer, which effectively activated the reactive polymer resulting in faster neutralization rates. However, the use of AMPD buffer solution is limited since in the final application, a solid polymer film, AMPD can be easily washed away. We sought a low vapor pressure base as a replacement of AMPD base-buffer. We chose the viscous liquid polyethyleneimine (PEI), which was mixed with the polymer and in this system, fast DFP neutralization kinetics ($t_{1/2}$: 0.2 hr)

were observed. We have prepared crosslinked films with PEI covalently incorporated within the reactive terpolymer network.

DFP neutralization kinetic study was performed to see effect of polymer concentration and buffer using water-soluble p(NIP-*co*-VBIPAM) with different compositions.

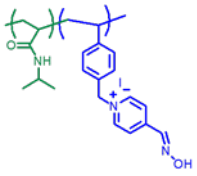

p(NIP-*co*-VBIPAM)

NIP	VBIPAM	Water-solubility
90	10	O
80	20	O
70	30	Δ

Figure 3.34 Water-soluble poly(NIP-*co*-VBIPAM) with different compositions (O means water-soluble, Δ means poorly water-soluble)

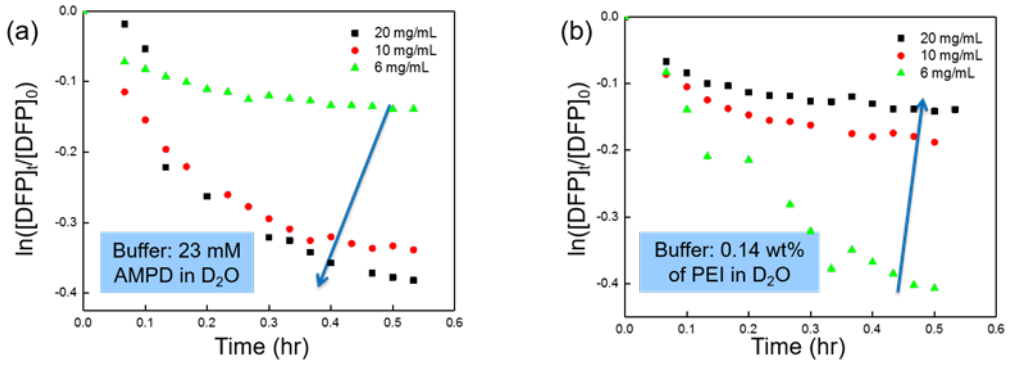

Figure 3.35 DFP neutralization kinetic study: effect of polymer (p(NIP-co-VBIPAM) with 90:10) concentration and buffer solutions

The rate of DFP neutralization was affected by polymer solution concentrations indicating that 4-pyridine aldoxime was involved non-catalytically in the hydrolysis of DFP. The water-soluble polymer, p(NIP-co-VBIPAM) with ratio of NIP:VBIPAM = 90:10 shows that higher polymer solution concentration in 23 mM AMPD buffer results in faster DFP neutralization. However, there was no large difference between 10

mg/mL and 20 mg/mL compared to 6 mg/mL. In the case of neutralization performed in the presence of PEI, lower polymer concentration results in faster DFP neutralization. From this data, we can conclude that 4-PAM is not catalytic in the neutralization of DFP. Also, the threshold polymer concentration (minimum polymer solution concentration showing fastest DFP neutralization) would be around 10 mg/mL in AMPD buffer solution.

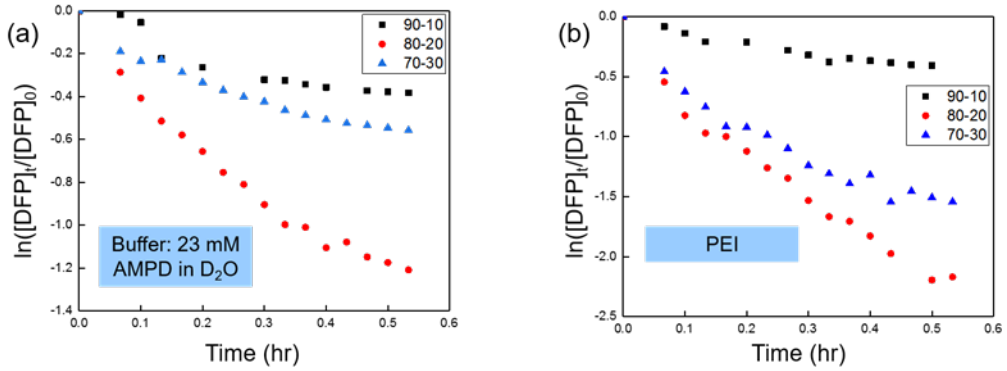

Figure 3.36 DFP neutralization kinetic study: effect of polymer with different compositions and buffer solutions

Above DFP neutralization plots are obtained from the fastest DFP neutralization result of each polymer concentration. NIP:VBIPAM = 90:10 (20 mg/mL in AMPD or 6 mg/mL in PEI), 80:20 (20 mg/mL), 70:30 (12 mg/mL-highest concentration). Depending on the polymers, the highest concentrations to be obtained were different. From the comparison among polymers with different compositions, polymer with higher PAM mol% as well as better water solubility results in fastest DFP neutralization in both AMPD and PEI buffered solutions. The fastest DFP neutralization was obtained from 20 mg/ml of p(NIP-co-VBIPAM) with 80:20 ratio in 0.6 wt% of PEI buffer solution. Based on this result, we have chosen the water-soluble p(NIP-VBBP-VBIPAM) sample with 20 mol% of VBIPAM for further optimization.

3.6 Conclusion

Due to the presence of AAc in polymer chains affecting overall pH, DFP neutralization catalyzed by the terpolymer could not be clearly concluded in that neutralization reaction saturated at low % of DFP destruction giving a non-linear curve. Neutralization of DFP by terpolymer containing AAc from hydrolyzed NIP was not suitable to conduct pseudo-first kinetic order. Ultimately, AMPD should assist PAM to enhance nucleophilic reactivity. However, AMPD will be easily washed away because of small molecular weight. For protective garment applications, we should find the replacement of AMPD rendering pH of polymer basic.

From ^{1}H NMR study of mixtures of PAM and NIP or vinylbenzyl chloride and PAM, we found the right synthesis route to avoid undesired NIP hydrolysis. NIP can be stable at room temperature and vinylbenzyl iodide can be functionalized with PAM at room temperature. DFP neutralization kinetic rate had been studied in various conditions controlling concentration of polymer solutions, buffer solutions (AMPD or PEI), and solubility of terpolymer in water or organic solvent. Up to now, the best result was water-soluble, terpolymer, p(NIP-VBBP-VBIPAM) with 20 mol% of VBIPAM with assistance of PEI activation reaching to half-life ~ 10 min and high % of DFP denomination.

Develop water-soluble terpolymers with maximized amount of VBIPAM and minimized hydrophobic VBBP. To achieve this, we can choose other hydrophilic monomers like HEMA or PEG-DMA instead of NIP. Also, we need to investigate the minimum mol % of VBBP in terpolymer in order to perform as photo-initiator and

reducing hydrophobicity. PEI was found as a good organo-base to activate PAM as a strong organo-nucleophile. We need to more care about molar ratio between amine from PEI and oxime from PAM. Build up more systematic DFP neutralization kinetic study based on solubility of terpolymer, mol% of VBBP in terpolymer and molar ratio between PEI and PAM.

CHAPTER 4

EVALUATION: MOISTURE VAPOR TRANSMISSION RATE (MVTR), CWA PERMEATION STUDY AND SELF-EXFOLIATION STUDY

4.1 Introduction

Protective clothing against toxic chemicals or biological hazards have been engineered to reduce the potential for the direct skin contact by resisting permeation, penetration or degradation. Before commercializing those materials, various standard and reliable tests are performed by quantitatively measuring the permeation of liquids and gases through protective clothing materials under continuous contact of the test chemical or examining undesirable physical changes.[1–3,46–52] With that, the breakthrough detection time, standardized breakthrough time, permeation rate, and cumulative permeation can be determined to evaluate the effectiveness of a clothing material as a barrier to the test chemical. ASTM (American Society for Testing and Materials) documents numbers of typical test methods for protecting garments. For example, F1407 suggests the permeation of liquids through protective clothing materials can be determined by using a permeation cup.[1] Basically, it measures weight loss from the cup resulting from chemical diffusion to and evaporation from the surface of the clothing specimen that faces the air. Regardless of its simplicity, there are several experimental limitations. If the weight loss occurs slowly due to the low volatility of the chemical, it will be difficult to trace the weight changes with time. Also, if the target

chemical is too toxic, then it is dangerous to test in open system. Especially, our system (SERP) targets significantly toxic OP-based nerve agents which can give us deleterious effects even with trivial amounts (LD_{50} of DFP: 1.3 mg/kg) requiring test methods to encompass small detection limits and a close system. Furthermore, SERP provides a protection against toxins by chemically neutralizing to non-toxic compounds as well as physically impeding permeation through. Therefore, it is necessary to quantitatively analyze a collection of permeants at given time by using detecting techniques including flame ionization, photo ionization, electro-chemical, ultraviolet and infrared spectrophotometry, gas and liquid chromatography, calorimetry, length-of-stain detector tubes, and radionuclide tagging/detection counting.

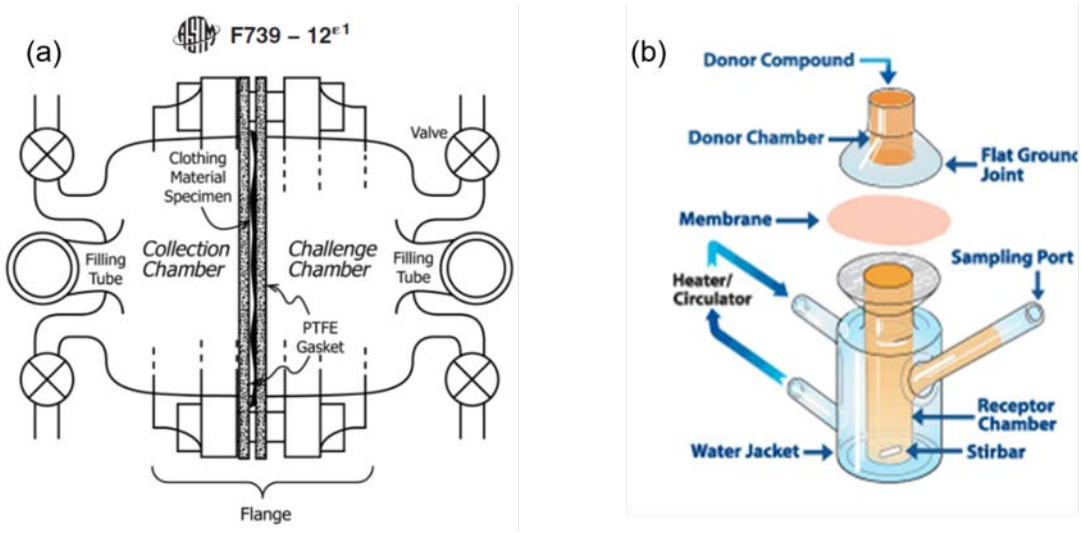

Figure 4.1 Permeation cell: F739 (a) and Franz cell (www.permeagear.com)

With those reasons, design of permeation test cells such as F739 and Franz cell[53] is a good candidate in that a sample material separates donor chamber for chemicals and receptor chamber for collecting permeants. The receptor chamber can be directly connected to the adequate detector which can provide the chemical identity and the relative amount if permeants consist of multi-components in real time. The permeation

test should be proceeding multi-times to obtain reliable values considering many factors such as film thickness, humidity, and detection limit.

4.2 Project Goal

- ✓ Understand SERP barrier abilities by examining resistance to permeation, % permeation through membrane, physical degradation or erosion rate and identifying permeants.
- ✓ Develop breathable layers with good moisture vapor transmission rate (MVTR), not limiting barrier ability.
- ✓ Control film thickness, crosslinking density, hydrophilicity of polymer and relative humidity.

4.3 Experimental, and Results and Discussion

4.3.1 Moisture Vapor Transmission Rate (MVTR)

Figure 4.2 Dynamic Moisture Permeation Cell (DMPC), image provided from Natick

The moisture vapor transmission rate (MVTR) of polymer coated films on ePTFE is measured in Natick. ePTFE is used due to its high breathability. The measurement condition is top cell with 95 % and bottom cell with 5 % relative humidity at 30 °C.

The flow rate is 2,000 cm^3/min. Polyethyleneimine (PEI) solution (6 wt%) in MeOH was spin-coated on ePTFE. MVTR was measured by Pearl Yip at Army Natick and shown to have excellent moisture permeability, 8399 g/m2·day. MVTR data for various substrates is shown in ***Figure 4.3***.

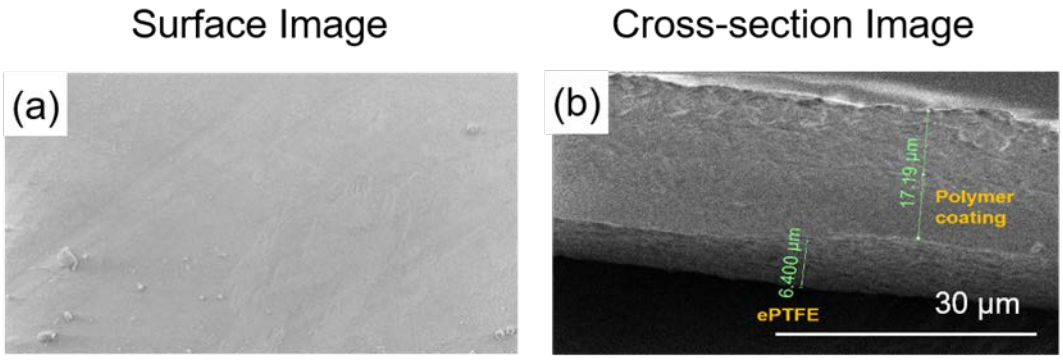

Sample	Water Vapor Flux [g/m^2·day]
ePTFE Membrane	16411
Gore-Tex Membrane	5809
Thin film on ePTFE	8399

Figure 4.3 Surface and cross-section image of breathable thin film on ePTFE and MVTR values.

4.3.2 Permeation test using Franz Cell and GC-MS

Ideally, OP-based toxins diffusing into the polymer films are neutralized before penetrating out of the layer. Therefore, the neutralization rate should be much faster than permeation rate. Even if permeation rate is fast, we can induce a long journey for toxins by increasing a film thickness. However, this physical hindrance will be an obstacle to achieve high breathability. To attain brief ideas, we've tried simple permeation experiments using Franz Cell. The hydrophilic polymers with an acid-

sensitive crosslinker cured on ePTFE was placed between donor chamber and receptor chamber. The receptor chamber was filled with organic solvent (hexane or dichloromethane) with internal standard (3mL). One of CWA simulants, diethyl chlorophosphate (DCP) (100 μL, 120 mg) was placed in the donor chamber. After each time interval, 1~2 μL of solution from receptor chamber was sampled and inserted into a gas chromatography-mass spectroscopy (GC-MS). However, we could not detect any from receptor chamber during observation time. It maybe because the concentration of DCP in receptor chamber is much more dilute than detection limit of GC-MS. We need to optimize the detection limit and concentration in receptor chamber. For quantitative investigation, a calibration curve was constructed using 5 different solutions with known concentration of DCP and constant concentration of hexadecane. Based on the response ratio between DCP and the internal standard (hexadecane) from the GC-MS data, we can obtain a product to standard ratio and hence quantify the measurements. The limit of detection was 1~3 μg which was calculated from injection volume and concentration. This stagnant and simple test will provide information on chemical identity of permeants.

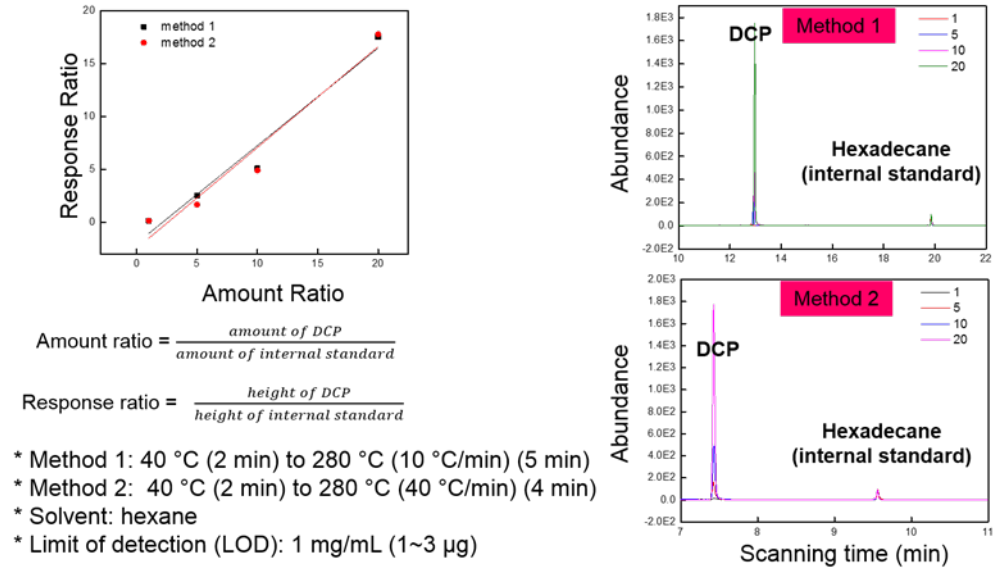

Figure 4.4 Calibration curve for GC-MS measurement of permeated DCP

4.3.3 CWA Permeation By Surface-enhanced Raman Spectroscopy (SERS)

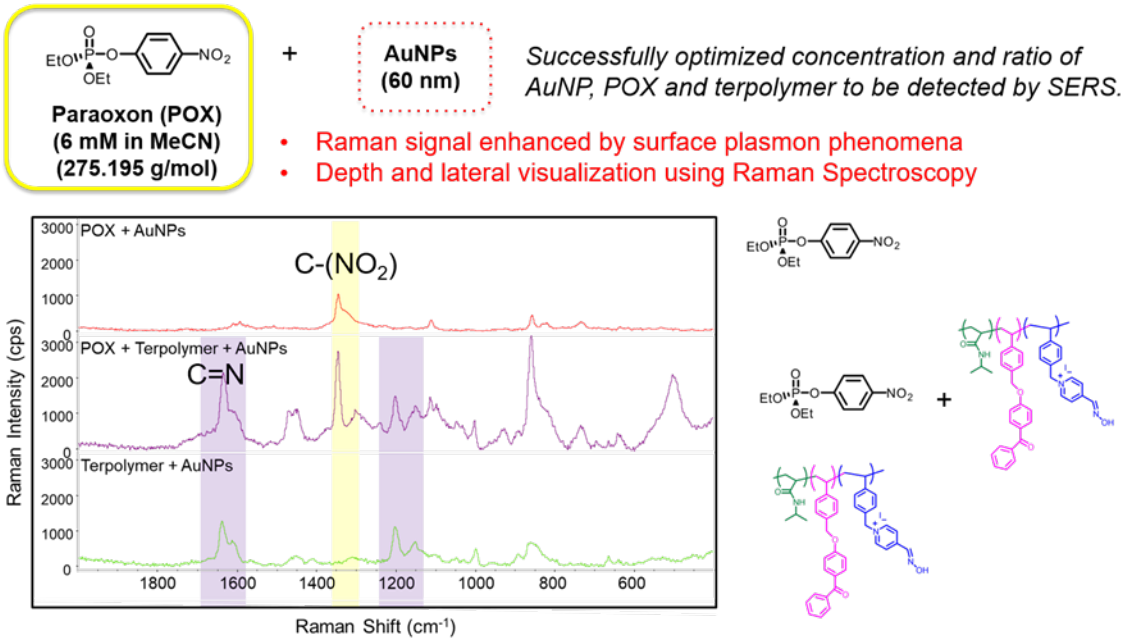

Figure 4.5 Schematic illustration of Surface-enhanced Raman Spectroscopy; target CWA simulant (paraoxon)

We have explored a new surface-enhanced Raman spectroscopy (SERS) technique that was developed in collaboration with Professor L. He (UMass, Food Science). This technique can be used to spatially monitor the diffusion of a CWA analogue, paraoxon

– (POX), through a polymer thin film. POX shows a weak Raman signal at 1350 cm^{-1}, which is greatly enhanced in the presence of 60 nm gold nanoparticles. To perform these analyses, an aqueous gold nanoparticle (AuNP) solution (0.5 mg/mL) was drop-cast on top of the film to be studied. After letting the AuNP diffuse into the film for 1 hr, 5 or15 μL of POX solution (6 mM in acetonitrile) was dropped on the surface of the film. We have continued to optimize the conditions to maximize detection. By combining AuNPs and adjusting concentration of AuNPs solution, we could successfully collect spectra to determine where each component (POX, terpolymer and mixture of two) show clear Raman signal peaks.

We prepared a polymer solution and prepared crosslinked films on ePTFE supports. We measured depth-mapping of SERS every 5 min after changing the surface with a 5 μL droplet of POX solution (20 mM in MeCN). Using a Raman microscope, depth mapping was performed by collecting spatially resolved spectra at depth intervals of every 3 μm. These slices are combined to give a plot of POX concentration as a function of area and depth. Results from a typical series of scans is shown in **Figure 4.6**. We observed that the diffusion of POX appeared to start at the top of the film and proceeds into the depth of the film over time. Position of the sample, flatness of the sample, and drop size have a strong impact on the quality of the results. While we do not yet fully understand this behavior, we believe that the highly humidified state of the sample may lead to isotropic diffusion like that found in the diffusion of ink in a liquid. At 30 min of exposure to POX, we could see evidence of neutralized POX by the appearance of a peak due to 4-nitrophenol at 1345 cm^{-1}. From these measurements we still do not know %

POX neutralization quantitatively. ^{31}P NMR measurement will complement these experiments to provide quantitative POX neutralization data. The experiments do confirm that a 30-um film of our material is not saturated or permeated by a highly concentrated drop of POX, even after 30 minutes.

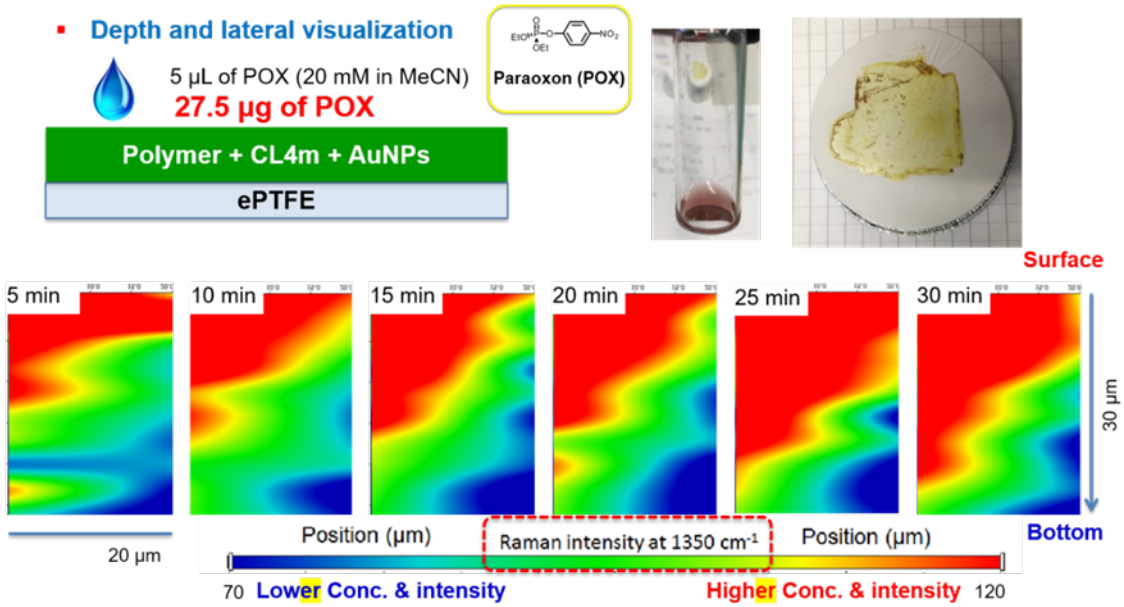

Figure 4.6 Visually shown depth-mapping of SERS exhibiting CWA permeation through crosslinked terpolymer

4.4 Conclusion

We have improved the breathability of the self-exfoliating and reactive polymer (SERP) by changing the system from bulk-hydrogel type of polymer films to thin polymer layer obtained from spin-coating of polymer solution and subsequent photo-irradiated crosslinking. The biggest change from the previous system to current linear polymer system is we have reduced film thickness significantly (150 µm to 10 µm). However, the control of film thickness is not exact in the lab. Therefore, we need more studies to achieve firmly controlled film thickness and MVTR.

For the study of CWA permeation through SERP layer, we used on *in situ* permeation cell connected to FID (Flame ionization detector). By doing so, we quantitatively observed the small amount of CWA, that permeated through the film in the closed system. Currently, our collaborator to Prof. Tim Swager (MIT), prepared this equipment.[54] In the future, we can go there to measure our samples. As a different approach, we use Surface-enhanced Raman Spectroscopy (SERS) to observe the permeation of CWA and decontaminated CWA. Also, by utilizing depth-mapping, we can see the concentration variation with different time intervals in the depth and width. Therefore, we could visually observe the CWA diffusion through films.

CHAPTER 5

CONCLUSION

As a protection against chemical warfare agents (CWAs), we've proposed self-exfoliating and reactive polymer (SERP). Our main targeting toxins are organophosphate (OP)-based nerve agents, which can be easily hydrolyzed by strong bases or nucleophiles. SERP materials would be coated on personal or soldier's garments so that the neutralization reaction of OP can occur at mild conditions without generating excess heat at ambient temperature. To achieve self-exfoliation, we've developed acetal/ketal-based acid-sensitive crosslinkers and studied their hydrolysis kinetic rate in solution and film states at different pH, hydrophilicity, and crosslinking density using ^{1}H NMR, UV-Vis spectroscopy and GC-MS.

To demonstrate neutralization of toxic OP compounds, we used DFP as Sarin or VX simulants. In early stages of this research, we had focused on finding better organo-nucleophiles. We have been exploring quaternary halides, histidine, aldoxime and pyridine-aldoxime (PAM) as a candidate of nucleophilic reactant. Among all candidates we chose PAM as a promising reactant for neutralizing DFP. We believed that PAM is a catalytic reactant, but we demonstrated reaction rate can be affected by concentration of PAM so we decideded to call PAM as a nucleophilic reactant. We designed and synthesized nucleophilic, photo-crosslinkable and hydrophilic terpolymer by conventional free radical polymerization. We investigated this terpolymer can neutralize DFP even faster with assistance of PEI as a base by deprotonating hydrogen

on the oxime rendering a lone pair electron on the oxime very reactive. It was realized that concentration of polymer solutions, hydrophilicity of polymer (water-solubility) and mol% of PAM-containing moiety, VBIPAM and base buffer can significantly affect DFP neutralization rate. So far, we have achieved the fastest DFP neutralization rate with half-life ~10 min. Also, we confirmed that SERP layer coated on ePTFE can also neutralize DFP with half-life ~30 min.

Also, we investigated breathability of SERP films coated on ePTFE. By changing system from a bulk-hydrogel film to a thin film layer spin-coated on ePTFE and subsequent photo-irradiated crosslinking, we have achieved high breathability with ~10 μm thickness. As a protection, it is important to observe how fast the CWA can permeate through films. Ideally, neutralization of DFP should be much faster than CWA permeation. Using Surface-enhanced Raman Spectroscopy (SERS), we observed CWA diffusion in the film by depth mapping with concentration variations and neutralized CWA (non-toxic) in the different depth. Unfortunately, we could not quantitatively investigate the permeation rate utilizing SERS, we could only obtain brief idea on how fast they can permeate.

CHAPTER 6

FUTURE WORK

As a future work, we will perform quantitative study of CWA permeation through SERP films using a diffusion cell equipped with the GC-MS which is set up in MIT. By doing so, we can expect that we will understand how fast CWA can permeate through our film quantitatively. Also, we can collaborate with the national lab where it can use real agents for testing with permission.

Also, we are working on making cellulose-based film containing nucleophilic PAM units which can be used as a CWA-agent decontaminating material. We are currently optimizing the amount of PAM in the cellulose-based film, the thickness of films and corresponding breathability by measuring moisture-vapor transmission rate (MVTR) collaborate with Natick Army Research Lab. This material can be spray coated, so uniform and thin layer can be made.

REFERENCES

(1) ASTM International. ASTM F1407:2012 Standard Test Method for Resistance of Selection of Chemical Protective Clothing Materials to Liquid Permeation - Permeation Cup Method. **2012**, 3–8 DOI: 10.1520/F1407-12.1.

(2) ASTM Commitee F23.30. F739 - Standard Test Method for Permeation of Liquids and Gases through Protective Clothing Materials under Conditions of Continuous Contact. **2012**, *i*, 1–12 DOI: 10.1520/F0739-07.2.

(3) Chao, K. P.; Wang, P.; Chen, C. P.; Tang, P. Y. Assessment of Skin Exposure to N,N-Dimethylformamide and Methyl Ethylketone through Chemical Protective Gloves and Decontamination of Gloves for Reuse Purposes. *Sci. Total Environ.* **2011**, *409* (6), 1024–1032 DOI: 10.1016/j.scitotenv.2010.11.034.

(4) Murthy, N.; Thng, Y. X.; Schuck, S.; Xu, M. C.; Fréchet, J. M. J. A Novel Strategy for Encapsulation and Release of Proteins: Hydrogels and Microgels with Acid-Labile Acetal Cross-Linkers. *J. Am. Chem. Soc.* **2002**, *124* (42), 12398–12399 DOI: 10.1021/ja026925r.

(5) Khaja, S. D.; Lee, S.; Murthy, N. Acid-Degradable Protein Delivery Vehicles Based on Metathesis Chemistry. *Biomacromolecules* **2007**, *8* (5), 1391–1395 DOI: 10.1021/bm061234z.

(6) Paramonov, S. E.; Bachelder, E. M.; Beaudette, T. T.; Standley, S. M.; Lee, C. C.; Dashe, J.; Fréchet, J. M. J. Fully Acid-Degradable Biocompatible Polyacetal Microparticles for Drug Delivery. *Bioconjug. Chem.* **2008**, *19* (4), 911–919 DOI: 10.1021/bc7004472.

(7) Knorr, V.; Russ, V.; Allmendinger, L.; Ogris, M.; Wagner, E. Acetal Linked Oligoethylenimines for Use as pH-Sensitive Gene Carriers. *Bioconjug. Chem.* **2008**, *19* (8), 1625–1634 DOI: 10.1021/bc8001858.

(8) Kim, B.; Lee, E.; Kim, Y.; Park, S.; Khang, G.; Lee, D. Dual Acid-Responsive Micelle-Forming Anticancer Polymers as New Anticancer Therapeutics. *Adv. Funct. Mater.* **2013**, *23* (40), 5091–5097 DOI: 10.1002/adfm201300871.

(9) Binauld, S.; Stenzel, M. H. Acid-Degradable Polymers for Drug Delivery: A Decade of Innovation. *Chem. Commun. (Camb).* **2013**, *49* (21), 2082–2102 DOI: 10.1039/c2cc36589h.

(10) Palmieri, F.; Adams, J.; Long, B.; Heath, W.; Tsiartas, P.; Willson, C. G. Design of Reversible Cross-Linkers. **2007**, *1* (4), 307–312.

(11) Heath, W. H.; Palmieri, F.; Adams, J. R.; Long, B. K.; Chute, J.; Holcombe, T. W.; Zieren, S.; Truitt, M. J.; White, J. L.; Willson, C. G. Degradable Cross-Linkers and Strippable Imaging Materials for Step-and-Flash Imprint Lithography. *Macromolecules* **2008**, *41* (3), 719–726 DOI: 10.1021/ma702291k.

(12) Zhou, H.; Blackwell, J. M.; Lee, H. B. R.; Bent, S. F. Highly Sensitive, Patternable Organic Films at the Nanoscale Made by Bottom-up Assembly. *ACS Appl. Mater. Interfaces* **2013**, *5* (9), 3691–3696 DOI: 10.1021/am4002887.

(13) Jhaveri, S. B.; Carter, K. R. Triggered Decomposition of Polymeric Nanoparticles Triggered Decomposition of Polymeric Nanoparticles. **2007**, *40* (22), 7874–7877 DOI: 10.1021/ma071750x.

(14) Koylu, D.; Carter, K. R. Stimuli-Responsive Surfaces Utilizing Cleavable Polymer Brush Layers. *Macromolecules* **2009**, *42* (22), 8655–8660 DOI: 10.1021/ma901627c.

(15) Jain, R.; Standley, S. M.; Fréchet, J. M. J. Synthesis and Degradation of pH-Sensitive Linear Poly (Amidoamine) S. *Macromolecules* **2007**, *40*, 452–457 DOI: 10.1021/ma062319v.

(16) Wang, Y.; Morinaga, H.; Sudo, A.; Endo, T. Synthesis of Amphiphilic Polyacetal by Polycondensation of Aldehyde and Polyethylene Glycol as an Acid-Labile Polymer for Controlled Release of Aldehyde. *J. Polym. Sci. Part A Polym. Chem.* **2011**, *49* (3), 596–602 DOI: 10.1002/pola.24425.

(17) Tomlinson, R.; Klee, M.; Garrett, S.; Heller, J.; Duncan, R.; Brocchini, S. Pendent Chain Functionalized Polyacetals That Display pH-Dependent Degradation: A Platform for the Development of Novel Polymer Therapeutics. *Macromolecules* **2002**, *35* (2), 473–480 DOI: 10.1021/ma0108867.

(18) Shimoda, A.; Sawada, S. ichi; Kano, A.; Maruyama, A.; Moquin, A.; Winnik, F. M.; Akiyoshi, K. Dual Crosslinked Hydrogel Nanoparticles by Nanogel Bottom-up Method for Sustained-Release Delivery. *Colloids Surfaces B Biointerfaces* **2012**, *99*, 38–44 DOI: 10.1016/j.colsurfb.2011.09.025.

(19) Wang, K.; Lu, J.; Yin, R.; Chen, L.; Du, S.; Jiang, Y.; Yu, Q. Preparation and Properties of Cyclic Acetal Based Biodegradable Gel by Thiol-Ene Photopolymerization. *Mater. Sci. Eng. C* **2013**, *33* (3), 1261–1266 DOI: 10.1016/j.msec.2012.12.024.

(20) Kim, S.; Linker, O.; Garth, K.; Carter, K. R. Degradation Kinetics of Acid-Sensitive Hydrogels. *Polym. Degrad. Stab.* **2015**, *121*, 303–310 DOI: 10.1016/j.polymdegradstab.2015.09.014.

(21) Bromberg, L.; Schreuder-Gibson, H.; Creasy, W. R.; McGarvey, D. J.; Fry, R. A.; Hatton, T. A. Degradation of Chemical Warfare Agents by Reactive Polymers. *Ind. Eng. Chem. Res.* **2009**, *48* (3), 1650–1659 DOI: 10.1021/ie801150y.

(22) Kim, K.; Tsay, O. G.; Atwood, D. A.; Churchill, D. G. Destruction and Detection of Chemical Warfare Agents. *Chem. Rev.* **2015**, *111* (9), 5345–5403 DOI: 10.1021/cr100193y.

(23) Bharathi, S.; Wong, P. T.; Desai, A.; Lykhytska, O.; Choe, V.; Kim, H.; Thomas, T. P.; Baker, J. R.; Choi, S. K. Design and Mechanistic Investigation of Oxime-Conjugated PAMAM Dendrimers as the Catalytic Scavenger of Reactive Organophosphate †. *J. Mater. Chem. B* **2014**, *2*, 1068–1078 DOI: 10.1039/c3tb21267j.

(24) Cox, J. R.; Ramsay, O. B. Mechanisms of Nucleophilic Substitution in Phosphate Esters. *Chem. Rev.* **1964**, *64* (4), 317–352 DOI: 10.1021/cr60230a001.

(25) Mcbain, A. J.; Ledder, R. G.; Moore, L. E.; Carl, E.; Gilbert, P.; Catrenich, C. E. Effects of Quaternary-Ammonium-Based Formulations on Bacterial Community Dynamics and Antimicrobial Susceptibility Effects of Quaternary-Ammonium-Based Formulations on Bacterial Community Dynamics and Antimicrobial Susceptibility. *Appl. Environ. Microbiol.* **2004**, *70* (6), 3449–3456 DOI: 10.1128/AEM.70.6.3449.

(26) Marciano, D.; Goldvaser, M.; Columbus, I.; Zafrani, Y. Catalytic Degradation of the Nerve Agent vx by Water-Swelled Polystyrene-Supported Ammonium Fluorides. *J. Org. Chem.* **2011**, *76* (20), 8549–8553 DOI: 10.1021/jo201600d.

(27) Mahato, T. H.; Prasad, G. K.; Singh, B.; Acharya, J.; Srivastava, A. R.; Vijayaraghavan, R. Nanocrystalline Zinc Oxide for the Decontamination of Sarin. *J. Hazard. Mater.* **2009**, *165* (1–3), 928–932 DOI: 10.1016/j.jhazmat.2008.10.126.

(28) Honda, H.; Ogawa, Y.; Kuwabara, J.; Kanbara, T. Emission Behavior of Secondary Thioamide-Based Cationic Pincer Platinum (II) Hiroya Honda , [a] Yasuyuki Ogawa , [a] Junpei Kuwabara , [a] and Takaki Kanbara * [a]. *Eur. J. Inorg. Chem.* **2014**, *201* (Ii), in press DOI: 10.1002/ejic.201)).

(29) Hirakawa, T.; Sato, K.; Komano, A.; Kishi, S.; Nishimoto, C. K.; Mera, N.; Kugishima, M.; Sano, T.; Ichinose, H.; Negishi, N.; Seto, Y.; Takeuchi, K. Experimental Study on Adsorption and Photocatalytic Decomposition of Isopropyl Methylphosphonofluoridate at Surface of TiO 2 Photocatalyst. *J. Phys. Chem. C* **2010**, *114*, 2305–2314 DOI: 10.1021/jp910911x.

(30) Cochran, R.; Kalisiak, J.; Küçükkilinç, T.; Radić, Z.; Garcia, E.; Zhang, L.; Ho, K. Y.; Amitai, G.; Kovarik, Z.; Fokin, V. V.; Sharpless, K. B.; Taylor, P. Oxime-Assisted Acetylcholinesterase Catalytic Scavengers of Organophosphates That Resist Aging. *J. Biol. Chem.* **2011**, *286* (34), 29718–29724 DOI: 10.1074/jbc.M111.264739.

(31) Chiarini, M.; Gillitt, N. D.; Bunton, C. A. The Oxidation of Thioanisole by Peroxomolybdate in Micelles of Cetylpyridinium Chloride. *Langmuir* **2002**, *18* (10), 3836–3842 DOI: 10.1021/la0117404.

(32) Chen, L.; Bromberg, L.; Schreuder-Gibson, H.; Walker, J.; Alan Hatton, T.; Rutledge, G. C.; Chemical Protection Fabrics via Surface Oximation of Electrospun Polyacrylonitrile Fiber Mats. *J. Mater. Chem.* **2009**, *19* (16), 2432 DOI: 10.1039/b818639a.

(33) Bromberg, L.; Pomerantz, N.; Schreuder-Gibson, H.; Hatton, T. A. Degradation of Chemical Threats by Brominated Polymer Networks. *Ind. Eng. Chem. Res.* **2014**, *53* (49), 18761–18774 DOI: 10.1021/ie501055g.

(34) Bromberg, L.; Klichko, Y.; Chang, E. P.; Speakman, S.; Straut, C. M.; Wilusz, E.; Hatton, T. A. Alkylaminopyridine-Modified Aluminum Aminoterephthalate Metal- Organic Frameworks As Components of Reactive Self-Detoxifying Materials. *Interfaces (Providence).* **2012**.

(35) Bromberg, L.; Hatton, T. A. Poly(N-Vinylguanidine): Characterization, and Catalytic and Bactericidal Properties. *Polymer (Guildf).* **2007**, *48* (26), 7490–7498 DOI: 10.1016/j.polymer.2007.10.040.

(36) Bromberg, L.; Creasy, W. R.; McGarvey, D. J.; Wilusz, E.; Hatton, T. A. Nucleophilic Polymers and Gels in Hydrolytic Degradation of Chemical Warfare Agents. *ACS Appl. Mater. Interfaces* **2015**, *7* (39), 22001–22011 DOI: 10.1021/acsami.5b06905.

(37) Mondloch, J. E.; Katz, M. J.; Isley III, W. C.; Ghosh, P.; Liao, P.; Bury, W.; Wagner, G. W.; Hall, M. G.; Decoste, J. B.; Peterson, G. W.; Snurr, R. Q.; Cramer, C. J.; Hupp, J. T.; Farha, O. K. Destruction of Chemical Warfare Agents Using

Metal–organic Frameworks. *Nat. Mater.* **2015**, *14* (March), 512–516 DOI: 10.1038/nmat4238.

(38) Morales-Rojas, H.; Moss, R. A. Phosphorolytic Reactivity of O - Iodosylcarboxylates and Related Nucleophiles. *Chem. Rev.* **2002**, No. 102, 2497–2551 DOI: 10.1021/cr9405462.

(39) Osovsky, R.; Kaplan, D.; Rotter, H.; Nir, I.; Columbus, I. Hydrothermal Degradation of Chemical Warfare Agents on Activated Carbon: Rapid Chemical-Free Decontamination. *Ind. Eng. Chem. Res.* **2013**, *52* (28), 9705–9708 DOI: 10.1021/ie401517a.

(40) Singh, N.; Karpichev, Y.; Sharma, R.; Gupta, B.; Sahu, A. K.; Satnami, M. L.; Ghosh, K. K. From α-Nucleophiles to Functionalized Aggregates: Exploring the Reactivity of Hydroxamate Ion towards Esterolytic Reactions in Micelles. *Org. Biomol. Chem.* **2015**, *13* (10), 2827–2848 DOI: 10.1039/c4ob02067g.

(41) Sit, R. K.; Fokin, V. V; Amitai, G.; Sharpless, K. B.; Taylor, P.; Radic, Z. Imidazole Aldoximes E Ff Ective in Assisting Butyrylcholinesterase Catalysis of Organophosphate Detoxi Fi Cation. **2014**.

(42) Smith, B. M. Catalytic Methods for the Destruction of Chemical Warfare Agents under Ambient Conditions. *Chem. Soc. Rev.* **2008**, *37* (3), 470–478 DOI: 10.1039/b705025a.

(43) Soman, M.; Dfp, B.; Hammondt, P. S.; Forster, J. S. A Polymeric Amine-Copper (I I) Complex as Catalyst for the Hydrolysis of 1 , Z , Z-Trimethylpropyl. **1991**, 1925–1931.

(44) Verma, A. K.; Srivastava, A. K.; Singh, B.; Shah, D.; Shrivastava, S. Kinetic Study of the Degradation of Diethylchlorophosphate and Sarin on Carbon-Supported Oxime. *Carbon N. Y.* **2012**, *50* (8), 3103–3106 DOI: 10.1016/j.carbon.2012.02.054.

(45) Whiteside, T.; Carreira, L.; Hilal, S. Estimation of Phosphate Ester Hydrolysis Rate Constants. II. Acid and General Base Catalyzed Hydrolysis. *QSAR Comb. Sci.* **2007**, *26* (5), 587–595 DOI: 10.1002/qsar.200630100.

(46) Precision, S. Standard Practice for Probability Sampling of Materials 1. **2016**, 10–13 DOI: 10.1520/E0105-16.Copyright.

(47) Specimens, P.; Glycol, E.; Duty, H.; Package, S.; Arms, S.; Grade, R.; Base, P.; Base, P.; Resistant, F.; Base, H. Standard Practices for. **2015**, *i* (Reapproved 2013), 3–9 DOI: 10.1520/D0543-14.2.

(48) Method, S. T. Standard Test Method for Rubber Property — Effect of Liquids 1. *Change* **2012**, *i*, 1–15 DOI: 10.1520/D0471-12.ASTM.

(49) American, A.; Standard, N. Standard Practice for Use of the Terms Precision and Bias in ASTM Test Methods 1. *Test* **2011**, No. C, 1–12 DOI: 10.1520/E0177-10.2.

(50) That, M.; Normally, P.; Data, D. Standard Test Method for Thickness of Textile Materials 1. **2002**, *7* (November 1995), 1–5 DOI: 10.1520/D1777-96R15.2.

(51) American, A.; Standard, N. Coated Fabrics 1. *Test* **2000**, *9* (September), 1–25 DOI: 10.1520/D0751-06R11.Copyright.

(52) ASTM International. Standard Test Method for Resistance of Protective

Clothing Materials to Permeation by Liquids or Gases Under Conditions of Intermittent. **1999**, *9*, 1–11 DOI: 10.1520/F1383-12E01.2.

(53) Rolland, P.; Bolzinger, M. A.; Cruz, C.; Briançon, S.; Josse, D. Human Scalp Permeability to the Chemical Warfare Agent VX. *Toxicol. Vitr.* **2011**, *25* (8), 1974–1980 DOI: 10.1016/j.tiv.2011.06.021.

(54) Gibson, P.; Schreuder-Gibson, H. Influence of Hydration State on Permeation Testing and Vapor Transport Properties of Polymer Films. *INDA Assoc. Nonwoven Fabr. Ind. - INDA/TAPPI Int. Nonwovens Tech. Conf. 2009, INTC 2009* **2009**, *2* (4), 876–915.

PUBLICATIONS:

1. Self-exfoliating and Reactive Polymer (SERP) as a Protection against Chemi cal Warfare Agents (CWAs), Soeun Kim, Kenneth R Carter, in preparation, **2019**.
2. Mechanical Properties and Moisture Transport Behavior of Acid-Sensitive Hydrogels, Sachin Bhaladhare, Soeun Kim, Kenneth R Carter, *Journal of Appl ied Polymer Science*, **2018**, submitted.
3. Degradation kinetics of acid-sensitive hydrogels, Soeun Kim, Olga Linker, Kim Garth and Kenneth R. Carter, *Polymer Degradation and Stability*, **2015**, *121*, 303-310.

PRESENTATIONS:

1. Breathable Polymer Layer as A Protection against Chemical Warfare Agents (CWAs), Soeun Kim, Yinyong Li, Kenneth R Carter, *Dynamic Multifunctional Materials for a Second Skin 2017 Program Review*, Pittsburgh, PA, June 14th (2017)
2. Reactive Polymer Layer against Organophosphate Nerve Agents, Soeun Kim and Kenneth R Carter, *The 12th National Graduate Research Polymer Conference*, Akron, OH, USA, June 19-22 (2016)-Oral
3. Nucleophilic NPs for CWA Threat Reduction, Soeun Kim and Kenneth R Carter, *The 2015 ACS Fall Meeting*, Boston, MA, USA, August 16-20 (2015)-Oral
4. Auto-Exfoliation/Regeneration Functionality for CWA Threat Reduction, Soeun Kim, Charlotte Mallet, Kenneth R Carter, The 2014 *ACS Spring Meeting*, Dallas, TX, USA, March 17-20 (2014)-Poster